9950-808

DRL No. 135
Technical Report: MRI - 294

DOE/JPL - 955676-4
Distribution Category UC - 63

ANALYSIS OF DEFECT STRUCTURE IN SILICON

CHARACTERIZATION OF SEMIX MATERIAL

Silicon Sheet Growth Development for the Large Area Silicon Sheet Task of the Low-Cost Solar Array Project.

FINAL REPORT

by
R. Natesh
G. B. Stringfellow
A. V. Virkar
J. Dunn
T. Guyer

February, 1983

JPL Contract No. 955676

The JPL Low-Cost Silicon Solar Array Project is sponsored by the U.S. Department of Energy and forms part of the Solar Photovoltaic Conversion Program to initiate a major effort toward the development of low-cost solar arrays. This work was performed for the Jet Propulsion Laboratory, California Institute of Technology, by agreement between NASA and DOE.

MRI Materials Research, Inc.

Research
Development
Consulting and Testing
Of Materials

790 South 790 East
Centerville, Utah 84014
Telephone: (801) 298-4000

DRL No. 135
Technical Report: MRI - 294

DOE/JPL - 955676-1
Distribution Category UC - 63

ANALYSIS OF DEFECT STRUCTURE IN SILICON

CHARACTERIZATION OF SEMIX MATERIAL

Silicon Sheet Growth Development for the Large Area Silicon Sheet Task of the Low-Cost Solar Array Project.

FINAL REPORT

by
R. Natesh
G. B. Stringfellow
A. V Virkar
J. Dunn
T. Guyer

February, 1983

JPL Contract No. 955676

The JPL Low-Cost Silicon Solar Array Project is sponsored by the U.S. Department of Energy and forms part of the Solar Photovoltaic Conversion Program to initiate a major effort toward the development of low-cost solar arrays. This work was performed for the Jet Propulsion Laboratory, California Institute of Technology, by agreement between NASA and DOE.

MRI Materials Research, Inc.

Research
Development
Consulting and Testing
Of Materials

700 South 790 East
Centerville, Utah 84014
Telephone: (801) 298-4000

TECHNICAL CONTENT STATEMENT

TABLE OF CONTENTS

SECTION			Page
	LIST OF TABLES		5
	LIST OF FIGURES		6
1.	ABSTRACT		9
2.	QUANTITATIVE ANALYSIS OF DEFECTS		10
	2.1	INTRODUCTION	10
		2.1.1 Advantages of Quantitative Microscopy (QTM)	11
	2.2	EXPERIMENTAL PROCEDURE	13
		2.2.1 Chemical Polishing and Etching	13
	2.3	RESULTS AND DISCUSSIONS	18
		2.3.1 Measurement of Grain Boundary and Twin Boundary Length Per Unit Area	20
		2.3.2 Measurement of Precipitate Particles	23
		2.3.3 Dislocation Density Measurement	26
		2.3.4 Cell Efficiency Versus Twin Boundary Density	30
		2.3.5 Diffusion Length Versus Dislocation Density	30
		2.3.6 Cell Efficiency Versus Area of All Defects	31
		2.3.7 Cell Efficiency Versus Location of Wafers	34
		2.3.8 Unprocessed Wafers	37
		2.3.9 Numerical Significance of Measured Data	39

SECTION		Page
3.	EFFECT OF GRAIN BOUNDARY DENSITY ON CARRIER MOBILITY	42
	3.1 INTRODUCTION	42
	3.2 EXPERIMENTAL PROCEDURE	43
	3.3 RESULTS AND SAMPLE CALCULATIONS	46
	3.3.1 Thickness	46
	3.3.2 Resistivity	47
	3.3.3 Hall Const., Mobility, Carrier Conc., Carrier Type	48
	3.3.4 Normalized Mobilities	49
	3.3.5 Grain Boundary Density	50
	3.4 DISCUSSIONS	52
4	CONCLUSIONS	54
	4.1 QUANTITATIVE ANALYSIS OF DEFECTS	54
	4.2 EFFECT OF GRAIN BOUNDARY DENSITY ON CARRIER MOBILITY	55
5	REFERENCES	56
6	APPENDIX (Tables 1 thru 45)	92-137

LIST OF TABLES

Table No.	Title	Page
I	The Circumference and the Field of View on the Olympus Inverted PME Microscope	19
II	Grain Boundary and Twin Boundary Length Per Unit Area for the Semix Wafers	22
III	Precipitate Particle and Dislocation Pit Density for Semix Wafers	25
IV	Defect Density, Conversion Efficiency, and Diffusion Length of Semix Samples	29
V	Area of Influence of Structural Defects per Unit Volume of Semix Samples	33
VI	Defect Densities in Unprocessed Wafers	38
VII	Thickness Measurements on Sample G-12	46
VIII	Thickness Data for All Samples	46
IX	Measured Voltages On Sample G-12-2	48
X	Resistivity, Hall Mobility, Carrier Concentration, Hole Mobility, Normalized Hole Mobility, and Grain Boundary Density for All 20 Specimens	51

LIST OF FIGURES

Figure No.		Page
1A	Position of Wafers from UCP Ingot 5848-13C	59
1B	Relative Positions of the Measured Fields in the Semix Wafers	60
2	Region Showing High Twin Density in Semix A-13 (50X)	61
3	Region Showing a Large Number of Precipitates in Semix A-13(50X)	61
4	Large and Small Precipitates in Semix B-2 (1330X)	62
5	Precipitates in Semix B-2 (530X)	62
6	Many Grains and Grain Boundaries in Semix C-12 (50X)	63
7	Twin and Grain Boundaries in Semix C-12 (50X)	63
8	Large Number of Small Twin Boundaries in Semix D-8. These are not Typical Regions (66X)	64
9	Many Twin and Grain Boundary Region in Semix D-8 (66X)	64
10	Dislocations Piled up Between Twins due to Localized Strain in Semix D-8 (600X)	65
11	Dislocations Interacting with a Twin Boundary in Semix D-8 (1500X)	65
12	High Twin Density in Semix E-13 (50X)	66

Figure No.	Title	Page
13	Large Precipitate Particle Between Twins in Semix E-13 (530X)	66
14	Twin and Grain Boundary Structure in Semix F-2 (50X)	67
15	Small Precipitate Particles in Semix F-2 (200X)	67
16	Twins and Grain Boundaries in Semix G-12 (50X)	68
17	Region of High Twin Density in Semix G-12 (100X)	68
18	Dislocation pile-ups in Semix H-8 (1330X)	69
19	High Dislocation Density Between Twins in Semix D-8 (1330X)	69
20	Twin Boundary Length per Unit Area vs. Relative Position of the wafer in the ingot from Top of the Solidified Ingot	70
21	Dislocation Pit Density vs. Large Precipitate Particle Density	71
22	Solar Cell Efficiency vs. Twin Boundary Length Density	72
23	Diffusion Length vs. Dislocation Pit Density	73
24	Twin Boundary Length Per Unit Area vs. Grain Boundary Length per Unit Area	74
25	Solar Cell Efficiency vs. Precipitate Area	75
26	Solar Cell Efficiency vs. Dislocation Area	76
27	Solar Cell Efficiency vs. All Defect Area	77
28	Cell Map Showing Locations of Wafers	78

Figure No.	Title	Page
29	Twin Density vs. Distance from Ingot Axis	79
30	Cell Efficiency vs. Distance from Ingot Axis	80
31	Segregation of Impurities in Cast Silicon	81
32	Precipitate Density vs. Relative Position	82
33	Large Precipitate Density vs. Relative Position	83
34	Dislocation Density vs. Relative Position	84
35	Twin Boundary Density vs. Relative Position	85
36	Grain Boundary Density vs. Relative Position	86
37	Electrical Connections to get a Small Contact Area	87
38	Two Configurations for Resistivity Measurements	87
39	Two Configurations for Hall Voltage Measurements	88
40	Grid to Locate Center of a Given Field	88
41	Configuration to Determine Carrier Type	89
42	Mobility vs. Grain Boundary Density	90
43	Normalized Mobility vs. Grain Boundary Density	91

SECTION 1

ABSTRACT

Statistically significant quantitative structural imperfection measurements were made on samples from Ubiquitous Crystalline Process (UCP) Ingot 5848 - 13C. Important correlation was obtained between defect densities, cell efficiency, and diffusion length. Grain boundary substructure displayed a strong influence on the conversion efficiency of solar cells from Semix material. Quantitative microscopy measurements gave statistically significant information compared to other micro - analytical techniques. A surface preparation technique to obtain proper contrast of structural defects suitable for QTM analysis was perfected and is now being used routinely.

A study was made to determine the relationships between hole mobility and grain boundary density. Mobility was measured using the van der Pauw technique, and grain boundary density was measured using quantitative microscopy technique. Mobility was found to decrease with increasing grain boundary density.

SECTION 2

QUANTITATIVE ANALYSIS OF DEFECTS

2.1 INTRODUCTION

The objective of this work is to gain fundamental understanding of the role of structural imperfections and chemical impurities on solar cell performance.

The type, density, distribution, and electrical activity of such defects have significant effects on solar cell performance. Most of the processes designed to produce silicon crystals at low cost introduce a high density of defects in crystals, which have a distinct effect on solar cell efficiency.

The types of defects present in many of the low - cost silicon " sheets", produced by a variety of methodology, run the gamut from point defects to dislocations, planar defects such as twins and stacking faults, high and low angle grain boundaries, and second phase inclusions. The types of imperfections present and their density are a function of the specific method used for producing the silicon sheets.

In general, rapidly grown ribbon - type crystals produced by techniques such as the EFG process, the Web Dendritic method, etc., typically contain a relatively high population of dislocations usually arrayed along linear boundaries, a high density of twins, and chemical impurities in the form of precipitates. Sheets formed by slicing of cast crystals, such as SEMIX material, are generally polycrystalline in nature with grain diameters from a fraction of a millimeter to several millimeters, and twin boundaries oriented in different direction within many of the grains.

Quantitative analysis of surface defects was performed by using a Quantimet Quantitative Image Analyzer (QTM 720). The results were double checked by manually counting all the defects. The QTM 720 can differentiate and count 64 shades of grey levels between black and white contrasts. In addition, it can characterize structural defects by measuring their length, perimeter, area, density, spatial distribution, frequency distribution (in any preselected direction), and is programmable in these measurements. However, the QTM 720 is extremely sensitive to optical contrasts of various defects. Therefore, to obtain reproducible results, the contrasts produced by various defects must be similar and uniform for each defect types along the entire surface area of samples to be analyzed. To achieve this contrast uniformity, a chemical cleaning and polishing procedure was developed and perfected for the SEMIX samples described in this report. The cleaning and polishing procedure produced a very clean and even surface. Statistically significant quantitative data was measured and their significance is discussed.

2.1.1 ADVANTAGES OF QUANTITATIVE MICROSCOPY TECHNIQUE

There is significant advantage in using quantitative microscopy technique as described herein to analyze structural defects. Techniques such as transmission electron microscopy (TEM), scanning electron microscopy (SEM), while providing useful information, are usually performed at higher magnifications. For example, TEM analysis is usually carried out in the magnification range 10,000X to 300,000X. Because of the high magnification employed, the area of the field of view is very very small compared to the total surface area of the starting sample, such as a 2cm by 2 cm sample. Hence, the information obtained, although impressive, may not be statistically significant. However, in our quantitative microscopy technique as used in this report, the magnifications used are very low such as 100X to 1000X. In addition, a total of 62 fields was analyzed from a 2 cm by 2 cm sample. For grain boundary and twin boundary measurement, the total area analyzed was 1.49 cm^2 for a 2 cm by 2 cm sample i.e., a whopping 37% of total surface area was actually measured. For precipitate particles, the total area analyzed was 0.09 cm^2 i.e., 2.3% of the total surface area was measured. For dislocation pits, the total area measured was 0.37% of the total sample area. By way of comparision, if we were to analyze 62 fields from a 2 cm by 2 cm sample by TEM technique at 100,000X, the total area for 62 fields will be only 0.00000147 cm^2 which is 0.000037% of the sample surface area.

Therefore, the results obtained by quantitative microscopy technique as described in this report are statistically more significant and reliable than any other technique such as TEM, SEM, etc.

SECTION 2.2

EXPERIMENTAL PROCEDURE

2.2.1 CHEMICAL POLISHING AND ETCHING

Fifteen (15) samples from SEMIX's Ubiquitous Crystalline Process (UCP) Ingot 5848 - 13C were received by Materials Research, Inc., (MRI) from JPL for characterization of structural defects. These samples measured 2 cm by 2 cm and were designated by JPL as 1-4-13 (or A - 13), 2-10-2 (or B - 2), 3-10-12 (or C - 12), 4-10-8 (or D - 8), 1-2-13 (or E - 13), 2-9-2 (or F - 2), 3-9-12 (or G - 12), 4-9-8 (or H - 8), 1-10-13 (or T), 1-12-14 (or U), 2-5-1 (or V), 3-4-12 (or W), 3-4-16 (or X), 4-2-4 (or Y), and 4-2-8 (or Z). We notice that each sample is defined by three numbers. The first number refers to the section, the second number refers to the wafer number, and the third number refers to the cell number. Thus, sample A is located in section 1, wafer number 4, and cell number 13. The location of the samples is shown clearly in Figure 1 with respect to the center line of the casting ℄ - ℄ . From Figure 1A, it is clear that Ingot 5848 - 13 C is one- quarter (1/4) of the total casting. This quarter ingot was cut into four (4) sections. Each section was further sectioned into twelve (12) wafers, and sixteen (16) cells.

Samples T, U, V, W, X, Y, and Z were as - received samples. They were not subjected to any processing. Samples E, F, G, & H were fabricated into solar cells without gettering. Samples A, B, C, and D were gettered at 875° C for 1/2 hour and then processed into solar cells.

The QTM 720 apparatus is extremely sensitive to contrasts produced by various structural defects. It can distinguish 62 shades of grey levels between black and white. By remembering the exact shade, the QTM 720 is able to correctly count each defect types. Therefore, to obtain accurate and reproducible results, it is very important that each structural defect type be etched to identical contrast. MRI has now perfected a chemical cleaning, polishing, and etching procedure to produce contrasts to such a demanding requirement in these Semix samples. All chemicals used were Low Sodium MOS, Electronic Grade. The following procedures were used:

1) Grease, Dust and other Surface Contamination Removal

		time (min.)
a.	Sample immersed in trichloroethylene	3
b.	Sample rinsed in acetone	3
c.	Sample rinsed in 2- Propanol	3
d.	Compressed N_2 gas to blow off 2 - Propanol to prevent stain marks	0.5

2) Protective Coating Application

a. Using a fine paint brush, Apiezon Wax dissolved in trichloroethylene was applied to one surface of the silicon sample.

b. The wafer was then heated on a hot plate to about 120° C to accelerate evaporation of trichloroethylene. The Apiezon Wax melted and spread uniformly covering the entire surface. All of the trichloroethylene evaporated leaving behind a thin coating of the acid - resistant Apiezon Wax covering the surface.

3) Silicon Oxide Layer Removal

		time (min.)
a.	Sample was immersed in concentrated HF	4
b.	It was then rinsed in distilled water	4
c.	It was then rinsed in 2-propanol	4
d.	N_2 gas to blow off excess 2-propanol	0.5

The protective coating application is done for two reasons: i) to prevent attack and dissolution of samples from two surfaces. By using a wax coating, the coated surface is prevented from chemical attack during polishing and etching procedure, ii) the protective coating may be dissolved later in trichloroethylene and JPL may in future build a solar cell on that surface. Thus a direct correlation between cell efficiency and defect densities for each sample may be obtained.

4) Chemical Polishing Procedure

The chemical polishing solution is a mixture by volume of 1 part nitric acid (HNO_3) : 2 parts hydrofluoric acid (HF) : 3 parts acetic acid (CH_3COOH). The following procedure was used :

		time (min.)
a.	The wafer was immersed at 50 $\pm$ 3^{o} C in polishing solution	0.1-0.75
b.	It was then rinsed in deionized distilled water	4
c.	It was then rinsed in 2 - propanol	4
d.	N_2 gas blown to dry sample surface	0.5
e.	Sample was observed under micrscope and polishing was continued until a smooth flat surface was observed	0.1-0.75

5) Chemical Etching Procedure

The chemical etching solution consists of 2.5 gm. of chromium trioxide (CrO_3) dissolved in 15 ml. deionized distilled water and 15 ml. concentrated hydrofluoric acid (HF). The following procedure was used:

		time (min.)
a.	Sample was immersed in the chemical etching solution	0.1-0.3
b.	It was then rinsed in deionized distilled water	4
c.	It was then rinsed in 2 - propanol	4
d.	N_2 gas blown to dry sample surface	0.5
e.	Sample was observed under microscope and etching procedure was continued until dislocation pits are visibly observed	

The etching times for the Semix samples were as follows.

Sample No.	Etching Time (Sec.)
A-13	67
B-2	60
C-12	48
D-8	37
E-13	77
F-2	82
G-12	61
H-8	48
Average	60

SECTION 2.3

RESULTS AND DISCUSSION

MEASUREMENT OF GRAIN BOUNDARIES, TWIN BOUNDARIES, PRECIPITATE PARTICLES, AND DISLOCATION PITS

Using an Olympus Inverted Optical Metallurgical Microscope, Model PME , approximately 62 fields on each sample were analyzed for structural defects. Figure 1B shows the relative positions of the 62 fields that were observed on each sample. The feature under investigation is counted in each field and averaged over the 62 fields for a statistical average of the overall sample. The field of view of the microscope is a necessary quantity to know so that some dimensions can be given to the defect feature. Using a 0.01 cm - 0.001 cm calibrated standard microscope slide, the diameter of the field of view was measured at different magnifications. From this data, the circumference and the area of the field of view was determined. This data is tabulated in Table 1. Table 1 shows that as the magnification approximately doubles for successive objective setting, the diameter of field of view decreases by about half.

The defect measurements were done in three (3) separate steps. First, the grain boundary and twin boundary intersections were

TABLE I

The circumference and the field of view on the Olympus Inverted PME Microscope

Eye-piece Lens	Object-ive Lens	Magnifi-cation	Diameter of field of view (cm)	Circum-ference of field of view (cm)	Area of field of view (cm^2)
10X	5X	50X	0. 36	1. 13	0. 102
10X	10X	100X	0. 175	0. 55	0. 0241
10X	20X	200X	0. 089	0. 28	0. 00622
10X	40X	400X	0. 0435	0. 137	0. 00149
10X	100X	1000X	0. 0174	0. 055	0. 000238

Sample Calculation:

Circumference at 50X $= \pi D = (\pi)(0.36 \text{ cm}) = 1.13 \text{ cm}$

Area of field of view at 50X $= \dfrac{\pi D^2}{4} = \dfrac{\pi (0.36)^2}{4} = 0.102 \text{ cm}^2$

measured for all the 62 fields using a magnification of 100X in the polished condition. Next, the precipitate particles were measured for all the 62 fields using a magnification of 400X in the polished condition. Next, the sample was etched in the etching solution and immediately measurements were made for dislocation pits for all the 62 fields at a magnification of 1000X.

All of these measurements were made manually. Attempts were made to use the Quantitative Image Analyzer (Quantimet QTM 720). However, this was not successful since the contrast on the CRT was poor for the fine precipitates at 1000X. These manual measurements were done very carefully, the measurements were repeated, and found to be reproducible. All measured data is listed in Appendix.

2.3.1 Measurement of Grain Boundary and Twin Boundary Length Per Unit Area

Since grain boundaries can be location of efficient carrier recombination centers and act as sinks for impurities which can be detrimental to the efficiency of the solar cell,[1-4] the grain boundary length per unit area is an important quantity to know. Using a statistical method of counting the intersections of the grain boundaries and twin boundaries with a test line, the length per unit area can be calculated using the following relationship[5,6] :

$$L_A = (\pi/2) \cdot P_L \text{, where}$$

L_A = line length of grain boundaries or twin boundaries per unit area (cm/cm^2)

P_L = number of point intersections of grain boundaries or twin boundaries per unit length of test lines.

Figures 2, 6, 7, 8, 9, 12, 14, 16, and 17 show typical structures of twin boundaries and/or grain boundaries in the Semix samples. The Appendix Tables 1, 4, 7, 10, 13, 16, 19, and 22 contain a listing of the raw measured data for grain boundaries and twin boundaries. The information in the above tables has been summarized in Table II, along with calculated values for arithmetic mean and standard deviation.

Several tentative graphs are shown in order to determine any apparent relationship in the measured data. These graphs are preliminary and subject to revision as more and more samples are examined and better information about sample history is obtained from other sources (such as Semix Corporation, JPL, OCLI, etc.,). Figure 20 shows a plot of twin boundary length as a function of the distance of the wafer from top of the ingot. Figure 20 shows that, as a first approximation, twin boundary density (expressed as length/unit area) decreases as the distance from top of ingot increases. Samples A and E located at top of the ingot have higher densities and lower

<u>TABLE II</u>

Grain Boundary and Twin Boundary Length Per Unit Area for the Semix Samples

SEMIX Sample Number	Grain Boundary Length per unit area (cm/cm^2)	Twin Boundary Length per unit area (cm/cm^2)
A - 13	8.2 $\bar{x}$ = 2.9 σ = 2.0	99.0 $\bar{x}$ = 34.6 σ = 56.5
B - 2	4.5 $\bar{x}$ = 1.6 σ = 2.2	15.8 $\bar{x}$ = 5.6 σ = 9.3
C - 12	13.4 $\bar{x}$ = 4.7 σ = 2.7	31.9 $\bar{x}$ = 11.2 σ = 11.1
D - 8	13.8 $\bar{x}$ = 4.8 σ = 3.2	44.5 $\bar{x}$ = 15.6 σ = 17.1
E - 13	7.1 $\bar{x}$ = 2.5 σ = 2.1	68.5 $\bar{x}$ = 24 σ = 38
F - 2	5.4 $\bar{x}$ = 1.9 σ = 2.6	12.2 $\bar{x}$ = 4.3 σ = 6.8
G - 12	12.1 $\bar{x}$ = 4.2 σ = 2.6	40.7 $\bar{x}$ = 14.3 σ = 15.5
H - 8	9.4 $\bar{x}$ = 3.3 σ = 1.9	35.9 $\bar{x}$ = 12.6 σ = 13.3
Average	9.2	43.6

$$\bar{x} = \text{arithmetic mean} = \frac{\sum \text{features in all fields}}{\text{Total number of fields}}$$

$$\sigma = \text{standard deviation} = \left[\frac{1}{n-1} \sum_{i=1}^{n} (x_i - \bar{x})^2 \right]^{1/2}$$

solar cell efficiencies. To explain this phenomenon, data on crystal growth conditions are required, which is currently not available. Figure 24 is a plot of the data listed in Table II. As a first approximation, Figure 24 shows that as the grain boundary length/unit area increases, the twin boundary length/unit area increases rapidly at first then levels off and decreases. Assuming that nucleation of twin boundaries occur at grain boundaries, one would expect the twin boundary density to increase with decreasing grain size i.e., increasing grain boundary area. However, there are many interrelated unknown factors (regarding crystal growth conditions), which may make any possible definite relation between grain size and twin boundary density difficult to determine. The purpose of plotting twin boundary length versus grain boundary length is simply to pictorially depict observed relationship. Figure 24 does not imply that twin boundary area must depend upon grain boundary area. A further study will be required to see if there is any definite relationship between these variables.

2.3.2 Measurement of Precipitate Particles

The polished samples were observed at a magnification of 400 X, and the number of precipitate particles were counted in each field. There appeared to be two fairly distinct sizes of what was counted as precipitate particles. The large-sized defects were clearly recognized to be precipitate particles. However, there were smaller features, that could not be resolved clearly, which looked like precipitate particles. The only other possibilities were that these features are small stain marks or etch pits. Since there is some questions as to the identity of these features, observation of these samples at a higher magnification using a Scanning Electron Microscope (SEM) is recommended. However, for the time being, these features will be regarded as small precipitates, subject to correction later. The Appendix Tables 2, 5, 8, 11, 14, 17, 20 and 23 contain a listing of the raw measured data for precipitate particles in these Semix samples . The information contained in the above tables have been summarized in Table III , along with values for arithmetic mean and standard deviation. Small and large precipitate particle densities are listed separately in Table III.

TABLE III

Precipitate Particle and Dislocation Pit Density for Semix Samples

SEMIX Sample Number	Precipitate Particle Density (particles/cm^2)			Dislocation Pit Density (pits/cm^2)
	small	large	total	
A - 13	22×10^3 $\bar{x}$ = 33 σ = 36.5	745 $\bar{x}$ = 1.1 σ = 1.5	23×10^3	4.9×10^4 $\bar{x}$ = 12 σ = 23
B - 2	19.5×10^3 $\bar{x}$ = 29.1 σ = 18.1	444 $\bar{x}$ = 0.66 σ = 0.95	20×10^3	9.5×10^4 $\bar{x}$ = 23 σ = 45
C - 12	6.2×10^3 $\bar{x}$ = 9.2 σ = 7.7	65 $\bar{x}$ = 0.1 σ = 0.4	6.3×10^3	37×10^4 $\bar{x}$ = 89 σ = 62
D - 8	2.5×10^3 $\bar{x}$ = 3.8 σ = 4.0	152 $\bar{x}$ = 0.23 σ = 0.46	2.7×10^3	10×10^4 $\bar{x}$ = 24 σ = 51
E - 13	9.1×10^3 $\bar{x}$ = 13.5 σ = 10.6	400 $\bar{x}$ = 0.6 σ = 0.7	9.5×10^3	37×10^4 $\bar{x}$ = 89 σ = 96
F - 2	4.8×10^3 $\bar{x}$ = 7.2 σ = 10.5	740 $\bar{x}$ = 1.1 σ = 2.1	5.6×10^3	17×10^4 $\bar{x}$ = 40 σ = 111
G - 12	6.4×10^3 $\bar{x}$ = 9.6 σ = 8.0	140 $\bar{x}$ = 0.21 σ = 0.41	6.6×10^3	45×10^4 $\bar{x}$ = 108 σ = 161
H - 8	9.5×10^3 $\bar{x}$ = 14.1 σ = 10.9	250 $\bar{x}$ = 0.4 σ = 0.8	9.7×10^3	86×10^4 $\bar{x}$ = 204 σ = 235
Avg.	10.0×10^3	367	10×10^3	31×10^4

For precipitate particle density, 2.3% of the total area was measured.

For dislocation density, 0.37% of the total area was measured.

A sample calculation for small precipitate density in sample F-2 in Table III is shown below:

Magnification = 400X

Area of field = 0.00149 cm^2

$$\overline{X} \text{ for small precipitate} = \frac{447}{62} = 7.2 \quad \text{(see Appendix Table 17)}$$

$$\frac{\text{No. of small precipitates}}{\text{unit area}} = \frac{\text{(total no. of small precipitates counted)}}{\text{(total no. of fields) (area of a field)}}$$

$$= \frac{(447)}{(62)(0.00149 \text{ cm}^2)} \quad \text{(see Appendix Table 17)}$$

$$= 4.8 \times 10^3 \text{ precipitates/cm}^2$$

Figures 3, 4, 5, 13, and 15 show precipitate particles on some of the Semix samples. The large precipitate diameter is of the order of magnitude ~ 15 x 10^{-4} cm, while the small precipitate diameter is of the order of magnitude ~ 3 x 10^{-4} cm..

2.3.3 Dislocation Density Measurement

After etching each of the Semix wafers, the dislocation density was determined by counting the number of dislocation etch pits at 1000X in each field of view for approximately 57 fields per sample. The number of fields measured was slightly lower due to mechanical interference of the longer objective lens with the microscope stage. The Appendix Tables 3, 6, 9, 12, 15, 18, 21, and 24 list the raw measured data for dislocation number density. The information in the above tables have been summarized in Table III, along with calculated values for arithmetic mean and standard deviation. A sample calculation for wafer F-2 in Table III is as follows:

Magnification	=	1000X
Total number of dislocation pits counted	=	2334 from 59 fields
Area of Field	=	$0.000238\ cm^2$

$$\text{Dislocation Pit density} = \frac{\text{(total no. of dislocation pits counted)}}{\text{(total no. of fields) (Area of field)}}$$

$$= \frac{(2334)}{(59)\ (0.000238\ cm^2)} \quad \text{(see Appendix Table 18)}$$

$$= 1.7 \times 10^5 \text{ dislocation pits}/cm^2$$

Figures 10, 11, 18, and 19 show dislocation arrangements in some of the Semix samples.

Figure 21 shows a plot of dislocation density versus large precipitate density from the data listed in Table III (data for small precipitate was not used in Figure 21 since the identity of small precipitate was not positively established). Figure 21 shows that as the large precipitate density increased from sample to sample, the corresponding dislocation density decreased. This trend is quite clear even though some anomalies are present in Figure 21. This observation may be explained on the basis that dislocation lines constitute tubes of fast diffusion, with a diffusion coefficient close to the coefficient of self diffusion along grain boundaries. The rates of diffusion along such short-circuit paths are significantly higher than for volume diffusion, since the associated activation energies are much lower than for volume diffusion[8]. As dislocation density increases, larger number of short-circuit paths are now available for impurity atoms to migrate. This may result in a decrease in precipitate density. While the intrinsic properties of individual dislocations, dislocation networks, and grain boundaries are governed by the presence of space charge cylinders around defects, the typical electrical response of these structural defects is determined by the presence of impurities in association with the defects. The interaction energy between common impurities such as Fe, Ni, Cu and a dislocation are fairly high, so that impurity atmospheres and impurity precipitates can form at dislocations[9]. When defect intersections occur in crystals, the resulting electrical effects are more pronounced[10, 11]. Presence of impurities at or near crystallographic defects make them electrically active. When P is diffused into the crystals, the impurities from the defects are "gettered" due to reactions between P and impurities decorating the defects. As a result, the defects are no longer electrically active. However, the defects are still present within a diffusion length of beam-generated charge carriers. Hence, predominant electrical effects in silicon devices are caused by defect-impurity association (see Fig. 10, 11, & 19).

TABLE IV

Defect Density, Conversion Efficiency, and Diffusion Length of Semix Samples.

Semix sample number	Small precipitate density (cm^{-2})	Large precipitate density (cm^{-2})	Total precipitate density (cm^{-2})	Dislocation density (cm^{-2})	Grain boundary length per unit area (cm^{-1})	Twin boundary length per unit area (cm^{-1})	Cell efficiency* (%)	Diffusion length* (μm)
A - 13	22×10^3	745	23×10^3	4.9×10^4	8.2	99.0	7.2	53
B - 2	19.5×10^3	444	20×10^3	9.5×10^4	4.5	15.8	10.0	51
C - 12	6.2×10^3	65	6.3×10^3	37×10^4	13.4	31.9	9.7	41
D - 8	2.5×10^3	152	2.7×10^3	10×10^4	13.8	44.5	10.8	47
E - 13	9.1×10^3	400	9.5×10^3	37×10^4	7.1	68.5	6.2	35
F - 2	4.8×10^3	740	5.6×10^3	17×10^4	5.4	12.2	9.6	22
G - 12	6.4×10^3	140	6.6×10^3	45×10^4	12.1	40.7	9.5	19
H - 8	9.5×10^3	250	9.7×10^3	86×10^4	9.4	35.9	10.7	31

* data as given in reference No. 7

2.3.4 Cell Efficiency Versus Twin Boundary Density

Table IV lists the defect densities in these Semix samples as obtained by MRI along with the data for cell efficiency and diffusion length as obtained by OCLI[7]. The data for cell efficiency was plotted as a function of the observed data for different types of structural defects. Figure 22 shows a plot of cell efficiency versus twin boundary density. An approximate inverse relationship is observed. Plotting cell efficiency versus grain boundary density did not show any clear trend . The significance of Figure 22 is that the grain boundary substructure may influence cell efficiency in Semix material. In other words, the defect structure within grains may influence the cell efficiency more than the grain boundary itself. Furthermore, as mentioned in page 25, interactions of these substructures with one another and with impurity atmospheres may cause more pronounced electrical effects.

2.3.5 Diffusion Length Versus Dislocation Density

The numerical data for diffusion length was plotted in several ways using the various observed data for different types of structural defects listed in Table IV. Figure 23 shows a graphical plot of diffusion length versus observed dislocation density in the eight samples. The figure shows an important trend. An inverse relationship is observed between diffusion length and dislocation density. Since the average grain size in these samples is expected to be larger than the diffusion length in a single crystal Semix of the same doping level (data not currently available), the effective lifetime and diffusion length in the polycrystalline Semix samples is expected to be reduced by substructures within grains (such as twin boundary density, dislocation density, and precipitate particle density along with chemical segregation around these substructures).

2.3.6 Cell Efficiency Versus Area of All Defects

In an attempt to correlate the cell efficiency with various structural imperfections, it was tentatively assumed that the effectiveness (in reducing the cell efficiency) of various defect types was same. With this assumption, the total area of all structural defects was determined and summed.

The actual measurement on plane of polish of silicon wafers yields information in terms of length per unit area of structural features (listed in Table IV). However, these features are truly three-dimensional and, therefore, quantitative stereological relations can be used to convert these measured quantities to area per unit volume. For example, dislocation density measured in number /cm^2 is the same quantity as length /cm^3 of dislocations [5]. In order to determine the effect of various defects, the data in Table IV have been converted on a unit volume basis and is listed in Table V. The effect of defects on charge carriers will be in the immediate vicinity of the defects. Therefore , surface area of defects per unit volume is the most logical parameter to correlate efficiency with defect densities.

The precipitate matrix-interface area per unit volume (i. e. ,"area of influence" for precipitates) was calculated as follows :

$$S_{v(p)} = \pi d_1^2 \rho_1 + \pi d_2^2 \rho_2$$

Where d_1 and d_2 are the diameters of the large and small precipitates, and ρ_1 and ρ_2 are respective densities (number/cm^3). The precipitates exhibited binodal distribution. Smaller precipitates were on the average about 3 μm in diameter, while the larger precipitates were on the average about 15 μm in diameter. With this information, the surface area for small and large precipitates may be calculated, and these are listed in Table V.

With regards to dislocations, it was assumed that a cylindrical area around a dislocation is the effective area in reducing cell efficiency. The radius of this cylindrical area was assumed to be 20 Å. The reasoning for this assumption is that electrically active impurities will likely be located within 5 b from the core of the dislocation (where b is the Burgers Vector). Thus, the "area of influence" due to the dislocations is given by:

$$S_{v(d)} = 2 \pi R \Gamma$$

Where Γ = dislocation density (cm/cm^3)

and R = effective radius $\approx$ 20Å

In Table V, the respective areas of influence for these defects (per unit volume) are listed along with cell efficiency. It is interesting to note that the effective areas of the precipitate particles and dislocations is insignificant compared with the twin boundary area. It is further observed that at the defect densities observed, there is virtually no correlation between the cell efficiency and either the precipitate surface area or the dislocation surface area. This aspect is graphically demonstrated in Figures 25 and 26. Examination of Table V also shows that the grain boundary area, although not insignificant, is considerably smaller in these samples than the

TABLE V

Area of Influence of Structural Defects per Unit Volume of Semix Samples

Semix sample number	Surface area of small and large precipitates $4\pi r_1^2 d_1 + 4\pi r_2^2 d_2$ $r_1 = 3/2 \mu m$ $r_2 = 15/2 \mu m$ d_1, d_2 are precipitate densities cm^2/cm^3	Surface area of dislocation $2\pi R \Gamma$ where Γ is dislocation density and $R = 20Å$ cm^2/cm^3	Grain boundary surface area cm^2/cm^3	Twin boundary surface area cm^2/cm^3	Total areas of all types of structural defects cm^2/cm^3	Cell efficiency* (%)
A - 13	0.011	0.06	8.2	99.0	107.27	7.2
B - 2	0.008	0.12	4.5	15.8	20.428	10.0
C - 12	0.002	0.46	13.4	31.9	45.762	9.7
D - 8	0.002	0.126	13.8	44.5	58.428	10.8
E - 13	0.005	0.46	7.1	68.5	76.065	6.2
F - 2	0.006	0.214	5.4	12.2	17.82	9.6
G - 12	0.003	0.565	12.1	40.7	53.368	9.5
H - 8	0.004	1.081	9.4	35.9	46.385	10.7

* data as given in reference No. 7

corresponding twin boundary area. Once again there appears to be no definite correlation between grain boundary area and cell efficiency. Finally, upon examination of twin boundary area, it is seen that cell efficiency decreases with increasing twin boundary area (see Figure 22). Also shown in Figure 27 is a plot of cell efficiency versus total defect areas. Since twin boundary area is the predominant term, the overall behavior is similar to Figure 22.

2.3.7 Cell Efficiency Versus Location of Wafers

An important and definite correlation has been found between cell efficiency and location of the wafers with respect to the center line of ingot (Figure 1A) and in relation to the top center of the ingot. Figure 28 is a plan view of the top of the ingot, which is shown in three dimension in Figure 1A. The center line C in Figure 1A originates at O in Figure 28, and is perpendicular to the plane of paper. Figure 28 shows the distance of the center of a wafer from origin O. Thus, the center of cells A and E are located 1 cm along X-axis and 1 cm along Y - axis from O. Therefore, their center is located at $\sqrt{1^2 + 1^2} = \sqrt{2} = 1.414$ cm from the center line of ingot . The distance from ingot axis for the remaining cells were calculated. Figure 29 shows a definite relationship between twin boundary density and distance from ingot axis for the various cells. It is clear from Figure 29 that the twin boundary density decreases as the distance of the cells from ingot axis increases. Figure 30 shows important correlation between cell efficiency and distance from ingot axis. As the distance from the ingot axis increases, the cell effieciency also increases. Specifically, the cell efficiency increases with increasing distance from the center of the ingot towards its outer surface. For example, note that cells A - 13 and E - 13 have lower efficiency , while cells B - 2, F - 2, D - 8, H - 8 have much higher efficiencies. Furthermore, a definite relation also evolves with reference the location of the ingot. For example, note that the cells E - 13 and A - 13 were fabricated from wafers very close to the top center of the ingot. Cell E-13 came from a wafer which was just above cell A-13 (Figure 1A) Correspondingly, cell E-13 has lower efficiency (6.2%) compared to A-13 (7.2%). Even though these wafers are from adjacent location, the difference of 1% in cell efficiencies is significant. Similarly, cell F-2 is just above cell B-2 and correspondingly, cell efficiency for F-2 is smaller than that for B-2 (9.6% vs. 10.0% i.e., the differences is 0.4%). Note that these cells, which are considerably below cells E and A, have much higher efficiencies. Similarly cells G-12 and C-12 have efficiencies of 9.5% vs. 9.7% (difference is 0.2%) where G is above C. Cells H-8 and D-8 have efficiencies of 10.7% and 10.8% (difference 0.1%) where H is above D. Cells H and D came from the lowest section (4th section) of the ingot. These results are very remarkable in that they show a definite pattern of cell efficiency in relation to location in the ingot . A plausible explanation for this behavior is as follows:

It is assumed that this polycrystalline silicon ingot was fabricated by melting silicon in a refractory mold. Upon cooling, it is assumed that the material in contact with the mold is the first to solidify. Consequently, the topmost center part of the mold will be the last to solidify. Thus, any impurities which have higher solubilities in molten silicon will be rejected into the liquid upon freezing. Thus, the impurity concentration will be highest in the topmost center part of the ingot, while lowest in the bottom outermost part of the ingot. A schematic of the proposed impurity distribution in solidified ingot is shown in Figure 31. The region around A-B will have higher impurities then C (Figure 31) It is well known that certain impurities, which tend to segregate at various defects, render these defects electrically active. Thus, cells made from topmost center part of the ingot will have highest concentration of impurities and lowest cell efficiencies. This is also the region where highest concentration of twin boundary exists. If these impurities are associated with defects, the defects may become electrically active and reduce the cell efficiency drastically. The measured cell efficiencies clearly show this trend. Furthermore, as the variation of impurity concentration varies exponentially alons with distance in a zone melted or zone - refined body, the relaive variation in cell efficiency will incrase from bottom to the top of the ingot. The obervations clearly corroborate this hypothesis in that the adjacent cells at D and H vary only slightly in efficiency (0.1%) while cells A and E which are from the top of the ingot exhibit large variation (1.0%) in efficiency.

The present work, therefore, suggests avenues for further research in order to fully understand the role of defects on cell effieciency. For example, the precipitates and dislocations, at the densities observed, have no noticeable effect on cell efficiency. Among the defects characterizable by microscopy twin boundaries and grain boundaries seem to have the largest influence. Clearly then, the manufacturer should make process modifications in an attempt to reduce twin boundary densities.

A significant parameter may yet be related to trace impurities in the ingot. As pointed out above, the distribution of impurities in an ingot is most likely dependent upon the mode of solidification. However, the present analysis suggests that the impurity concentration will be highest in the topmost center part of the ingot. (The region of highest impurity concentration will be the region that solidified last. This region will be somewhat below the top center of the ingot). The future work therefore must focus on a thorough chemical analysis (with reference to trace elements) of wafers as a function or location in the ingot. Furthermore, detrimental impurities and their concentrations must be identified.

2.3.8 Unprocessed Wafers

Table VI lists the defect densities obtained on unprocessed wafers from UCP Ingot 5848 - 13C. Figures 32 thru 36 show the distribution of various defect types as a function depth for unprocessed, gettered, and non-gettered samples. The idea was to determine what effect, if any, gettering and processing may have on the distribution of defects. However, the data in the table and figures are not conclusive. The variation of defect densities in the unprocessed samples is considerable, requiring further study.

TABLE VI

Defect Densities in Unprocessed Wafers

Semix sample number	Small precipitate density (cm^{-2})	Large precipitate density (cm^{-2})	Dislocation density (cm^{-2})	Grain boundary length per unit area (cm^{-1})	Twin boundary length per unit area (cm^{-1})
1-10-13 (T)	44200	2035	6.0	7.88	79.2
1-12-14 (U)	29970	1705	1.1	3.14	29.2
2-5-1 (V)	26250	812	20.6	32	36.3
3-4-12 (W)	40370	2092	10.9	16.9	40
3-4-16 (X)	39050	2405	15.2	28.8	27.0
4-2-4 (Y)	23879	1916	37.2	16.9	34.8
4-2-8 (Z)	11430	693	16.9	13.9	51.2

2.3.9 Numerical Significance of Measured Data

The measured data for the Semix samples are listed in Appendix Tables 1 thru 24, and the information in these tables are summarized in Tables II, III, and IV. The defect structure characterization was done using a statistical sampling of each sample over a TV raster and from this an average value for each defect type in each sample was obtained [12-22].

Among these eight samples, the large precipitate density varied from 65 to 745 per cm^2, while the total (large and small) precipitate density varied from 2.7×10^3 to 23×10^3 per cm^2.

Grain boundary length per unit area varied from 4.5 to 13.8 cm/cm^2, whereas the twin boundary length per unit area varied from 12.2 to 99.0 cm/cm^2. Samples A-13 and E-13 had the higher twin boundary length per unit area, while the grain boundary length per unit area for these samples were in the middle range. Samples C-12, D-8, and G-12 had the higher numerical values for grain boundary length, but in the middle range for twin boundary length. Samples B-2 and F-2 had lower values for both grain boundary and twin boundary length. Figure 24 shows that as the grain boundary length/unit area increases, the twin boundary length/unit area also increases at first rapidly, but at higher values for grain boundary length/unit area,it levels off and gradually decreases.

Dislocation density in these samples varied from 4.9×10^4 to $86 \times 10^4/cm^2$.

Sample A-13 had the lowest dislocation density but highest large precipitate density (see Table IV). Samples C-12, G-12, and H-8 had lower precipitate density but had higher dislocation density. Therefore, an approximate inverse relationship was observed between dislocation density and precipitate density as shown in Figure 21.

Sample A-13 had the highest twin boundary length per unit area as well as the highest large precipitate density. Figures 2 and 3 show some regions in this sample that illustrate this observation.
Figures 4 and 5 show some precipitate particles in fields free of twin boundaries and grain boundaries in sample B-2 . This sample had lower twin boundary and grain boundary lengths per unit area but precipitate density was in the medium numerical value. Figures 6 and 7 show some twin boundary and grain boundary regions in sample C-12. Sample C-12 had higher grain boundary density. Sample D-8 had the highest grain boundary length per unit area and also a relatively high twin boundary density as illustrated in Figures 8 and 9. Figure 10 shows an area in sample D-8 where dislocations have piled up between twin boundaries Figure 11 shows another type of interaction between dislocations and a twin boundary. Such a boundary may be electrically active as discussed in page 21.

Figures 12 and 13 show a higher twin boundary density region, which is typical of sample E-13. Sample F-2 has a lower grain boundary and twin boundary length per unit area, but a high precipitate density. Figure 14 shows interaction between twin boundary and grain boundary, and Figure 15 shows a region of higher precipitate density in sample F-2. Figures 16 and 17 show sample regions in sample G-12 with typical grain boundary and twin boundary structures. Sample H-8 has the highest dislocation density and typical areas are illustrated in Figures 18 and 19. In Figure 18, the dislocations form simple networks. Figure 19 shows linear arrays of dislocations interacting with twin boundaries on either side

The standard deviation from the mean for all of the defect types is of the same order of magnitude as the mean itself. This shows that there is a large variation in the distribution of defects from one field to another in the same sample.

SECTION 3

EFFECT OF GRAIN BOUNDARY DENSITY ON CARRIER MOBILITY

3.1 INTRODUCTION

The objective of this work is to determine the relationship between carrier mobility and grain boundary density, that is grain boundary length per unit area, in cast polycrystalline silicon.

A polycrystalline wafer sliced from a cast mold will have many defects ranging from vacancies to precipitates, twins, dislocations, and grain boundaries. When considering the effect on carrier mobility, grain boundaries are thought to have the greatest influence.[23]

There are several reasons that grain boundaries are considered the limiting factor in mobilities. The most obvious is the high concentration of other defects at a boundary. Since there is a lattice mismatch at a boundary, there is bound to be a high vacancy density. These vacancies act as a sink for dopant atoms, thus resulting in an ionized impurity concentration near the boundary that is higher than the rest of the crystal matrix. Since ionized impurities act as scattering centers for charge carriers, mobilities will necessarily be lowered.

Another feature of a grain boundary is band bending. That is to say the conduction and valence bonds, at the grain boundary, are bent up and down respectively thus presenting an energy barrier for electrons and holes. This, too, should decrease mobility.

Carrier mobility was measured via the Hall effect[24-31] using a four-point-probe configuration. Important parameters such as resistivity, carrier type, and carrier concentration were also measured. Grain boundary density was measured by quantitative optical microscopy[32].

SECTION 3.2

EXPERIMENTAL PROCEDURE

Equipment List

Keithley Instruments model 225 current source
Hewlett Packard 412 A vacuum tube voltmeter
Keithley Instruments model 600 B electrometer
Harvey Wells model 1050A magnet power supply
Magnion 7" electromagnet
Power Logicon model 5C ultrasonic wire bonder
Nikon Optiphot optical microscope
Olympus OSM optical microscope
Hewlett Packard 3465 A Multi meter

Eight (8) SEMIX samples from UCP Ingot 5848-13 C were used in this study. These samples were designated by JPL as A-13, B-2, C-12, D-8, E-13, F-2, G-12, and H-8. The samples were first characterized for structural defects as described in an earlier report[32]. The specimens for Hall mobility measurements were obtained from each of the above 8 samples by scribing a line parallel to one of the edges,and then cleaving the sample along the scribed line. The cleaved piece was then broken into three smaller pieces. Therefore, initially there were 24 irregular specimens of sizes ranging from 2mm by 5mm to 5mm by 5mm. Due to breakage and handling problems only 20 specimens were eventually characterized. Thickness was measured by placing samples on edge and measuring them with a filar eyepiece at a magnification of about X100 with the Olympus microscope.

Electrical connections were made by mounting the sample on a PC board with four copper strips then, using an ultrasonic wire bonder, 18μm aluminum wire was bonded to the silicon surface and then to the copper strip (Fig. 1). This technique was used so that the contact area would be as small as possible and be bonded as close to the edge of silicon sample as possible so as to reduce the influence of the contacts on the measurements. The power and time settings for the silicon and copper bonds were 2 and 1.6, and 2.4 and 2 respectively.

Resistivity measurements were made using the configurations in Fig. 2. Current was passed through the contacts depicted in the figure and the corresponding potential induced at the other contacts was measured. This procedure was repeated in both configurations, with the current flowing in the forward and reverse directions and at 0.1 and 1mA to insure ohmic behavior in that region. The ammeter insures that the desired current is indeed what is flowing between the points in question.

Hall voltages were measured with the electrical connections in the configurations shown in Fig. 3. Current was passed through the contacts shown in each configuration and the potential across the other contacts was measured. The magnetic field, which is perpendicular to the face of the sample, was then applied. The voltage was then measured again. The difference between the two readings is the hall voltage. The procedure was repeated in both configurations with the current flowing in the forward and reverse directions. The sample was then turned around 180 degrees with respect to the magnetic field and the procedure was carried out again. This procedure negates the effects of any physical assymmetries in the experimental setup. Most of the samples were measured with a current of 1ma and an 8KG magnetic field. Some samples were run at different levels of current and magnetic field to facilitate more accurate voltage readings.

Grain boundary density was determined by examining the samples at 400X with the Nikon microscope. The diameter of the field of vision was determined with a calibrated microscope slide. The number of grain boundaries that intersected the circumference of the field of vision were then counted. Due to the irregular shapes and sizes of the samples the number of fields of vision per sample varied greatly. To preserve some statistical validity a grid was used to determine where to locate the center of a given field. See Fig. 4 for a portion of the grid. Each dot represents the center of a field of vision and there is 0.5mm between dots on a horizontal row.

SECTION 3.3

RESULTS AND SAMPLE CALCULATIONS

3.3.1 THICKNESS

The calibration of the filar eyepiece on the Olympus microscope when using the 10X objective is 0.9909 μm/div . Data taken for the three pieces from sample G-12 is shown in Table 1. Final results for all eight samples is shown in Table 2.

TABLE VII

THICKNESS MEASUREMENTS ON SAMPLE G-12

	INITIAL READING	FINAL READING	d(div)	d(μm)
1	276	564	288	285
2	361	653	292	289
3	208	526	318	315

d = 296μm max. % deviation = 6.4%

TABLE VIII

THICKNESS DATA FOR ALL SAMPLES

sample	d(μm)	max.% deviation
A - 13	266	2.4
B - 2	315	3.1
C - 12	304	1.2
D - 8	277	5.5
E - 13	305	3.5
F - 2	290	0.8
G - 12	296	6.4
H - 8	285	1.7

3.3.2 RESISTIVITY

Using the configurations (1) and (2) in Fig. 2, the resistances R_{ABCD} and R_{BCDA}, respectively, can be measured where

$$R_{ABCD} = \frac{\text{Potential across DC}}{\text{Current through AB}} = \frac{V_{DC}}{I_{AB}}$$

and

$$R_{BCDA} = \frac{\text{Potential across DA}}{\text{Current through BC}} = \frac{V_{DA}}{I_{BC}}$$

It was shown by Van der Pauw[33] that the following relation holds:

$$\exp\left[-\pi R_{ABCD}\left(\frac{d}{\rho}\right)\right] + \exp\left[-\pi R_{DCBA}\left(\frac{d}{\rho}\right)\right] = 1 \qquad \textit{equation (1)}$$

where d is the sample thickness and ρ is the resistivity of the sample. Since the resistances and thickness of a given sample are known, ρ can be determined by use of equation (1).

A calculation of ρ for the first of the C-12 samples, C-12-1, follows:

C-12-1

$$I = 1\text{mA} \qquad R_{ABCD} = \frac{.00145 + .0015}{2I} = 1.47\ \Omega$$

$$R_{BCDA} = \frac{.045 + .045}{2I} = 45\ \Omega$$

$$I = 100\mu\text{A} \qquad R_{ABCD} = \frac{.00015 + .00015}{2I} = 1.5\ \Omega$$

$$R_{BCDA} = \frac{.0045 + .0046}{2I} = 45.5\ \Omega$$

$\bar{R}_{ABCD} = 1.485$ ohm, $\bar{R}_{BCDA} = 45.25$ ohm; using these values and $d = 304\,\mu m$, equation (1) gives $\rho = 1.8\,\Omega$-cm.

3.3.3 Hall Const., Mobility, Carrier Conc., Carrier Type

The Hall const., mobility, carrier conc., and carrier type were determined using the configurations shown in Fig. 3. Data taken for sample G-12-2 is shown in Table 3. This is followed by sample calculations.

Sample: G-12-2

I = 1mA, B = 8KG, d = 296μm, ρ = 2.1Ω-cm

TABLE IX

MEASURED VOLTAGES ON SAMPLE G-12-2

Configuration 1

	$V_1(B=0)$	$V_2(B\neq0)$	V_H
+I +B	.05	.0515	.0015
-I +B	.056	.057	.001
+I -B	.056	.055	.001
-I -B	.051	.05	.001

Configuration 2

$V_1(B=0)$	$V_2(B\neq0)$	V_H
.056	.055	.001
.052	.051	.001
.052	.053	.001
.056	.057	.001

$$\overline{V_1-V_2} = \bar{V}_H = .0011V$$

$$\text{Hall const.} \equiv R_H = \frac{\bar{V}_H d}{BI} = \frac{(.0011V)(296 \times 10^{-4}cm)}{10^{-3}amps\ 8.5\times10^{-5}w/cm^2} = 393cm^3/coul$$

$$\text{Hall mobility} \equiv \mu_H = \frac{R_H}{\rho} = \frac{393}{2.1} = 187cm^2/v\text{-}sec$$

$$\text{Carrier conc.} \equiv P = \frac{1}{R_H q} = \frac{1}{393(1.6 \times 10^{-19}coul)} = 1.58 \times 10^{16}cm^{-3}$$

where q = charge of an electron.

Carrier type is determined by the following example:

> if V_1 is >0 when B = 0, there is an excess of negative charge near the contact D (ref. Fig. 5), when $B \neq 0$ and $V_2 > V_1$ the charge carrier is a hole since it travels in the direction of conventional current and is deflected by a force, $\vec{F} = q(\vec{V} \times \vec{B})$ thereby increasing the positive potential between B and D.

3.3.4 NORMALIZED MOBILITIES

Hole mobility may be given by the relation:[34]

$$\mu^P = \mu_{min} + \frac{\mu_{max} - \mu_{min}}{1 + \left(\frac{P}{P_{ref}}\right)^{\alpha}}$$

where μ_{min} = 47.7 cm^2/v-sec

μ_{max} = 495 cm^2/v-sec

P_{ref} = 6.3 X 10^{16} cm^{-3}

and

α = .76

The hole mobility normalized to a carrier conc. of P = $10^{16} cm^{-3}$, μ^*, is given by

$$\mu^* = \mu_H \left(\frac{\mu^{10^{16}}}{\mu^P}\right)$$

where μ_H is the hall mobility, and $\mu^{10^{16}}$ = 406 cm^2/v-sec.

3.3.5 GRAIN BOUNDARY DENSITY

The grain boundary density, G.B., is calculated by using the following relation from Brandon[35] :

$$G.B. = \left(\frac{\pi}{2}\right)\left(\frac{P_L}{N}\right) cm/cm^2$$

$$\text{where } P_L = \frac{\text{total number of intersections of grain boundaries with the test line}}{\text{unit length of the test line}}$$

and N = No. of fields of vision.

At 400X the diameter of the field of vision is .043 cm so the circumference, length of the test line, is $(\pi)(.043)$ cm.

A calculation of G.B. for sample D-8-1 follows:

D-8-1

$$P_L = 50 \qquad N = 59$$

$$G.B. = \left(\frac{\pi}{2}\right)\frac{50}{\pi(.043)\ 59} = 9.85\ cm/cm^2$$

A summary of results is listed in Table 4. This table lists data for resistivity, Hall mobility, carrier concentration, hole mobility, normalized hole mobility, and grain boundary density for all 20 specimens.

TABLE X

Resistivity, Hall Mobility, Carrier Concentration, Hole Mobility, Normalized Hole Mobility, and Grain Boundary Density for All 20 Specimens

SAMPLE	$\rho(\Omega\text{-cm})$	$\mu_H(cm^2/v\text{-sec})$	$P \times 10^{16}(cm^{-3})$	$\mu^P(cm^2/v\text{-sec})$	$\frac{\mu^{10^{16}}}{\mu^P}$	$\mu^* cm^2/v\text{-s}$	G.B. (cm/cm^2)
A-1	1.65	201	1.80	370	1.10	221	4.42
B-1	2.45	176	1.44	385	1.05	185	9.06
B-2	3.00	213	.97	408	1.00	213	16.97
B-3	1.85	212	1.58	379	1.07	227	12.41
C-1	1.80	337	1.02	405	1.00	337	2.12
C-2	1.69	198	1.86	368	1.10	218	15.17
C-3	2.20	187	1.51	382	1.06	198	11.86
D-1	2.20	178	1.59	378	1.07	190	9.85
D-2	2.15	177	1.64	376	1.08	191	6.43
D-3	3.10	85	2.36	351	1.16	99	16.16
E-1	1.86	274	1.26	393	1.03	282	0
E-2	1.75	226	1.58	379	1.07	242	.32
F-1	2.30	199	1.36	388	1.05	209	15.23
F-2	2.60	104	2.30	353	1.15	120	20.46
F-3	2.15	242	1.15	399	1.02	247	15.61
G-1	2.05	240	1.26	393	1.03	247	10.00
G-2	2.10	187	1.58	379	1.07	200	12.79
H-1	1.50	380	1.09	402	1.01	384	2.52
H-2	1.55	124	2.00	363	1.12	139	13.25
H-3	1.58	202	1.90	366	1.10	224	18.45

SECTION 3.4

DISCUSSIONS

When hole mobility is plotted as a function of grain boundary density a trend develops. That is, mobility decreased as a function of grain boundary density. This result, based on the electronic features of grain boundaries, is expected. But, it must be noted that while there is a clear trend, there is no clearly defined fundamental relationship evident.

It is noted that for grain boundary densities above all but the lowest values, the great majority of samples have mobility values centered near 200 cm^2/v-sec for raw data (Fig. 6) and 215 cm^2/v-sec for the normalized data (Fig. 7). It is also noted that within this region there is no defined trend between mobility and grain boundary density. Several explanations may be offered to explain this behavior.

It may be proposed that the range of grain boundary density is too small to allow conclusions to be drawn concerning a cause and effect relationship. Perhaps grain boundary densities spanning several orders of magnitude should be examined to determine if a fundamental relationship can be observed.

It may be reasoned that $\sim$200 cm^2/v-sec is the "characteristic" mobility for all but the most defect free samples. Those samples with much lower values are vastly different in the nature of their defect structure. One such difference may be the precipitate density. A precipitate will act as a scattering center and so it stands to reason that a sample with an extremely large precipitate density would have lower mobility values than would be expected based on grain boundary density alone.

Another factor that is likely to affect the mobility as a function of grain boundary density is the grain size distribution and the geometric distribution of grain boundaries on the samples themselves. Distances between grain boundaries ranged from ~100μm to more than a millimeter. There is no clearly defined relationship between mobility and grain sizes nor is there enough sample area available to get a statistically valid idea of the grain size distribution.

Geometric considerations must also be examined. That is to say, what is the actual distribution of grain boundaries on the sample. Grain boundary density does not take into account the uniformity of boundary distribution. It is reasonable to assume that two samples, one with grain boundaries uniformly distributed and the other with nearly all its boundaries concentrated in one portion of the sample, will have different mobility characteristics even if the grain boundary density is the same for both. Since there is no quantitative method to analyze and relate the "boundary distribution" to boundary density, ambiguous results are likely if boundary density is considered the only independent parameter.

SECTION 4

CONCLUSIONS

4.1 Quantitative Analysis of Defects

This work has resulted in a breakthrough in correlating the efficiency of solar cells from UCP Ingot 5848-13C with impurities and imperfections. Of the four types of structural imperfections measured, twin boundary density showed a remarkable effect on cell efficiency (Figures 22 and 27, Table V). It was clearly established that cell efficiency increases with decreasing twin boundary density.

A definite correlation was found between cell efficiency and location of wafers (Figure 30). As the distance from ingot axis increases, the cell efficiency also increases. At the top center of the ingot where higher concentration of impurities and twin densities exist, the cell efficiencies were found to be the lowest. Therefore, it appears that impurities interacting with twin boundaries in this region creates electrically active scattering surfaces which drastically reduce the cell effieciency. This may explain why the cell efficiency increases from a low of 6.2% in the top center of the ingot to a high of 10.7% towards the outer surfaces of the ingot.

Therefore, a modification of UCP casting technique to reduce or eliminate twin boundary surfaces and detrimental impurities will result in a significant increase in cell efficiency.

4.2 Effect of Grain Boundary Density on Carrier Mobility

Mobility measurements were made on twenty SEMIX samples using the van der Pauw technique. Grain boundary density was measured using quantitative microscopy technique. The mobility was found to decrease with increasing grain boundary density (Figures 42 and 43).

SECTION 5

REFERENCES

1. K. V. Ravi, Imperfections and Impurities in Semiconductor Silicon, John Wiley & Sons, New York, 1981.

2. Z. C. Putney and W. F. Regnault, Solar Cells, vol. 1, No. 3, p. 285-292, May, 1980.

3. G. H. Schwuttke, T. F. Ciszek, and A. Kron, "Silicon Ribbon Growth by a Capillary Action Shaping Technique", Final Report, DOE/JPL 954144, IBM Corporation, Hopwell Junction, New York, 1977.

4. B. L. Sapori and A. Baghdadi, Solar Cells, vol. 1, No. 3, p. 237-250, May, 1980.

5. E. E. Underwood, Quantitative Stereology, Addison-Wesley Publishing Company, Reading, Massachusetts, 1970.

6. E. E. Underwood, Metals Handbook, vol. 8, p. 37-47, American Society for Metals, Metals Park, Ohio, 1973.

7. P. A. Iles and D. C. Leung, "Silicon Solar Cell Process Development, Fabrication, and Analysis", 26th Monthly Report, JPL 955089, Optical Coating Laboratory, Inc., City of Industry, California, October, 1981.

8. J. Friedel, Dislocations, p. 290-292, Addison-Wesley Publishing Company, Reading, Massachusetts, 1964.

9. A. D. Kurtz, S. A. Kulin, and B. L. Averbach, Phys. Rev., vol. 101, p. 1285, 1956.

10. H. B. Serreze, J. C. Swartz, G. Entine, and K. V. Ravi, Mater. Res. Bull., vol. 9, p. 1421, 1976.

11. G. H. Schwuttke, T. F. Ciszek, and A. Kran, "Silicon Ribbon Growth by a Capillary Action Shaping Technique", Quarterly Report No. 6, DOE/JPL 954144, IBM Corporation, Hopwell Junction, New York, Dec. 15, 1976.

12. R. Natesh, H. A. Qidwai: "Quantitative Analysis of Defects in Silicon", One - Time Report on Crystal Etching Preparation Technique, DOE/JPL 954977, Materials Research, Inc., Technical Report: MRI - 259, 1978.

13. R. Natesh, J. M. Smith, T. Bruce, H. A. Qidwai: "Quantitative Analysis of Defects in Silicon", Final Report, DOE/JPL 954977, Materials Research, Inc., Technical Report: MRI - 276, 1980.

14. R. Natesh, J M. Smith: "Quantitative Analysis of Defects in Silicon", Monthly Technical Letter Progress Report No. 10, DOE/JPL 954977, Materials Research, Inc., Technical Report: MRI - 270, 1979.

15. R. Natesh, J. M. Smith, H. A. Qidwai, T. Bruce: "Quantitative Analysis of Defects in Silicon", Quarterly Progress Report, DOE/JPL 954977, Materials Research, Inc., Technical Report: MRI - 273, 1979.

16. R. Natesh, M. Plichta, J. M. Smith: "Analysis of Defect Structure in Silicon", Informal Technical Report, DOE/JPL 955676, Materials Research, Inc., Technical Report: MRI - 280, 1980.

17. R. Natesh, M. Mena, J. M. Smith, M. A. Sellani: "Analysis of Defect Structure in Silicon", Characterization of Silicon - on-Ceramics Material, Informal Technical Report, DOE/JPL 955676, Materials Research, Inc., Technical Report: MRI - 281, 1981.

18. R. Natesh, M. Mena, J. M. Smith, M. A. Sellani: "Analysis of Defect Structure in Silicon", Mobil Tyco EFG Samples, Informal Technical Report, DOE/JPL 955676, Materials Research, Inc., Technical Report: MRI - 282, 1981.

19. R. Natesh, M. Mena, M. A. Sellani: "Analysis of Defect Structure in Silicon", Single Crystal and Polycrystalline HEM Material, Informal Technical Report, DOE/JPL 955676, Materials Research, Inc., Technical Report: MRI - 283, 1981.

20. R. Natesh, M. Mena, J. M. Smith, M. A. Sellani: "Analysis of Defect Structure in Silicon", Characterization of HAMCO and EFG Solar Cells, Informal Technical Report DOE/JPL 955676, Materials Research, Inc., Technical Report: MRI - 284, 1981.

21. R. Natesh, M. Mena, J. M. Smith, M. A. Sellani: "Analysis of Defect Structure in Silicon", Characterization of HEM Solar Cell Material, Informal Technical Report, DOE/JPL 955676, Materials Research, Inc., Technical Report: MRI - 285, 1981.

22. R. Natesh, M. Mena, J. M. Smith, M. A. Sellani: "Analysis of Defect Structure in Silicon", Characterization of Mobil Tyco EFG Sheet Material, Informal Technical Report, DOE/JPL 955676, Materials Research, Inc., Technical Report: MRI - 286, 1981.

23. J. Y. M. Lee and I. C. Cheng, J. Appl. Phys., vol. 53, p. 490, 1982.

24. R. A. Smith, "Semiconductors," Cambridge University Press, London, 1959.

25. E. H. Putley, " The Hall Effect and Semiconductor Physics", Butterworth and Co. (Publishers), Ltd., London, 1960: Dover Publications, Inc., New York, 1968.

26. A. C. Beer, " Galvanomagnetic Effects in Semiconductors" , Academic Press, Inc., New York, 1963.

27. L. P. Hunter, Phys. Rev., vol. 94, p. 1157 - 1160, 1954.

28. L. P. Hunter, E. Hulbregtse, and R. Anderson, Phys. Rev., vol. 91, p. 1315 - 1320, 1953.

29. G. L. Pearson and J. Bardeen, Phys. Rev., vol. 75, p. 865 - 883, 1949.

30. K. Pigon, J. Appl. Phys., vol. 32, p. 2369 - 2371, 1961.

31. R. L. Petritz, Phys. Rev., vol. 110, p. 1254 - 1262, 1958.

32. R. Natesh, T. Guyer, and G. B. Stringfellow, " Analysis of Defect Structure in Silicon: Characterization of Samples from UCP Ingot 5848 - 13C ", Interim Report, Technical Report: MRI - 290, Materials Research, Inc., August, 1982 .

33. L. J. van der Pauw, Phillips Research Reports, vol. 13, p. 1 , 1958.

34. R. S. Muller and T. I. Kamins, "Device Electronics for Integrated Circuits," (New York: Wiley 1977) p. 26.

35. D. G. Brandon, "Modern Techniques in Metallography," (Princeton, N. J. : D. van Nostrand Company 1966) p. 241.

POSITION OF WAFERS FROM UCP INGOT 5848-13C

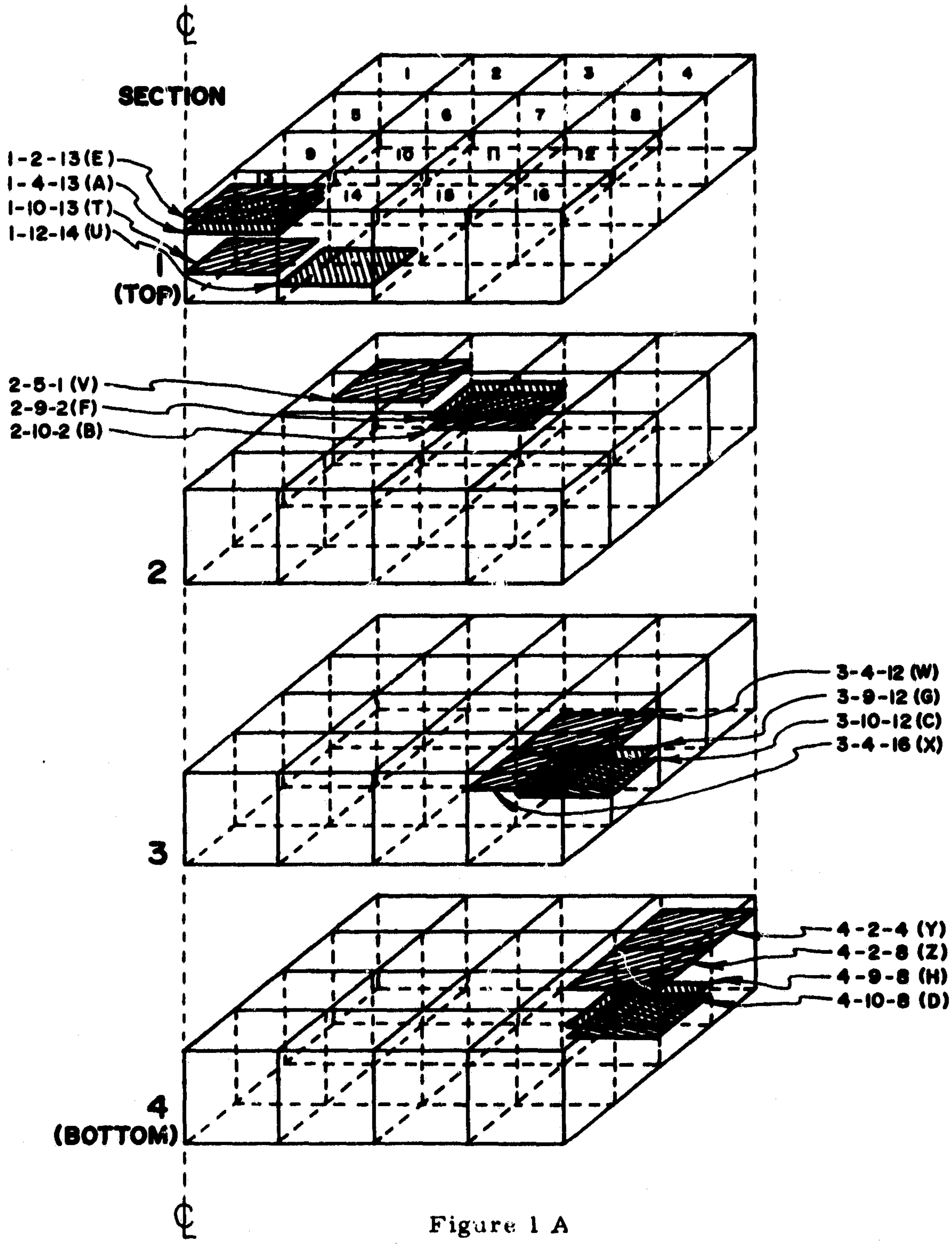

Figure 1 A

RELATIVE POSITIONS OF THE MEASURED FIELDS ON THE SEMIX WAFERS

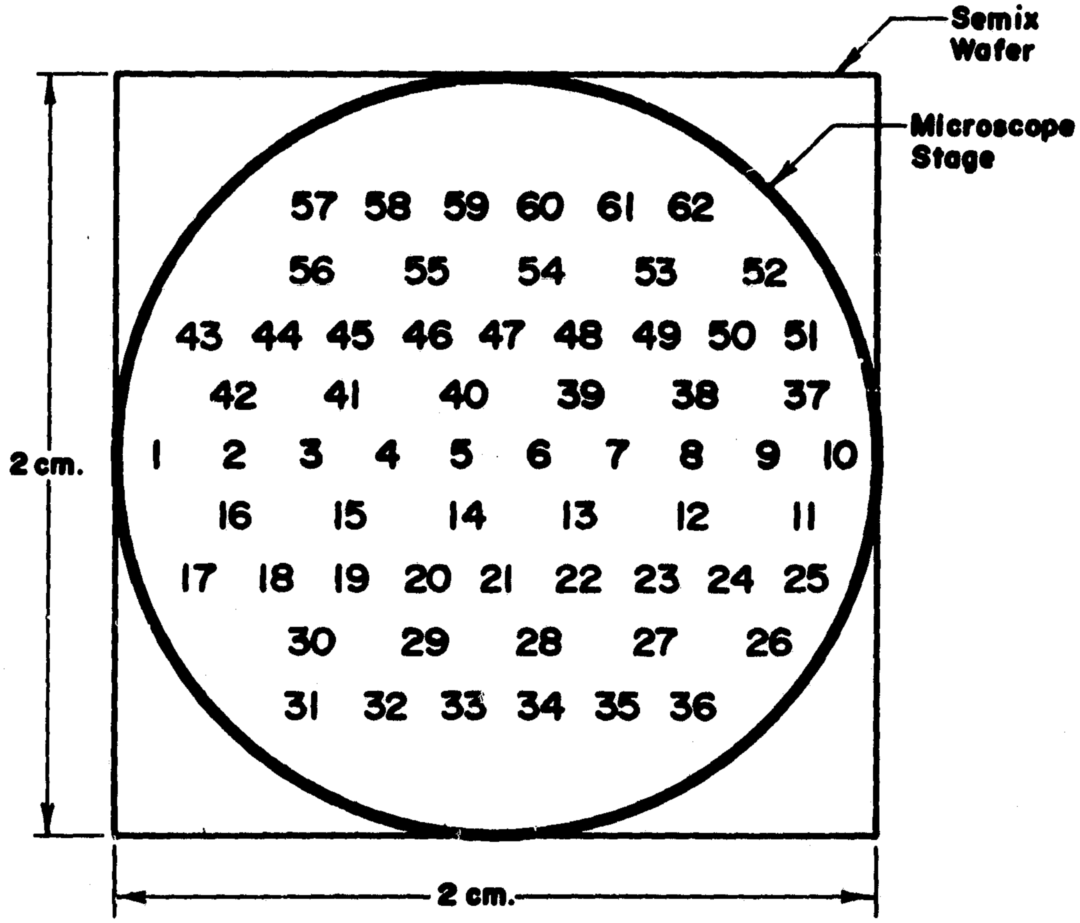

Figure 1 B

Fig. 2 Region Showing High Twin Density in Semix A-13(50X)

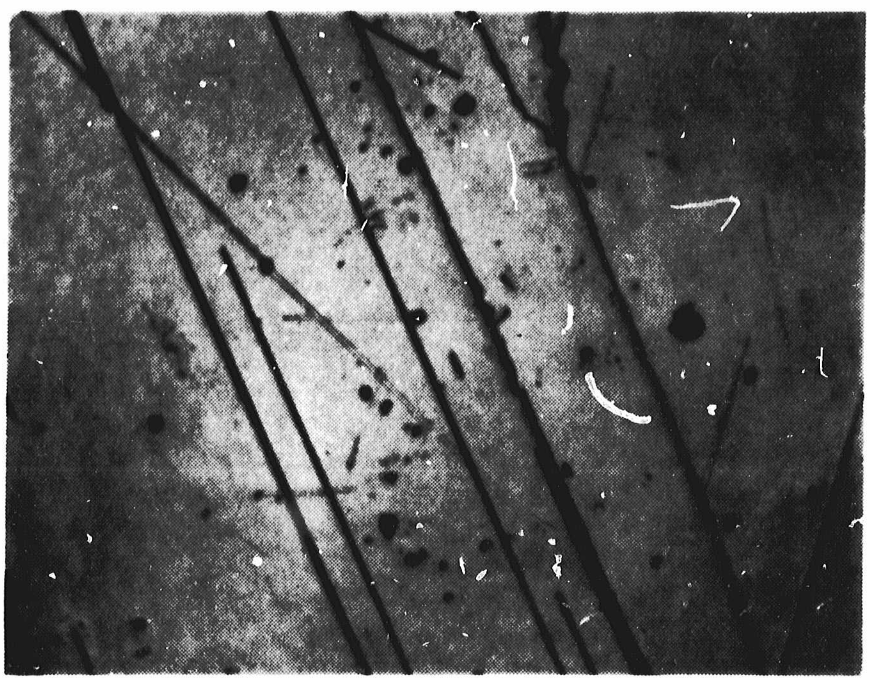

Fig. 3 Region Showing a Large Number of Precipitates in Semix A-13(50X)

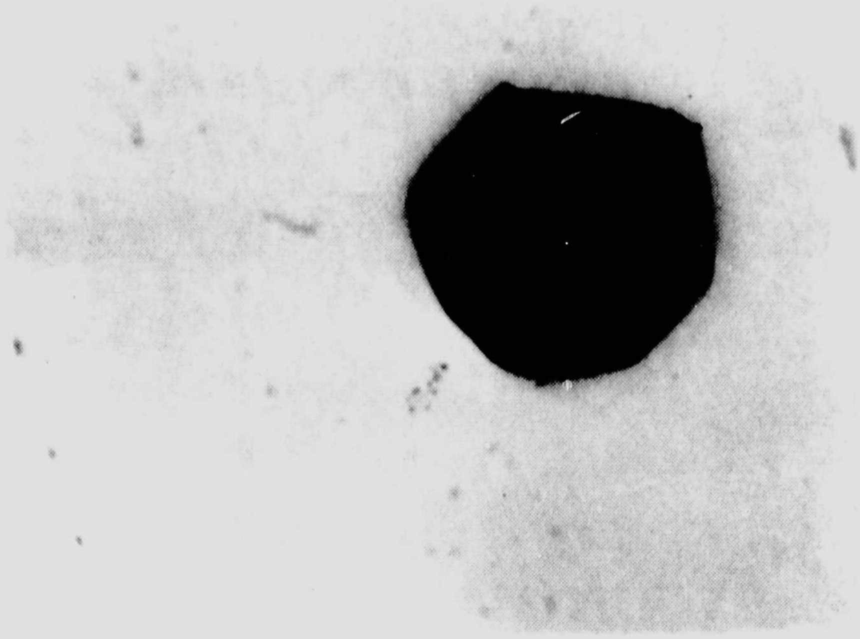

Fig. 4 Large and Small Precipitates in Semix B-2 (1330X)

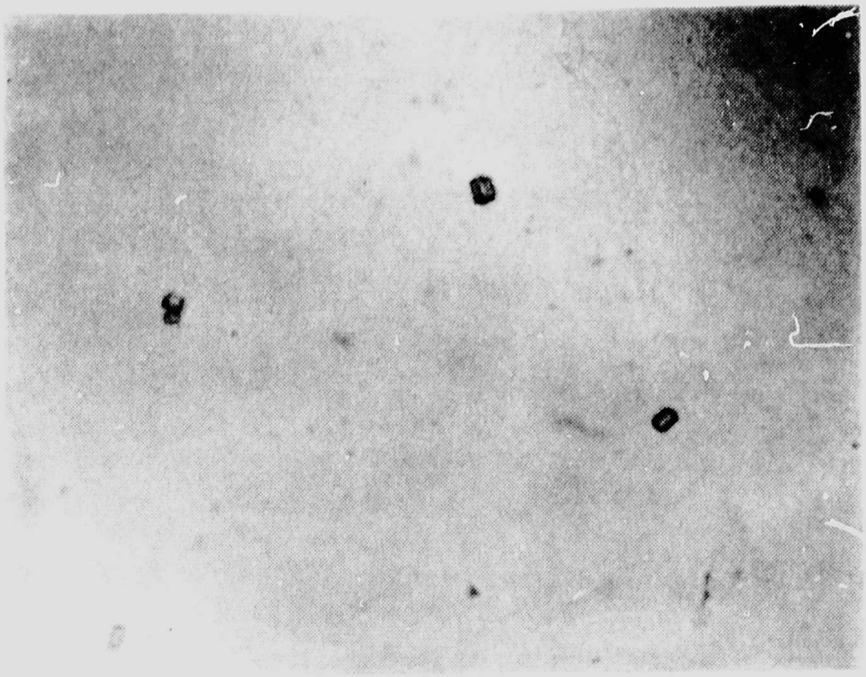

Fig. 5 Precipitates in Semix B-2 (530X)

Fig. 6 Many Grains and Grain Boundaries in Semix C-12 (50X)

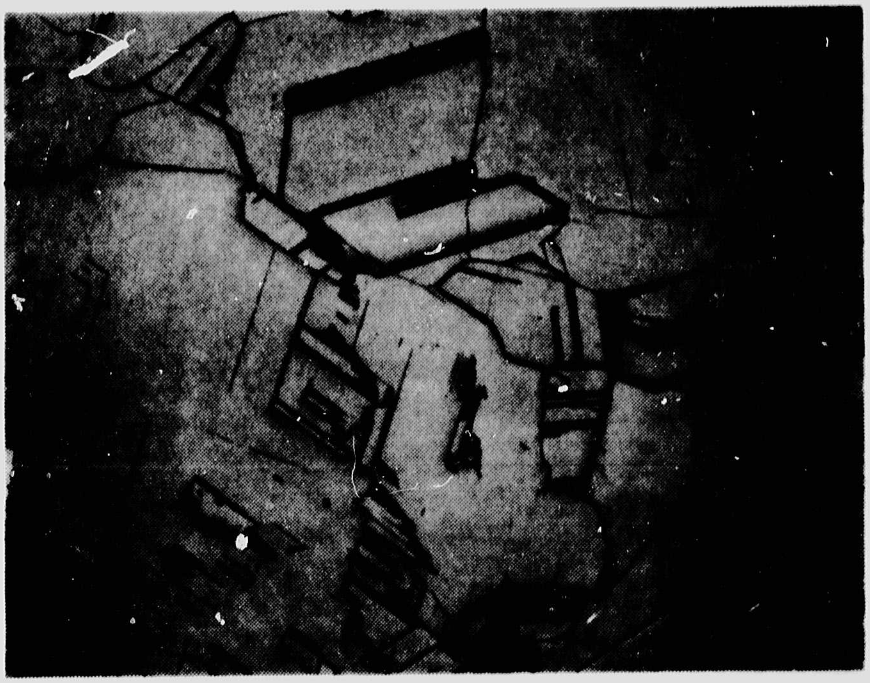

Fig. 7 Twin and Grain Boundaries in Semix C-12 (50X)

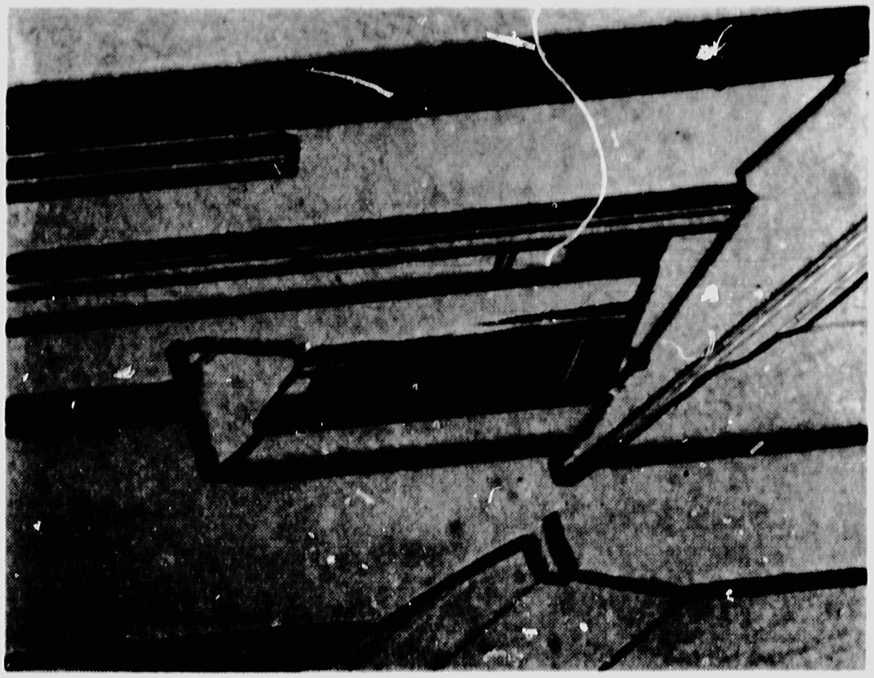

Fig. 8 Large Number of Small Twin Boundaries in Semix D-8. These are not Typical Regions (66X). Region marked "U".

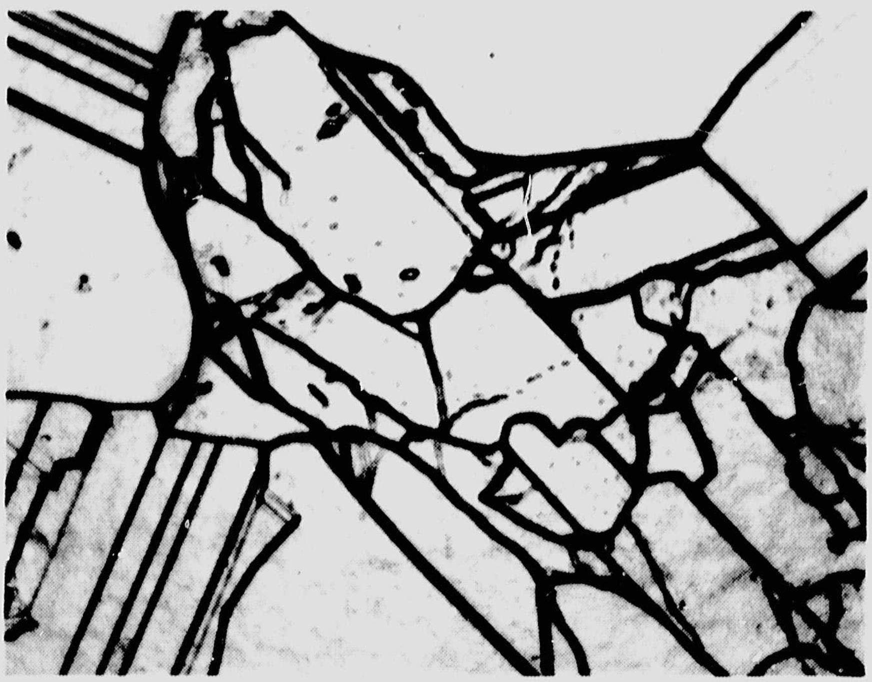

Fig. 9 Many Twin and Grain Boundary Region in Semix D-8 (66X)

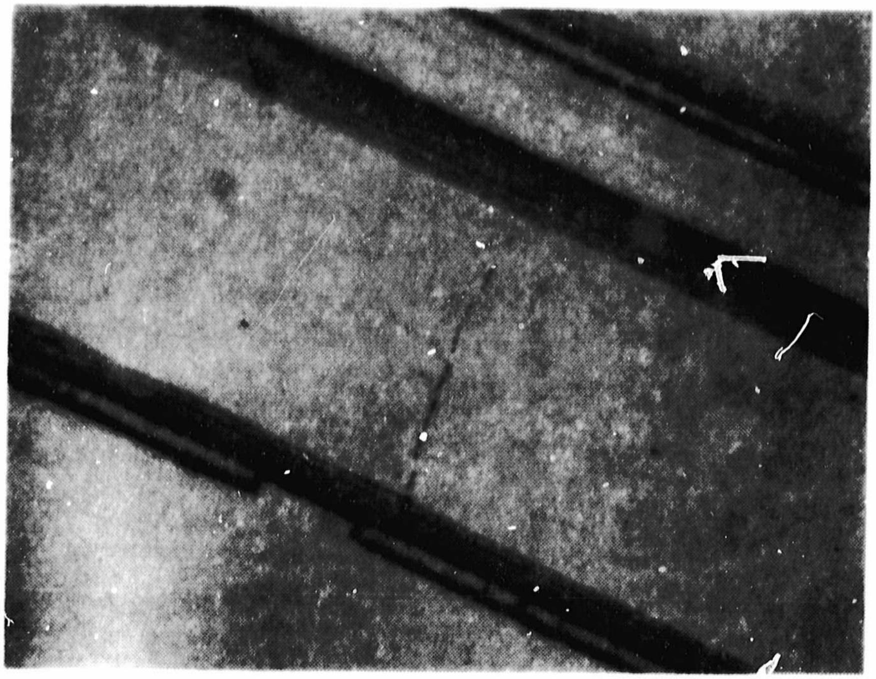

Fig. 10 Dislocations Piled up Between Twins due to Localized Strain in Semix D-8 (600X)

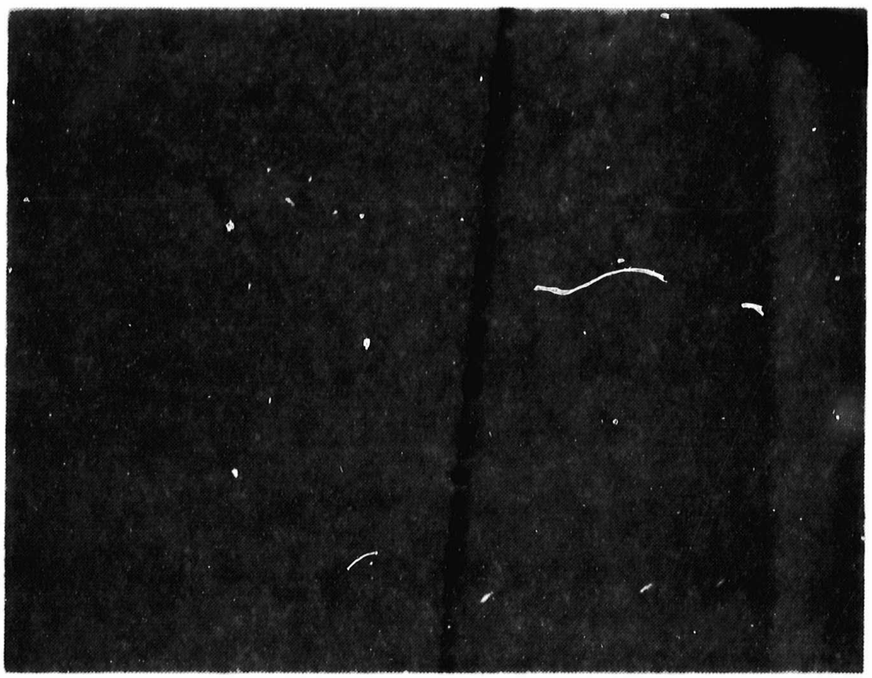

Fig. 11 Dislocations Interacting with a Twin Boundary in Semix D-8 (1500X)

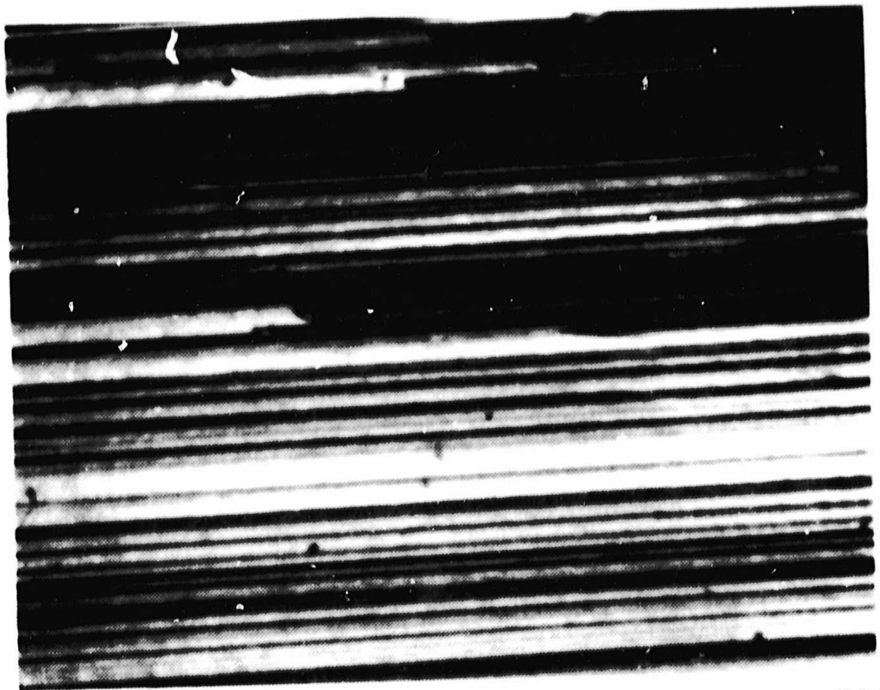

Fig. 12 High Twin Density in Semix E-13 (50X)

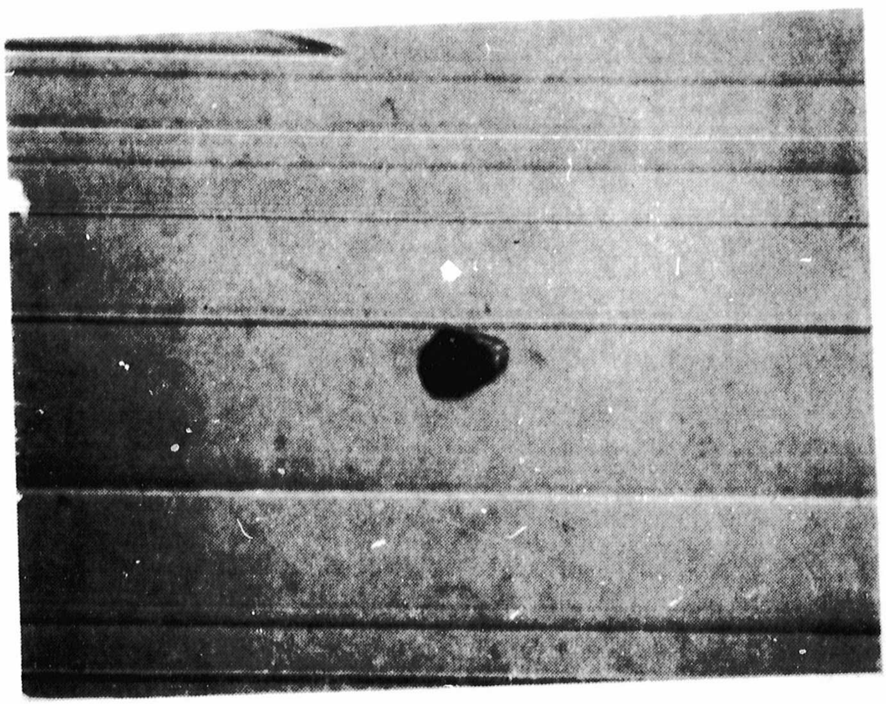

Fig. 13 Large Precipitate Particle Between Twins in Semix E-13 (530X)

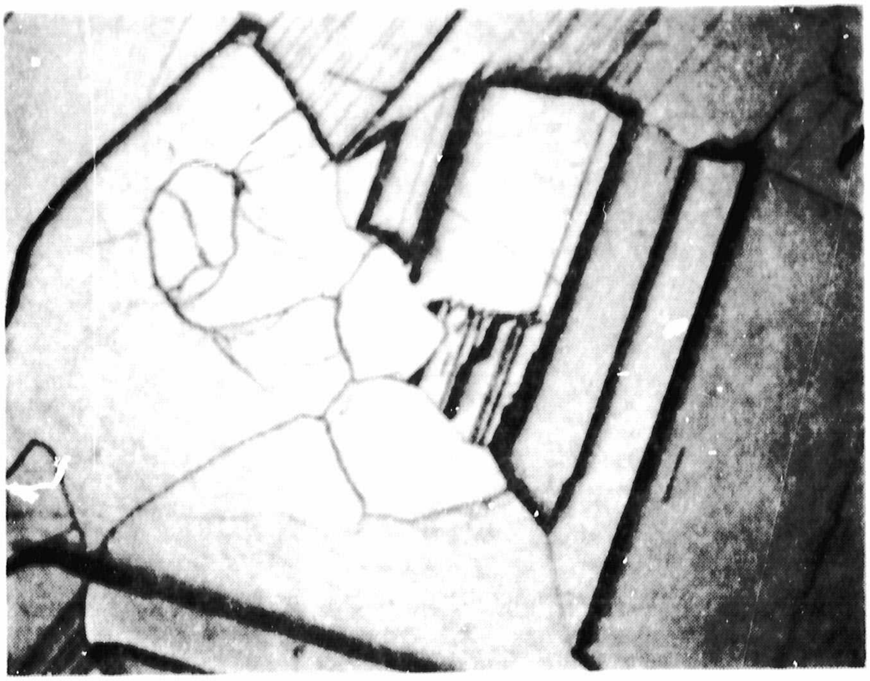

Fig. 14 Twin and Grain Boundary Structure in Semix F-2 (50X)

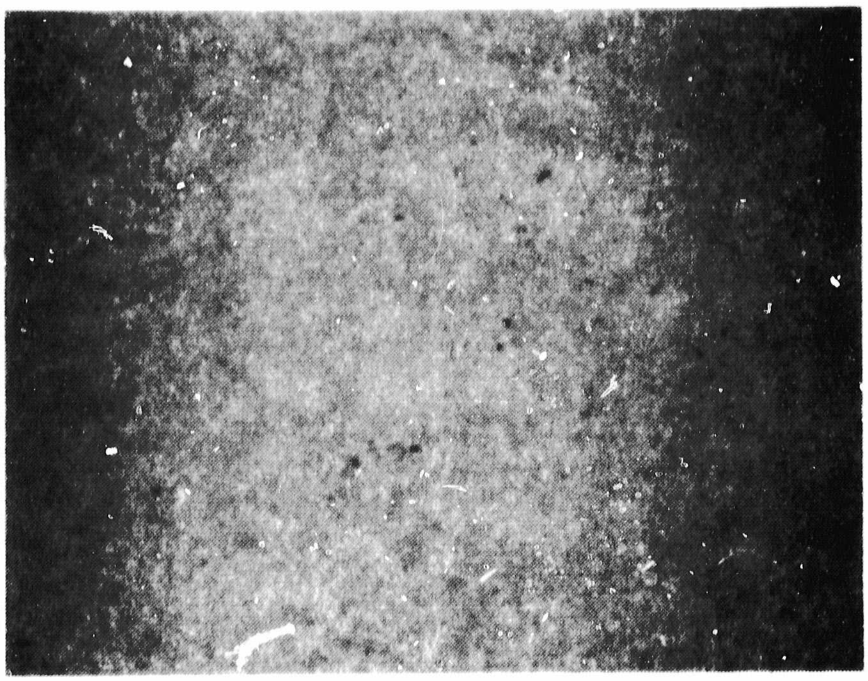

Fig. 15 Small Precipitate Particles in Semix F-2 (200X)

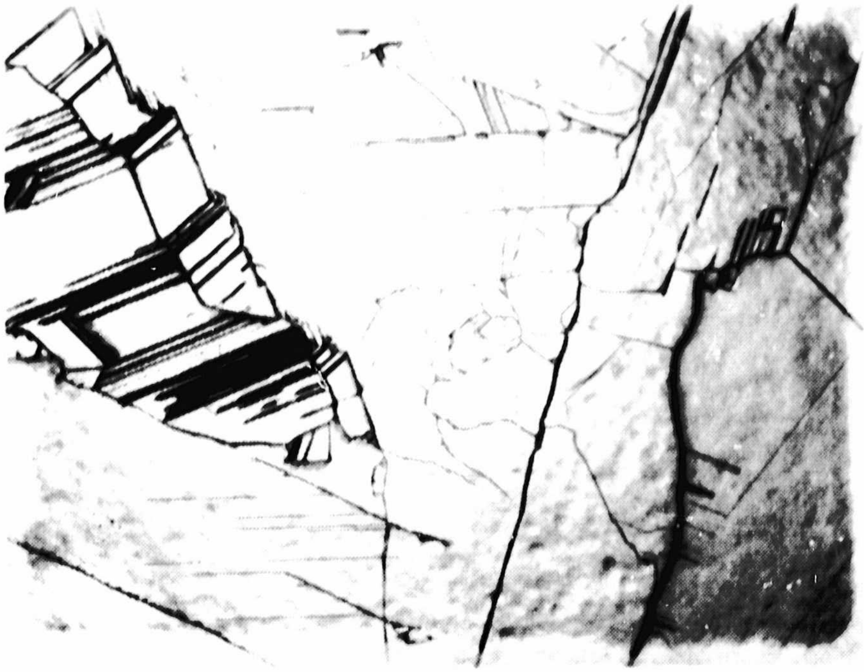

Fig. 16 Twins and Grain Boundaries in Semix G-12 (50X)

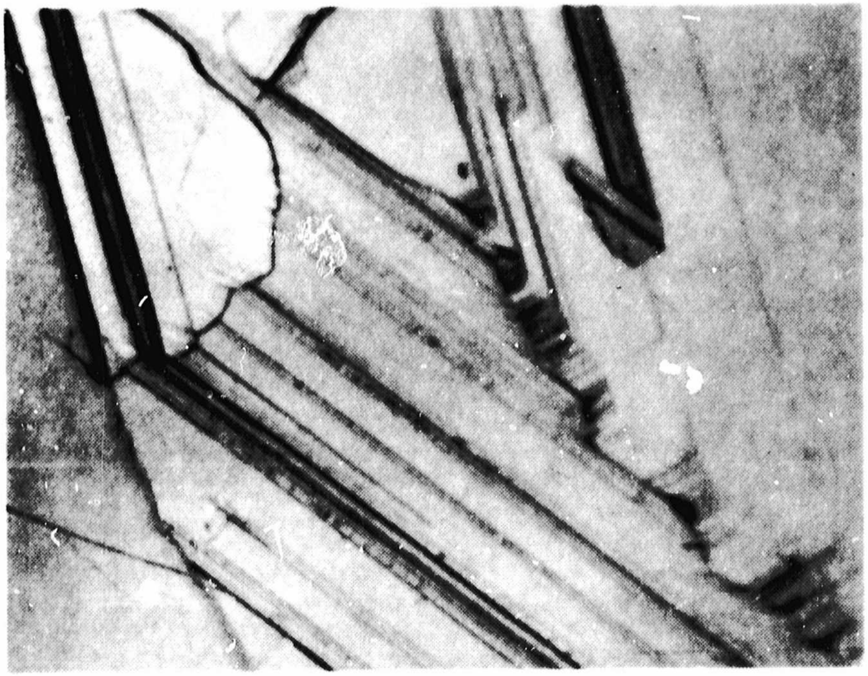

Fig. 17 Region of High Twin Density in Semix G-12 (100X)

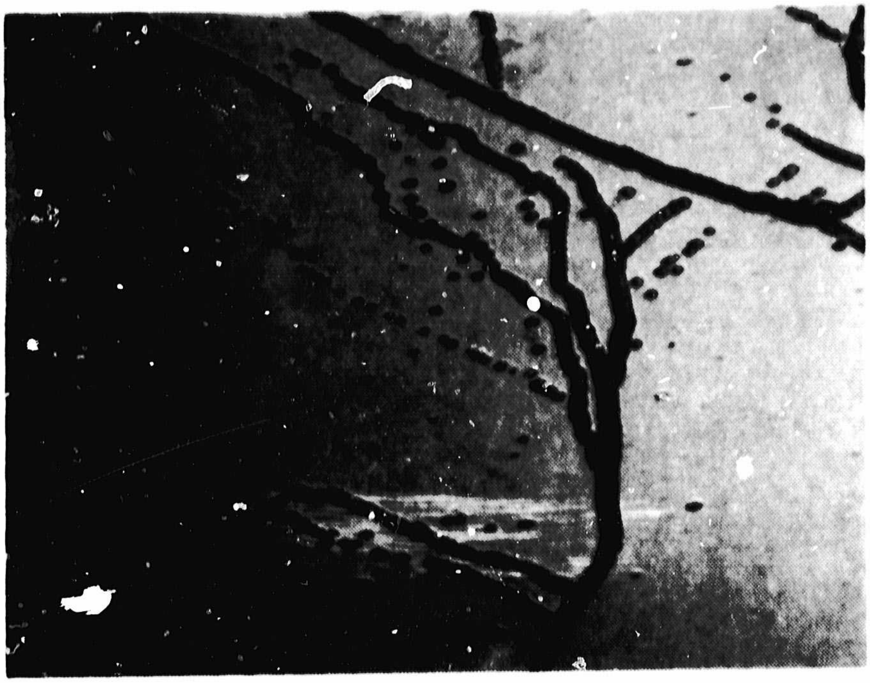

Fig. 18 Dislocation pile-ups in Semix H-8 (1330X)

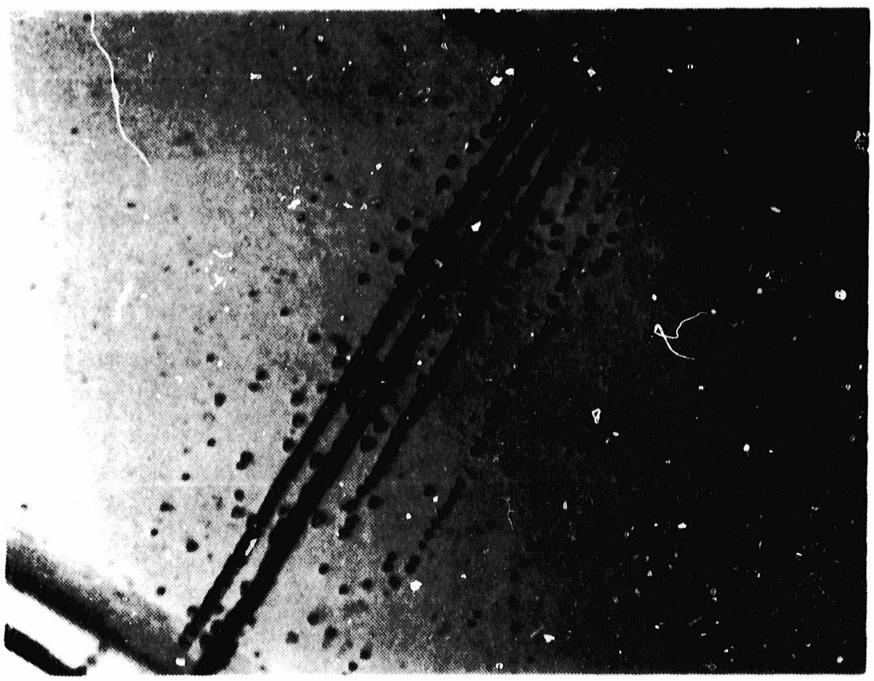

Fig. 19 High Dislocation Density Between Twins in Semix D-8 (1330X)

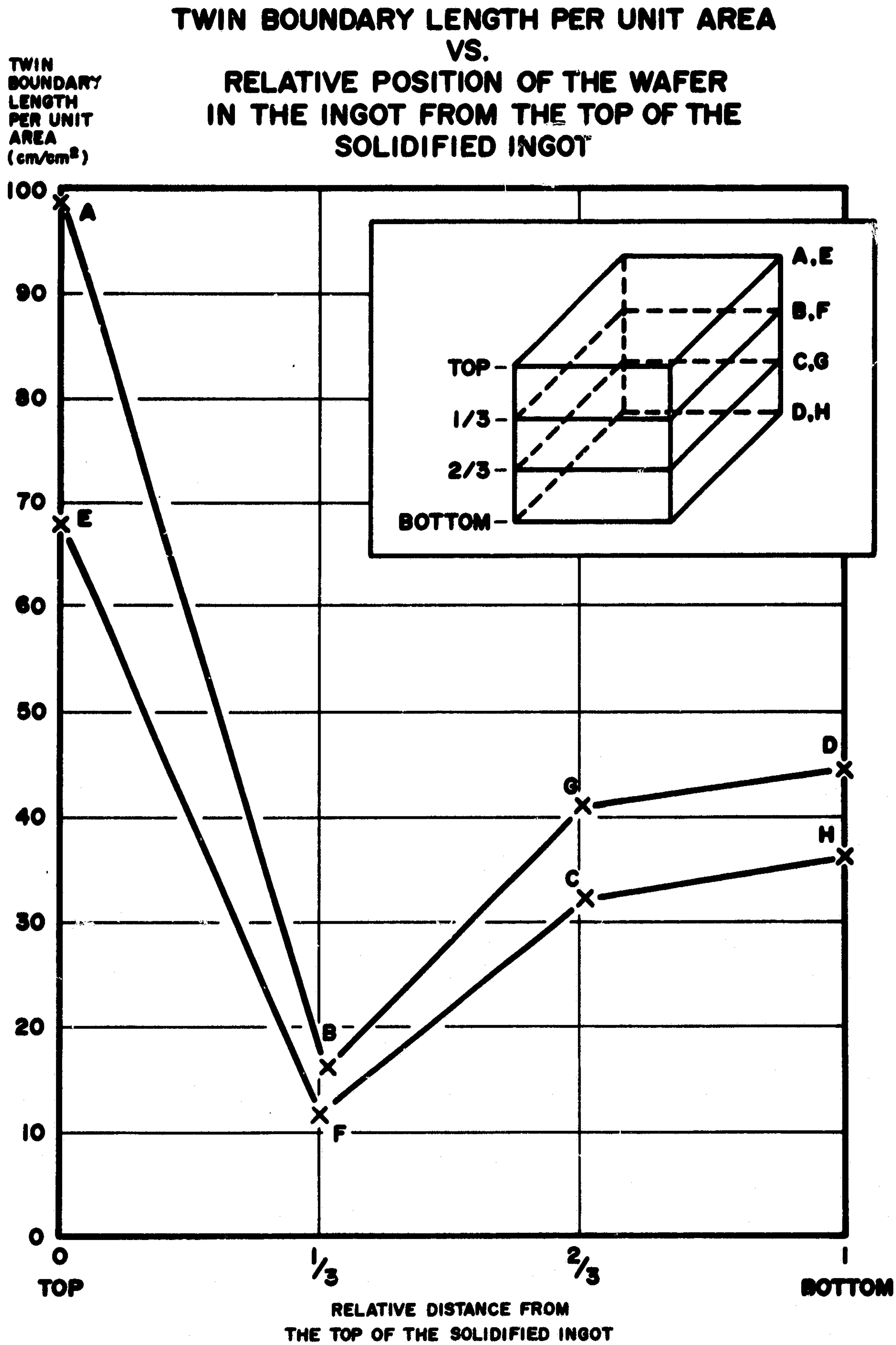
TWIN BOUNDARY LENGTH PER UNIT AREA
VS.
RELATIVE POSITION OF THE WAFER
IN THE INGOT FROM THE TOP OF THE
SOLIDIFIED INGOT
TWIN BOUNDARY LENGTH PER UNIT AREA (cm/cm²)
100
90
80
70
60
50
40
30
20
10
0
A
B
C
D
E
F
G
H
A,E
B,F
C,G
D,H
TOP
1/3
2/3
BOTTOM
0
TOP
1/3
2/3
1
BOTTOM
RELATIVE DISTANCE FROM
THE TOP OF THE SOLIDIFIED INGOT

Figure 20

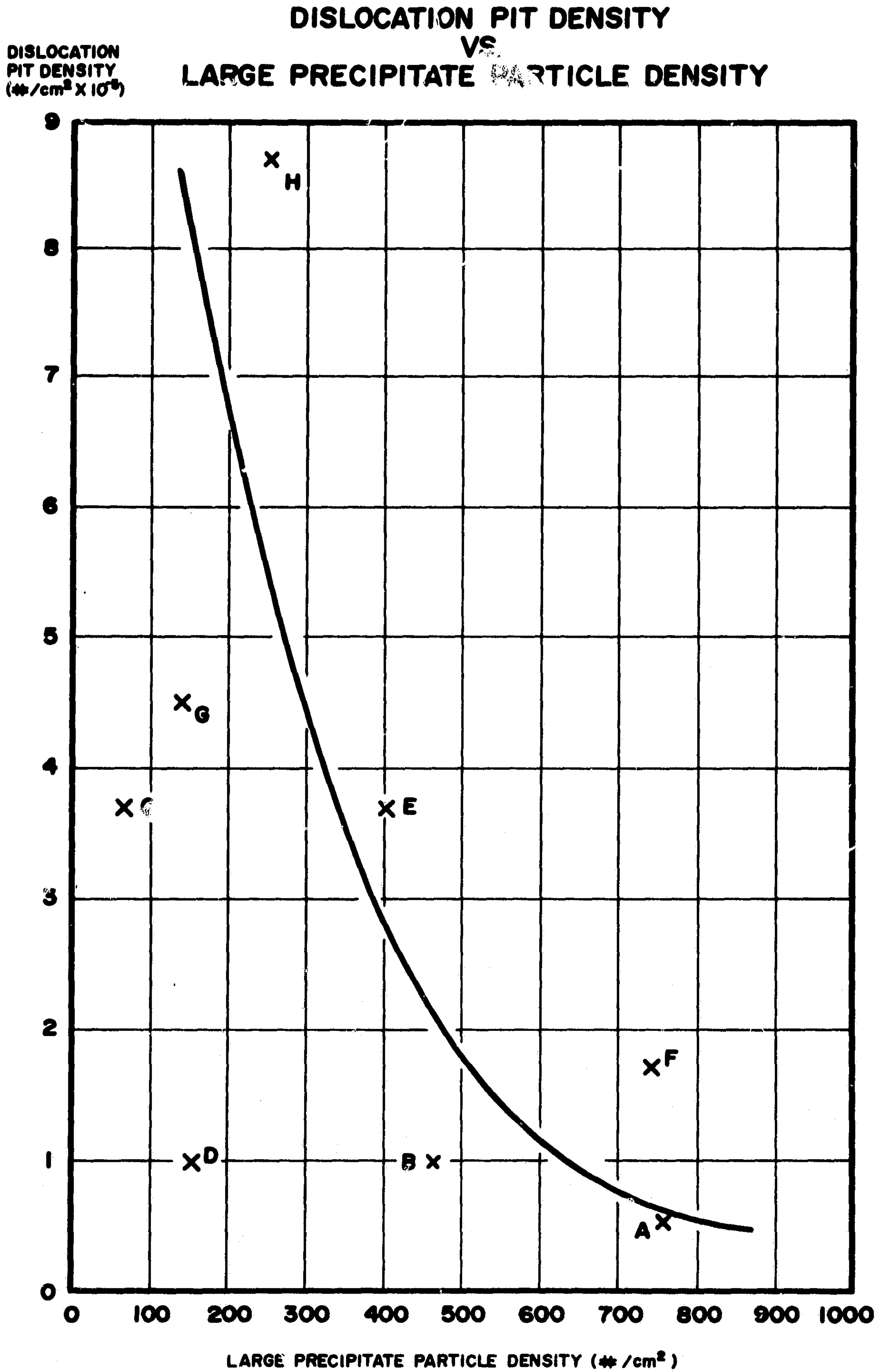
DISLOCATION PIT DENSITY
VS.
LARGE PRECIPITATE PARTICLE DENSITY
DISLOCATION PIT DENSITY (#/cm² X 10⁻⁵)
0
1
2
3
4
5
6
7
8
9
0
100
200
300
400
500
600
700
800
900
1000
H
G
E
F
D
B
A
LARGE PRECIPITATE PARTICLE DENSITY (#/cm²)

Figure 21

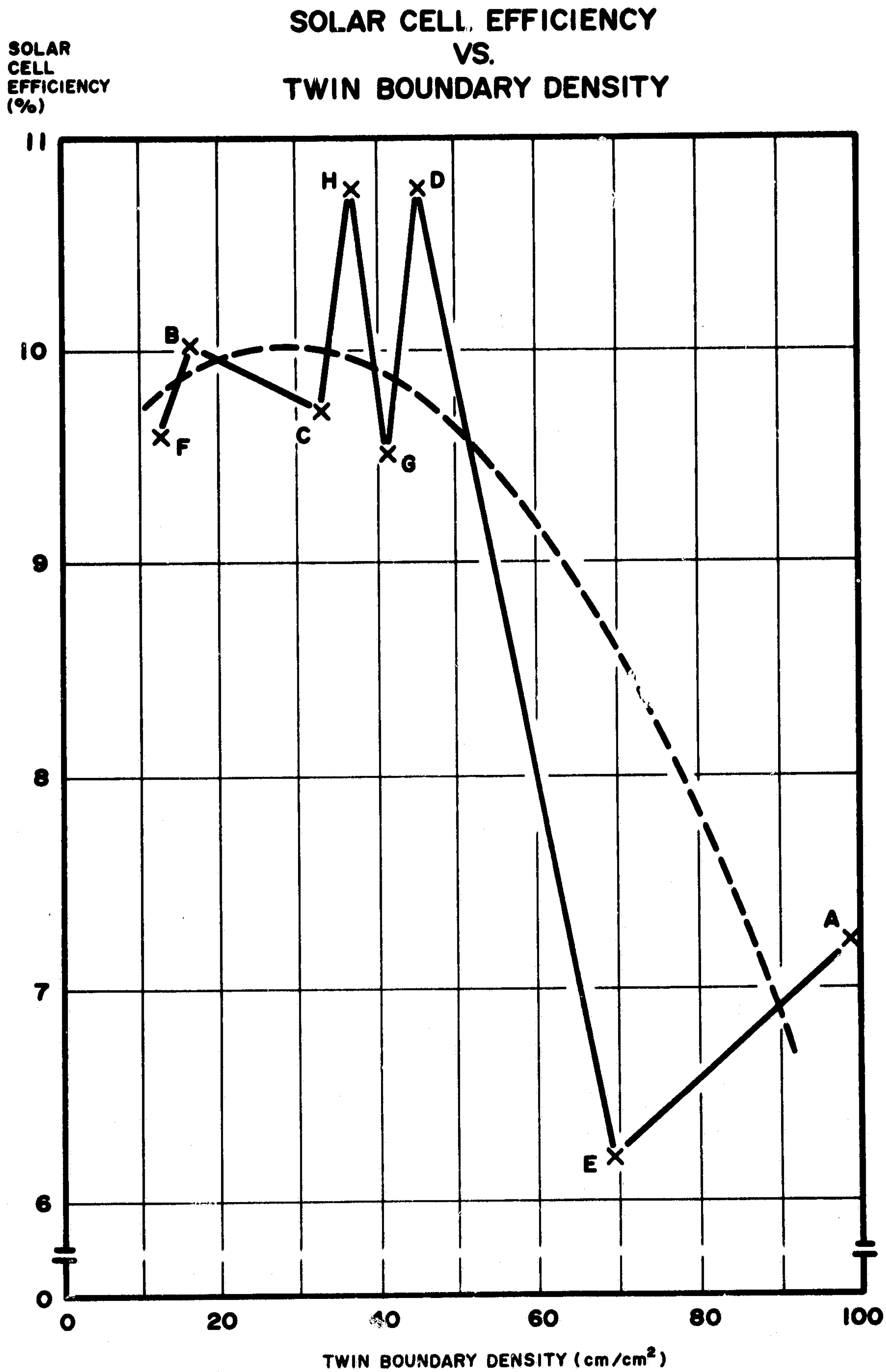
SOLAR CELL EFFICIENCY
VS.
TWIN BOUNDARY DENSITY
SOLAR
CELL
EFFICIENCY
(%)
11
10
9
8
7
6
0
H
D
B
F
C
G
A
E
0
20
40
60
80
100
TWIN BOUNDARY DENSITY (cm/cm²)

Figure 22

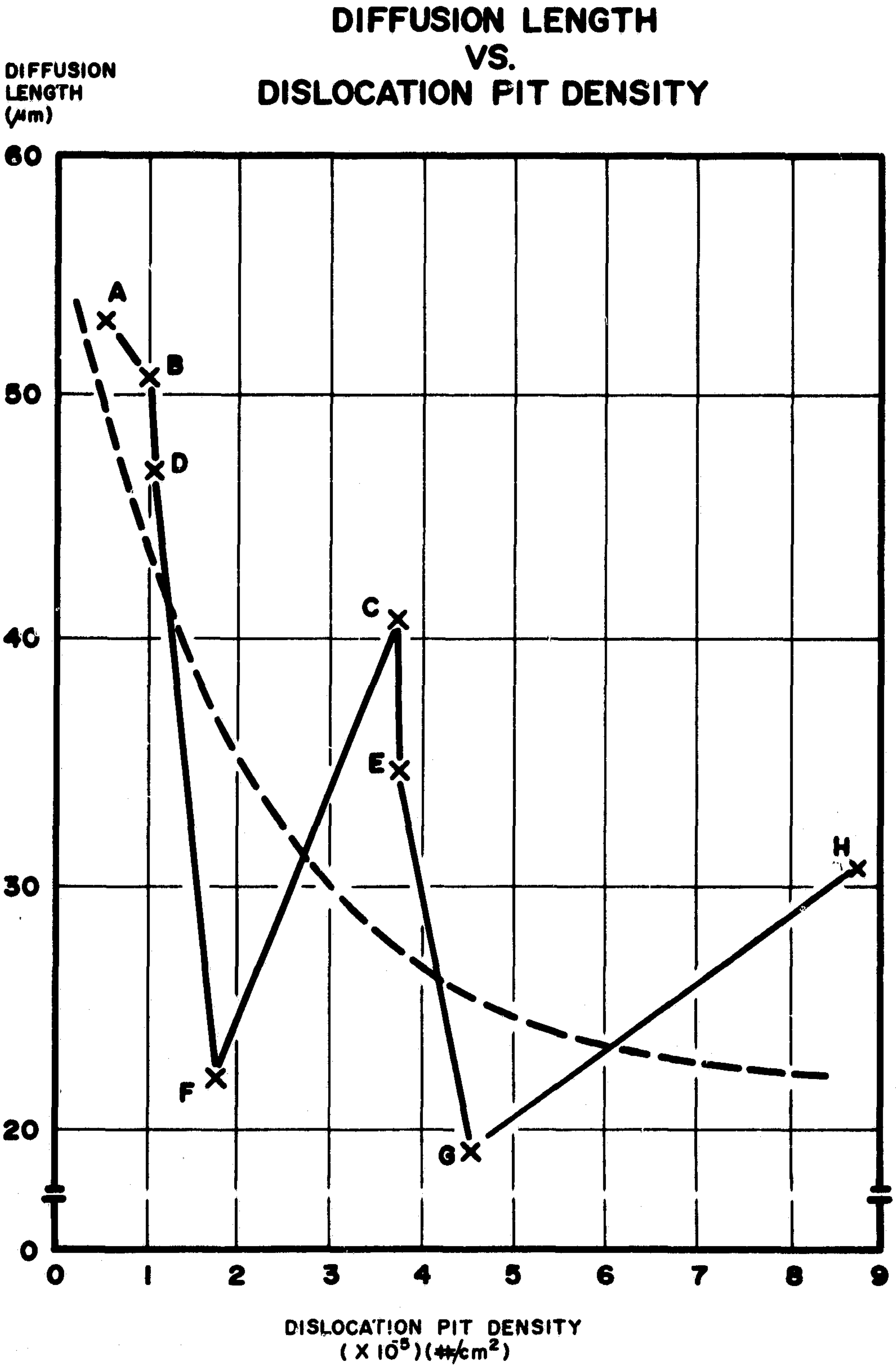
DIFFUSION LENGTH
VS.
DISLOCATION PIT DENSITY
DIFFUSION LENGTH (μm)
60
50
40
30
20
0
A
B
D
C
E
F
G
H
0
1
2
3
4
5
6
7
8
9
DISLOCATION PIT DENSITY
(X 10⁵)(#/cm²)

Figure 23

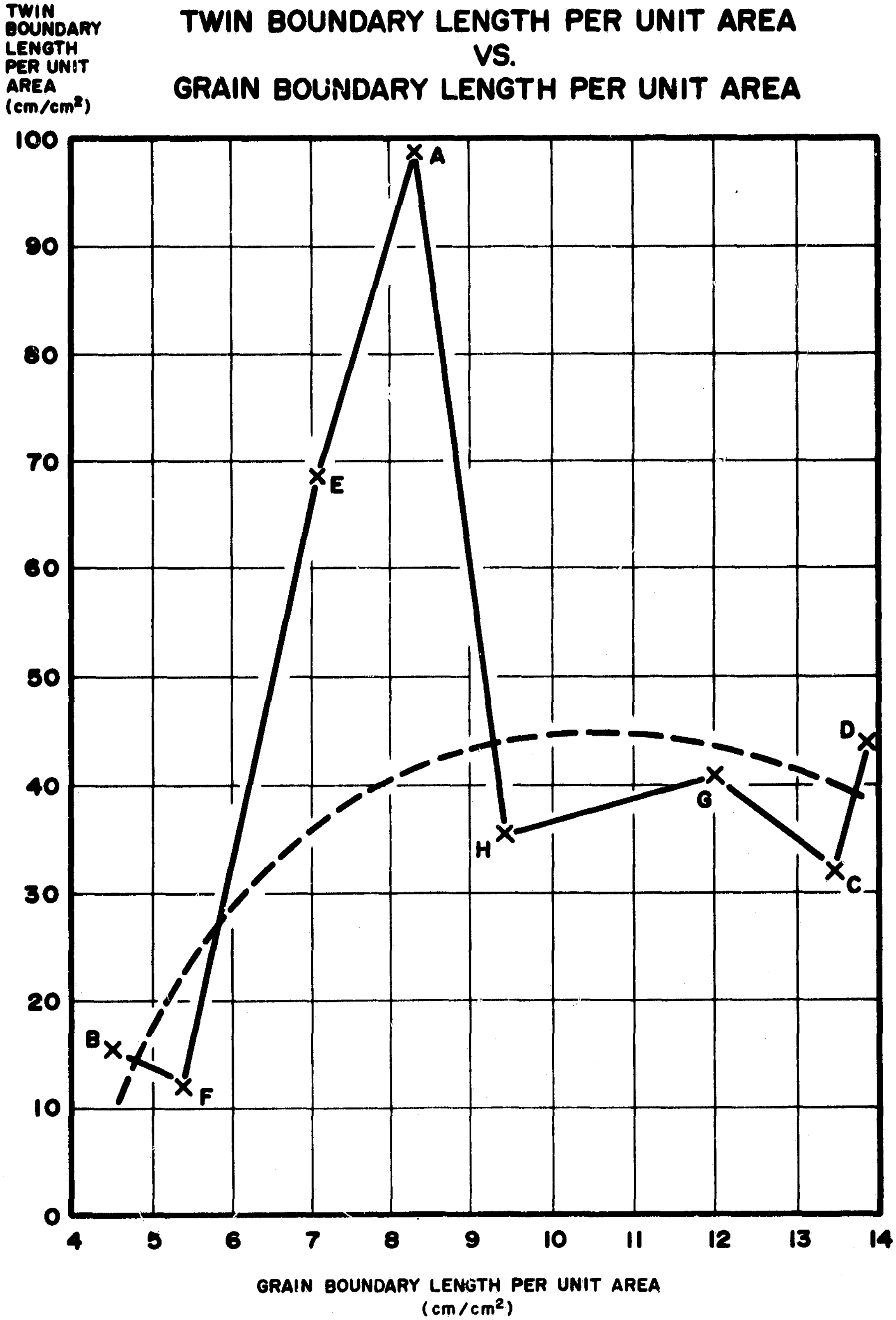
TWIN BOUNDARY LENGTH PER UNIT AREA (cm/cm²)
TWIN BOUNDARY LENGTH PER UNIT AREA
VS.
GRAIN BOUNDARY LENGTH PER UNIT AREA
100
90
80
70
60
50
40
30
20
10
0
A
E
H
G
D
C
B
F
4
5
6
7
8
9
10
11
12
13
14
GRAIN BOUNDARY LENGTH PER UNIT AREA
(cm/cm²)

Figure 24

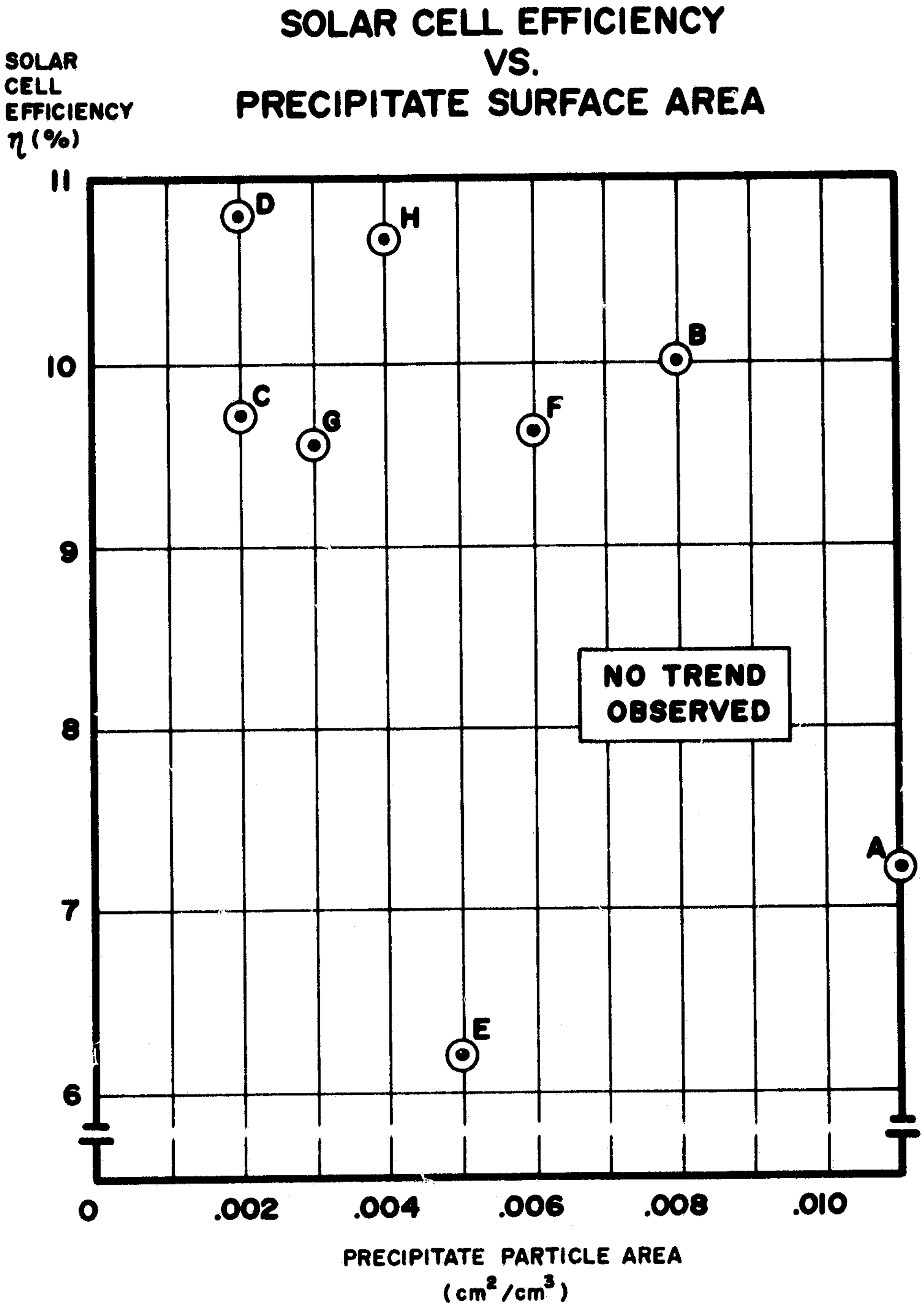
SOLAR CELL EFFICIENCY
VS.
PRECIPITATE SURFACE AREA
SOLAR
CELL
EFFICIENCY
η (%)
11
10
9
8
7
6
D
H
B
C
G
F
NO TREND
OBSERVED
A
E
0
.002
.004
.006
.008
.010
PRECIPITATE PARTICLE AREA
(cm²/cm³)

Figure 25

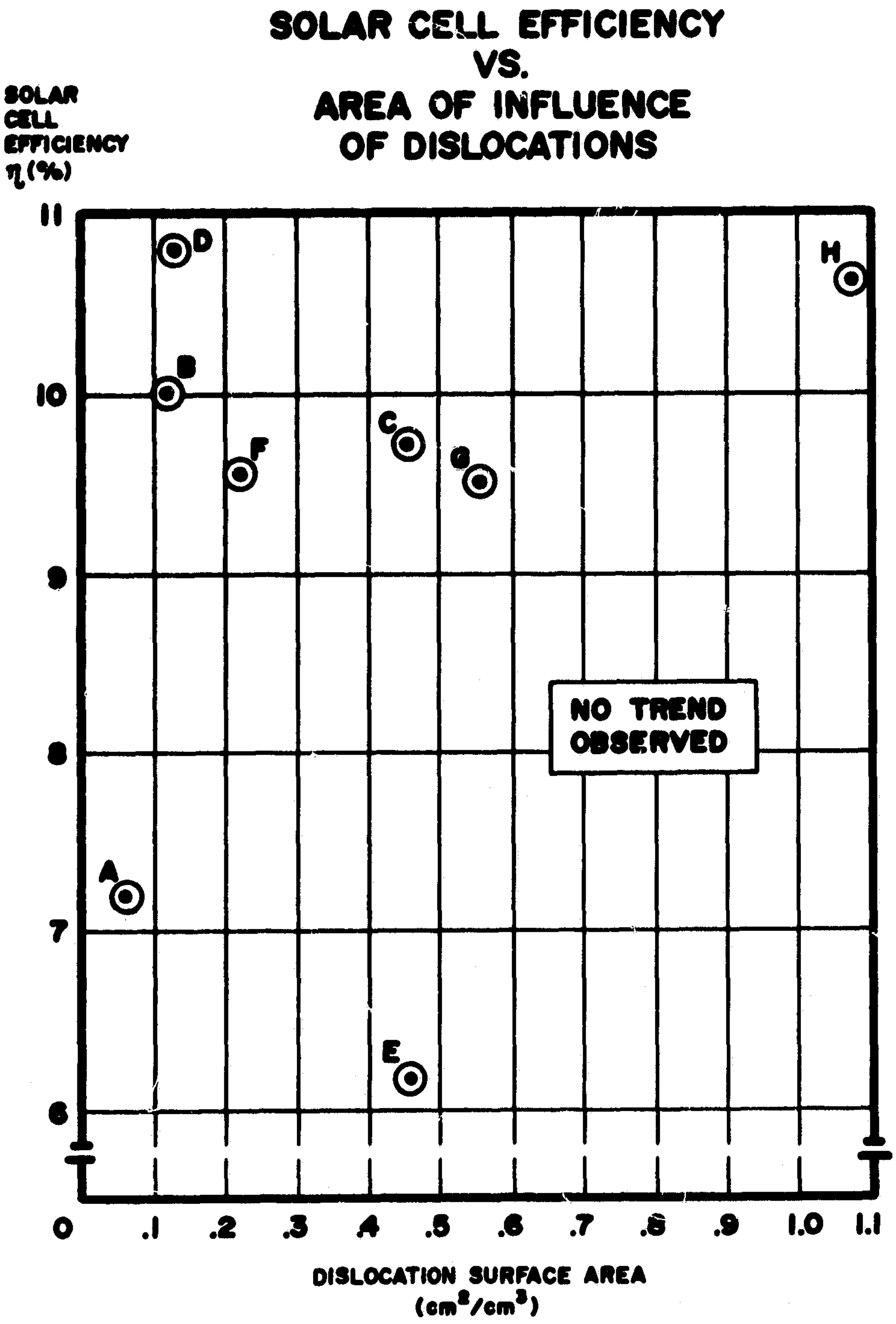
SOLAR CELL EFFICIENCY
VS.
AREA OF INFLUENCE
OF DISLOCATIONS
SOLAR
CELL
EFFICIENCY
η (%)
11
10
9
8
7
6
D
B
F
C
G
H
A
E
NO TREND
OBSERVED
0
.1
.2
.3
.4
.5
.6
.7
.8
.9
1.0
1.1
DISLOCATION SURFACE AREA
(cm²/cm³)

Figure 26

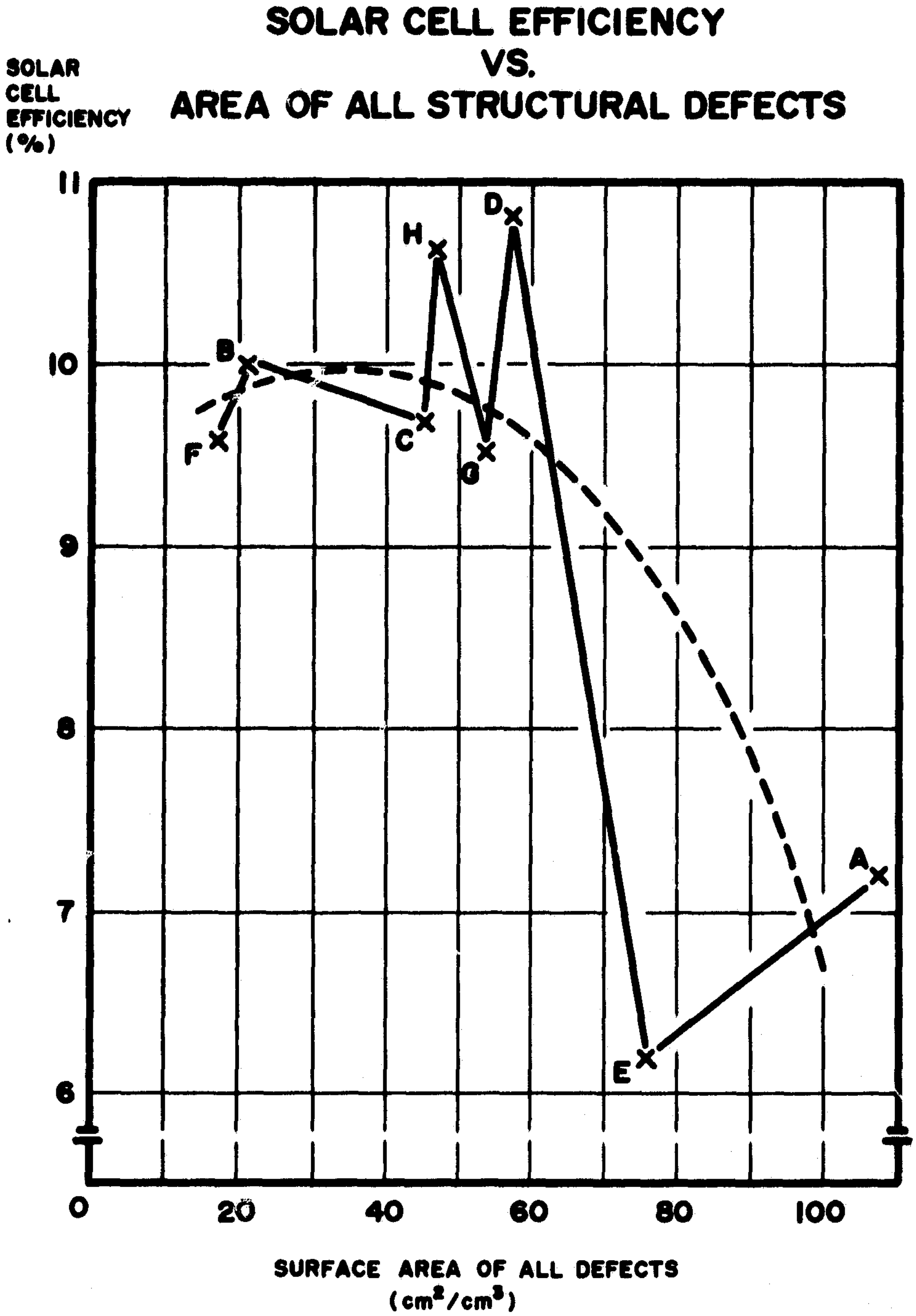
SOLAR CELL EFFICIENCY
VS.
AREA OF ALL STRUCTURAL DEFECTS
SOLAR CELL EFFICIENCY (%)
11
10
9
8
7
6
0
20
40
60
80
100
A
B
C
D
E
F
G
H
SURFACE AREA OF ALL DEFECTS (cm^2/cm^3)

Figure 27

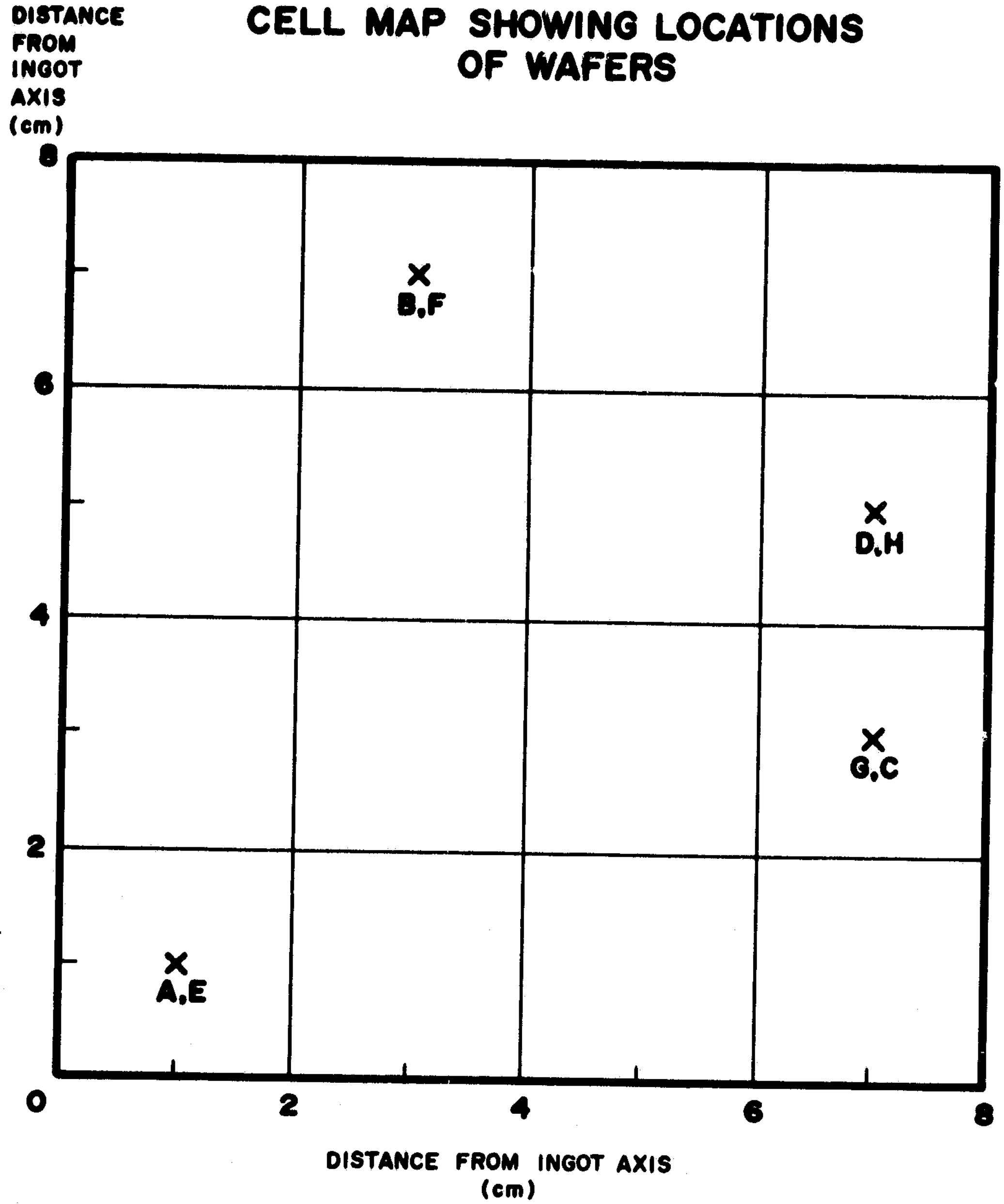
CELL MAP SHOWING LOCATIONS OF WAFERS
DISTANCE FROM INGOT AXIS (cm)
0
2
4
6
8
B,F
D,H
G,C
A,E
DISTANCE FROM INGOT AXIS (cm)

Figure 28

ORIGINAL PAGE IS
OF POOR QUALITY

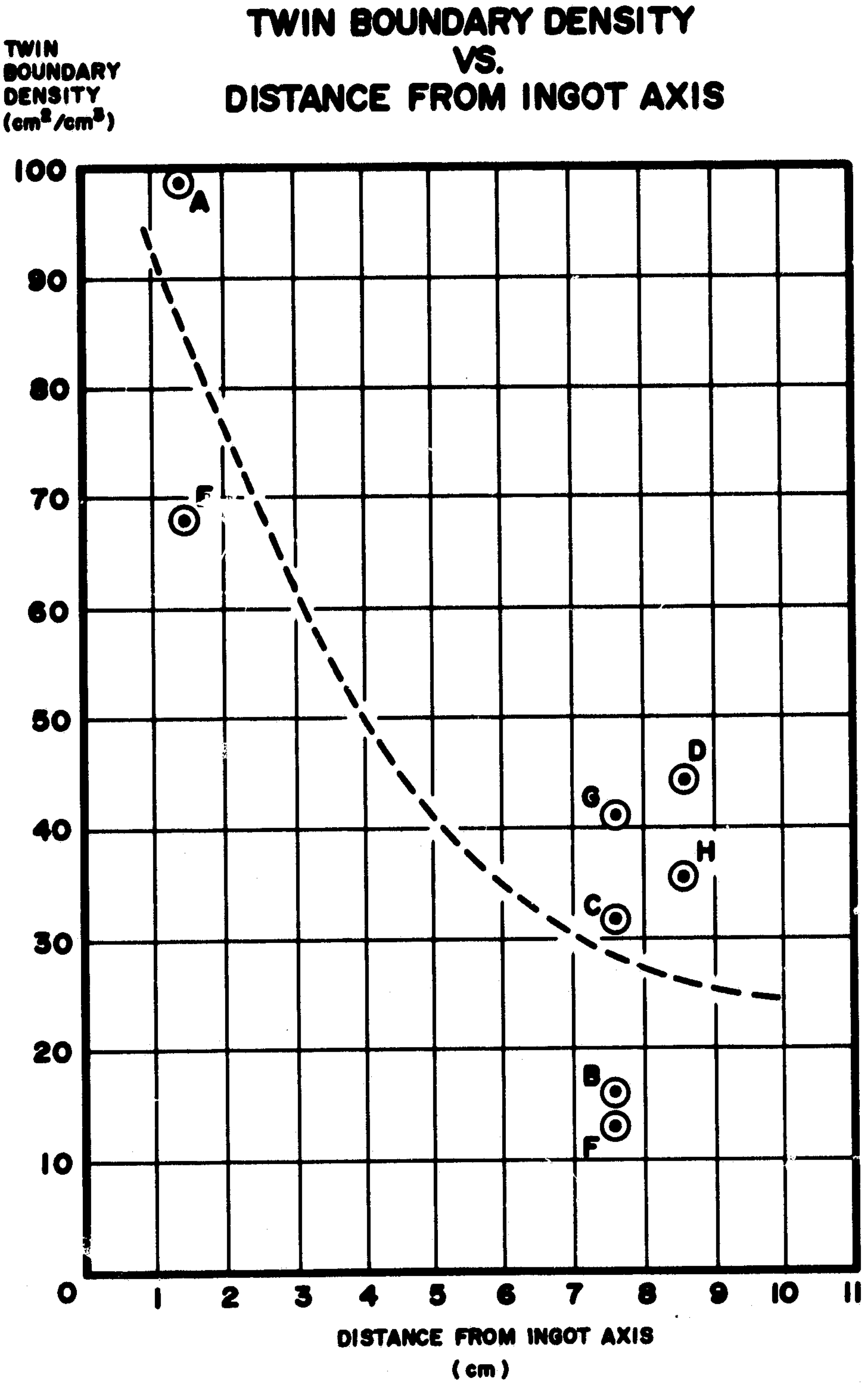

Figure 29

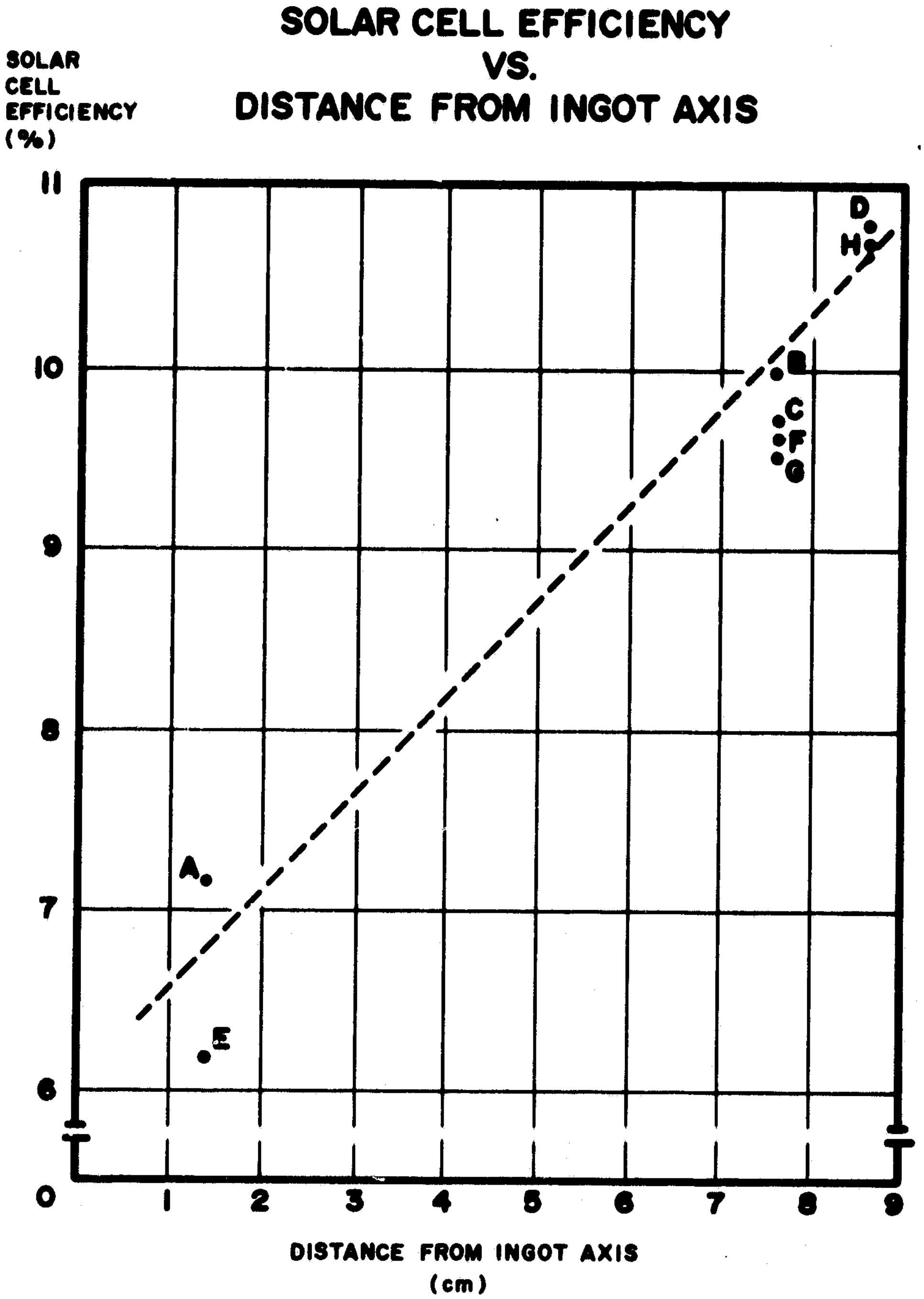
SOLAR CELL EFFICIENCY
VS.
DISTANCE FROM INGOT AXIS
SOLAR CELL EFFICIENCY (%)
11
10
9
8
7
6
0
1
2
3
4
5
6
7
8
9
A
B
C
D
E
F
G
H
DISTANCE FROM INGOT AXIS (cm)

Figure 30

SEGREGATION OF IMPURITIES IN CAST SILICON

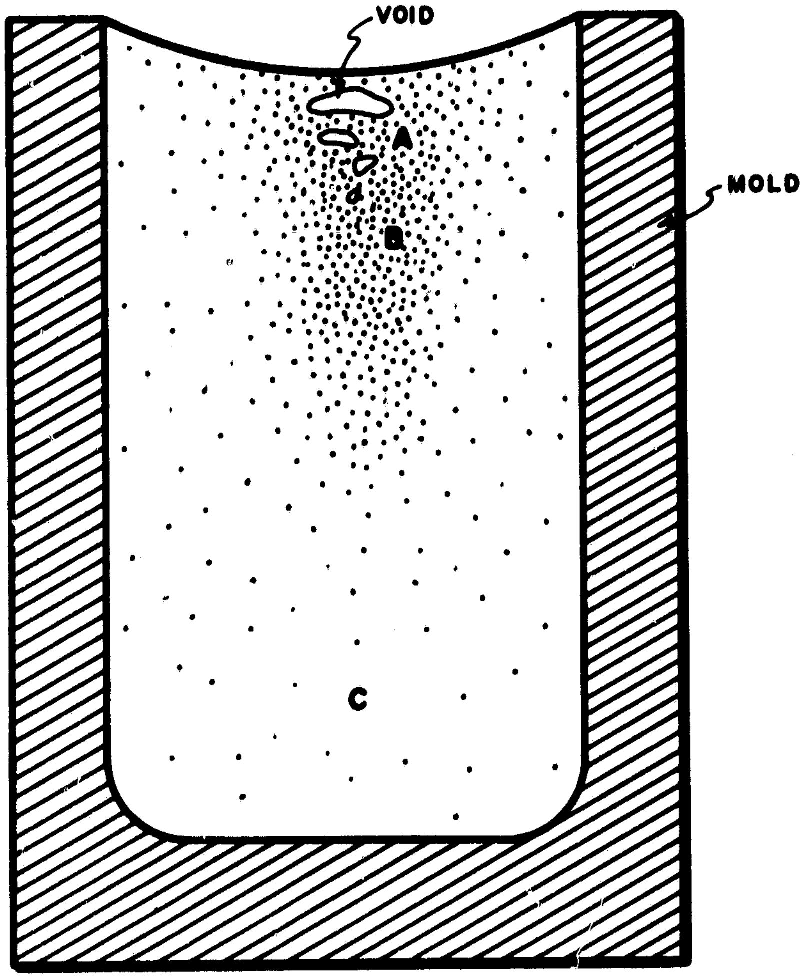

Figure 31

ORIGINAL PAGE IS
OF POOR QUALITY

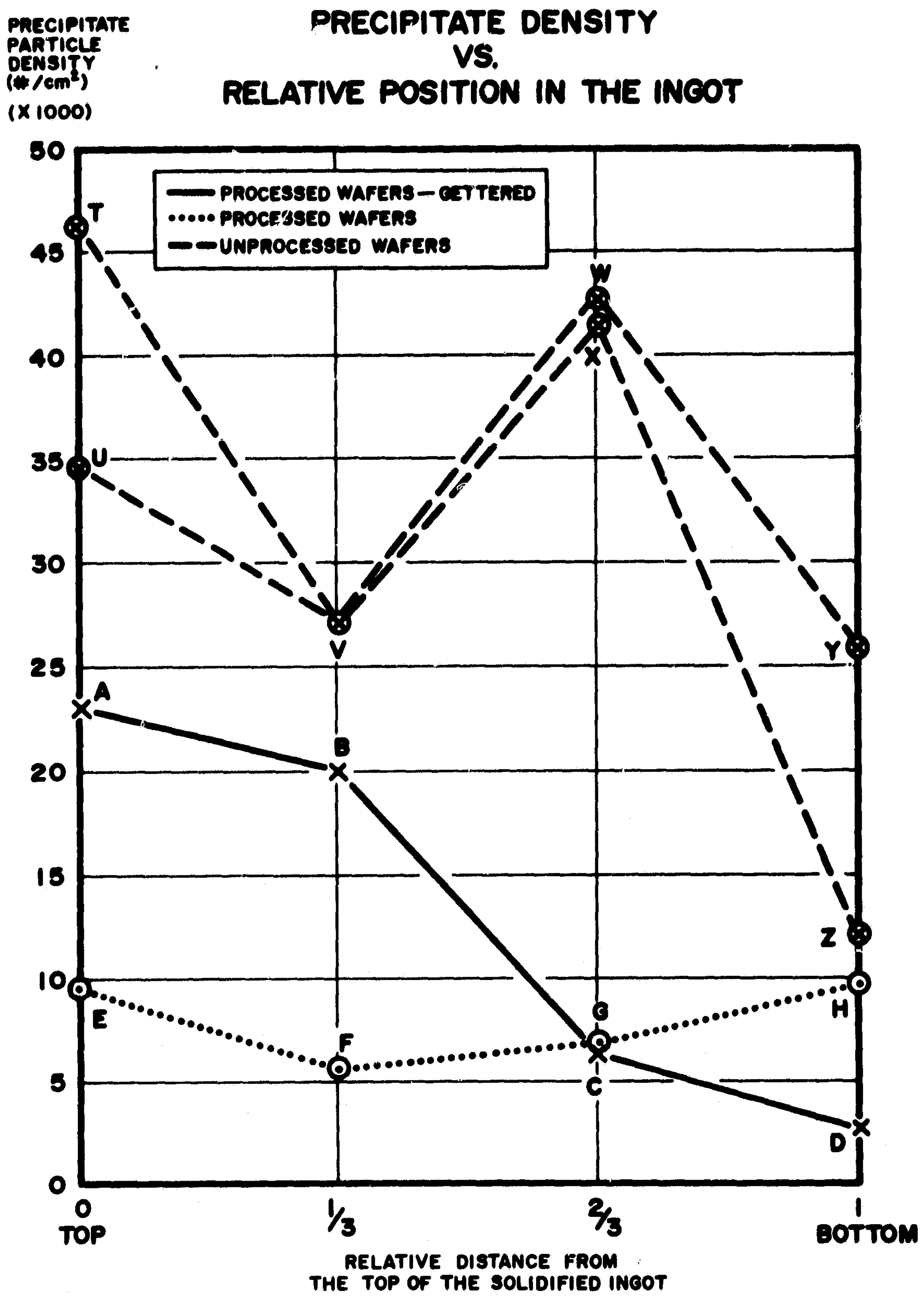

Figure 32

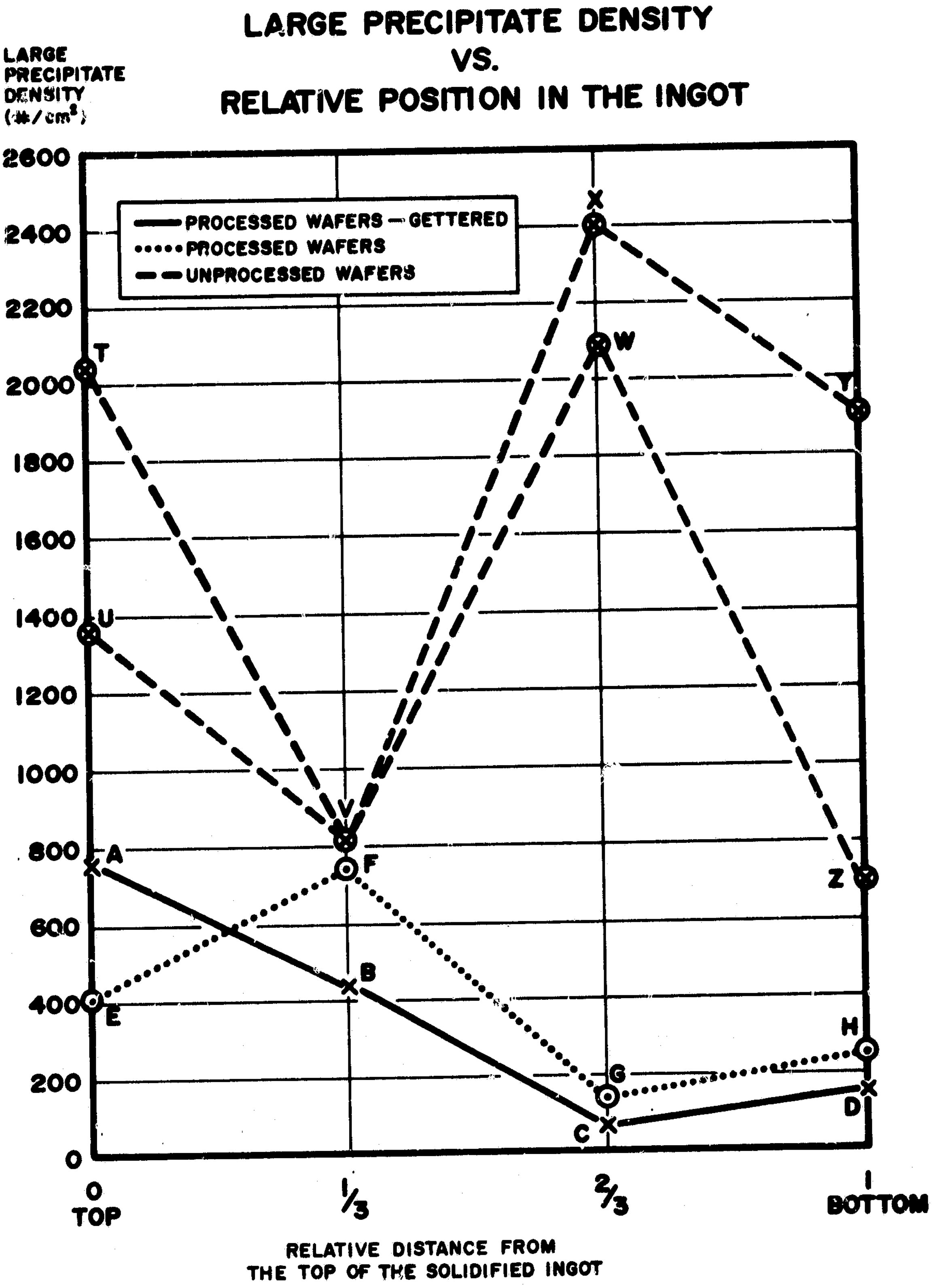
LARGE PRECIPITATE DENSITY
VS.
RELATIVE POSITION IN THE INGOT
LARGE PRECIPITATE DENSITY (#/cm²)
2600
2400
2200
2000
1800
1600
1400
1200
1000
800
600
400
200
0
PROCESSED WAFERS — GETTERED
PROCESSED WAFERS
UNPROCESSED WAFERS
T
U
V
W
X
Y
Z
A
B
C
D
E
F
G
H
0 TOP
1/3
2/3
1 BOTTOM
RELATIVE DISTANCE FROM THE TOP OF THE SOLIDIFIED INGOT

Figure 33

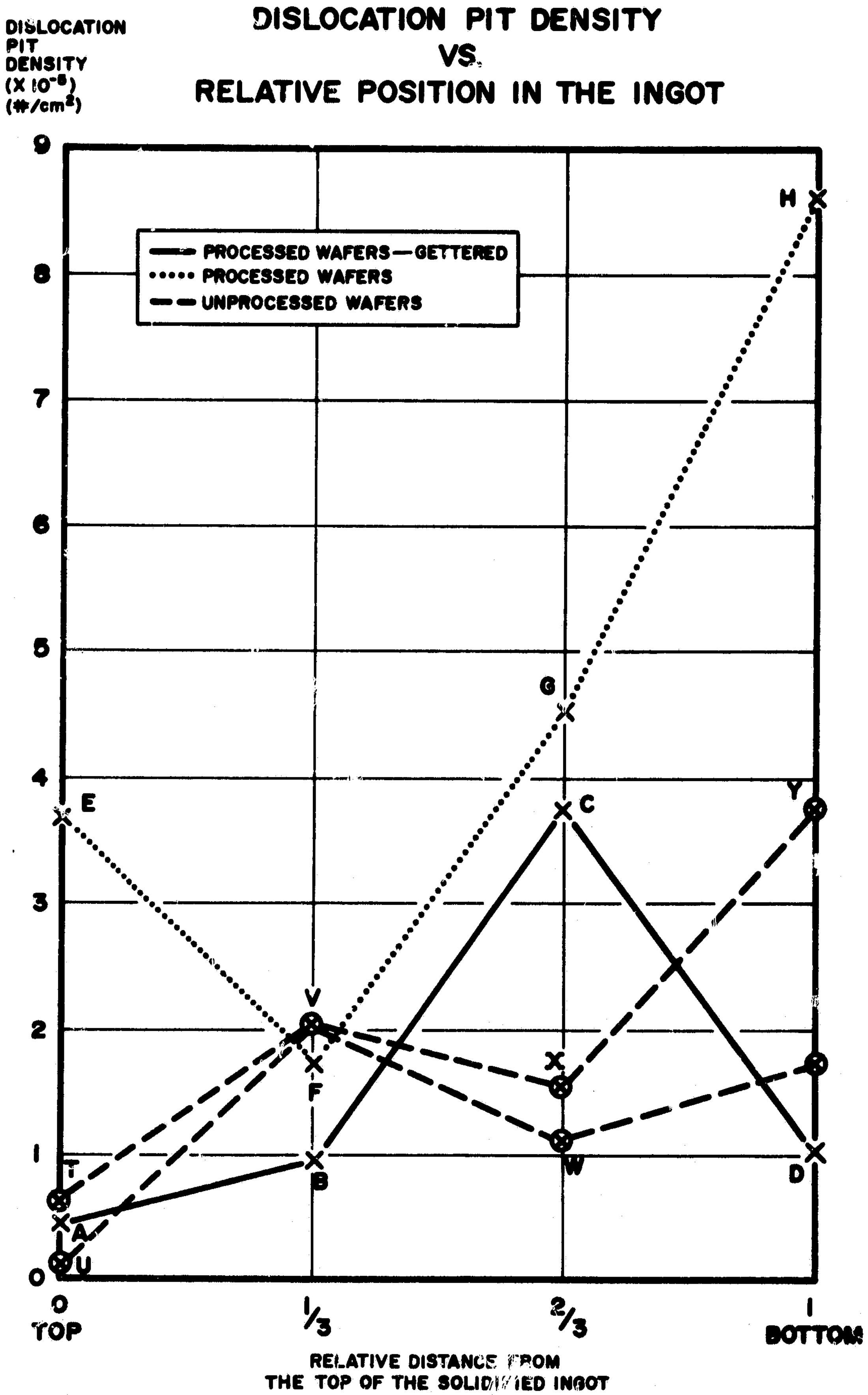
DISLOCATION PIT DENSITY
VS.
RELATIVE POSITION IN THE INGOT
DISLOCATION PIT DENSITY (X 10⁻⁵) (#/cm²)
9
8
7
6
5
4
3
2
1
0
PROCESSED WAFERS—GETTERED
PROCESSED WAFERS
UNPROCESSED WAFERS
H
G
E
C
Y
V
F
X
T
A
U
B
W
D
0
TOP
1/3
2/3
1
BOTTOM
RELATIVE DISTANCE FROM
THE TOP OF THE SOLIDIFIED INGOT

Figure 34

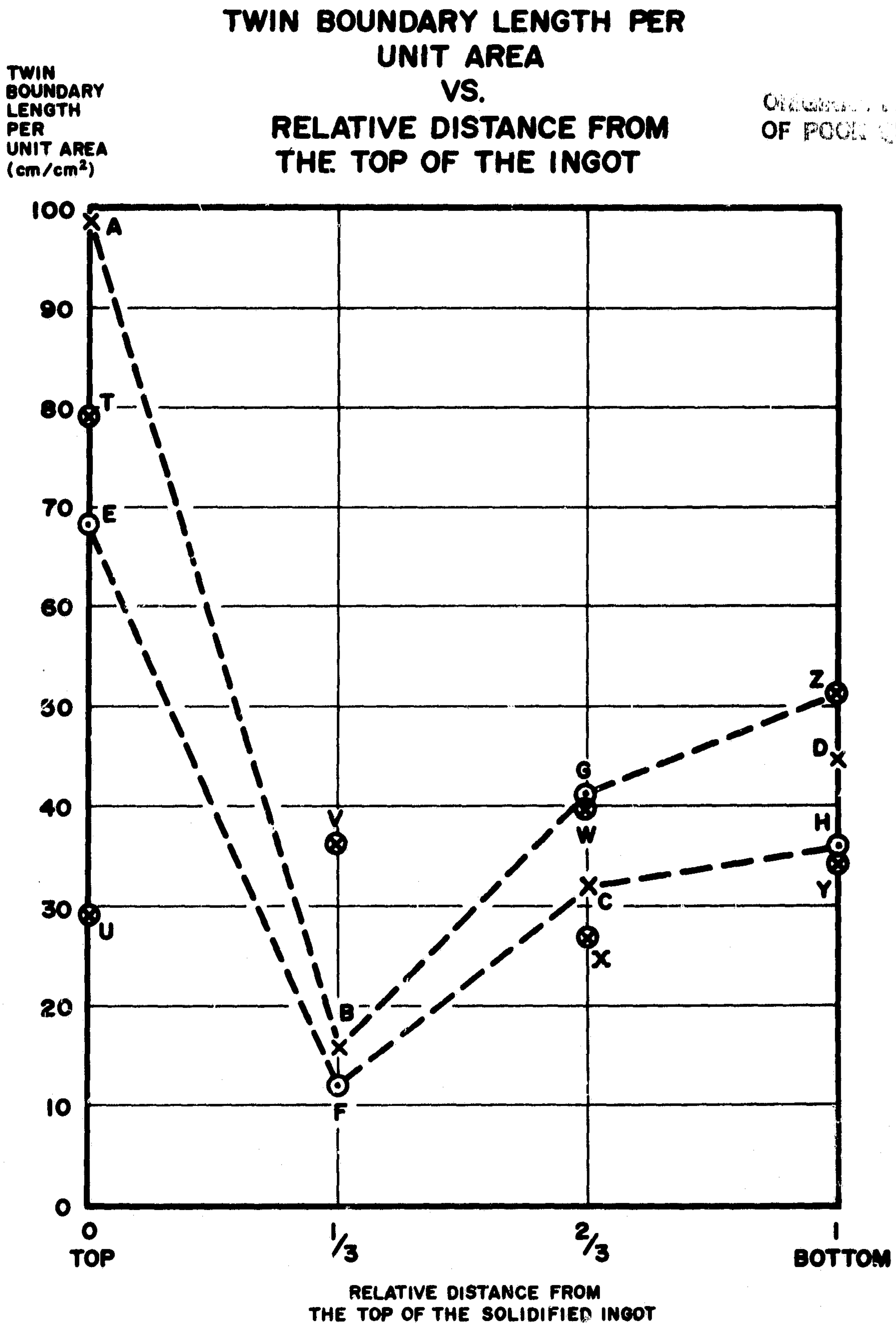

TWIN BOUNDARY LENGTH PER UNIT AREA VS. RELATIVE DISTANCE FROM THE TOP OF THE INGOT
TWIN BOUNDARY LENGTH PER UNIT AREA (cm/cm²)
100
90
80
70
60
50
40
30
20
10
0
A
T
E
U
V
B
F
G
W
C
X
Z
D
H
Y
0 TOP
1/3
2/3
1 BOTTOM
RELATIVE DISTANCE FROM THE TOP OF THE SOLIDIFIED INGOT

Figure 35

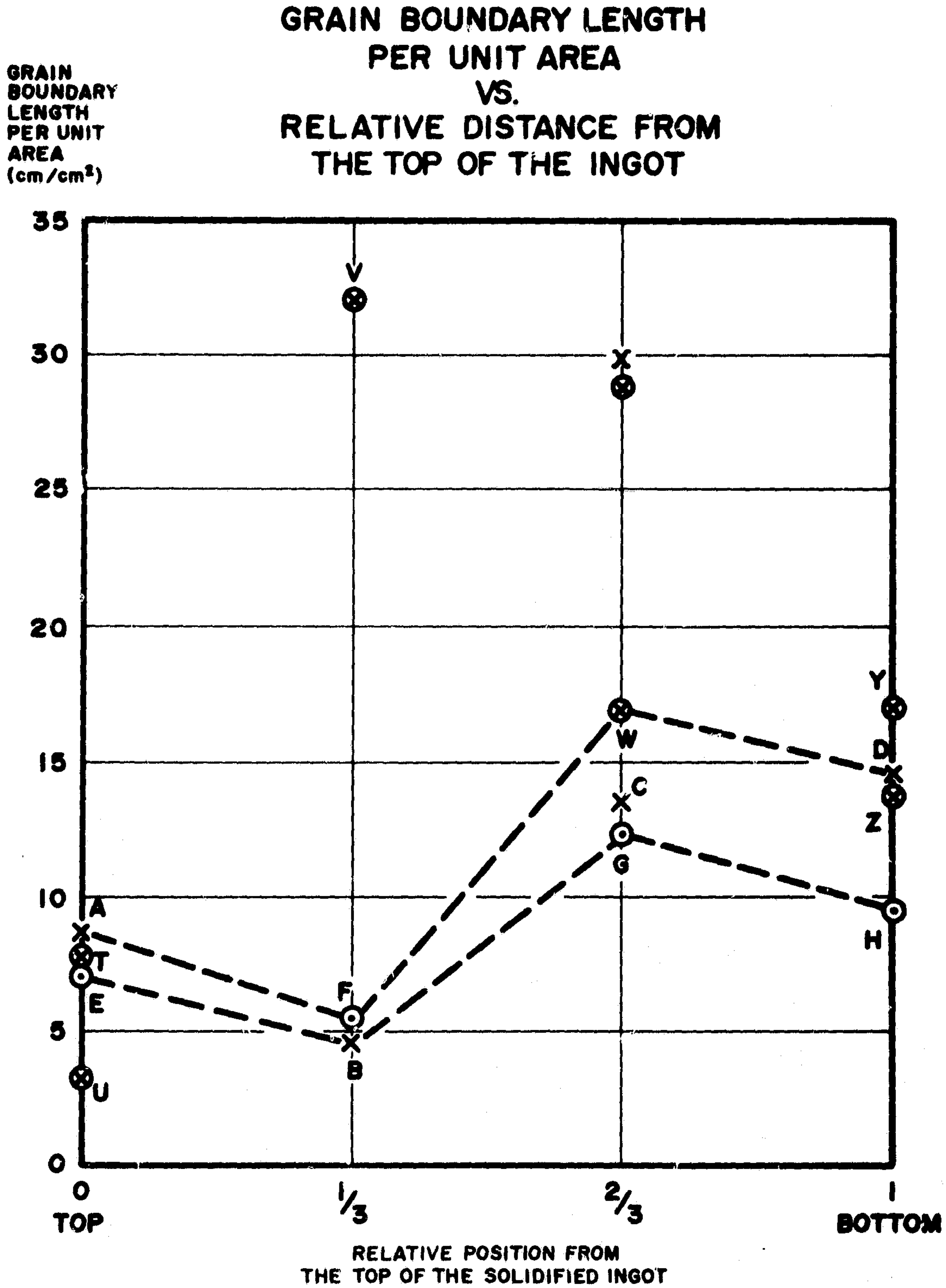
GRAIN BOUNDARY LENGTH
PER UNIT AREA
VS.
RELATIVE DISTANCE FROM
THE TOP OF THE INGOT
GRAIN BOUNDARY LENGTH PER UNIT AREA (cm/cm²)
35
30
25
20
15
10
5
0
V
X
W
Y
D
C
Z
G
H
A
T
E
F
B
U
0
TOP
1/3
2/3
1
BOTTOM
RELATIVE POSITION FROM
THE TOP OF THE SOLIDIFIED INGOT

Figure 36

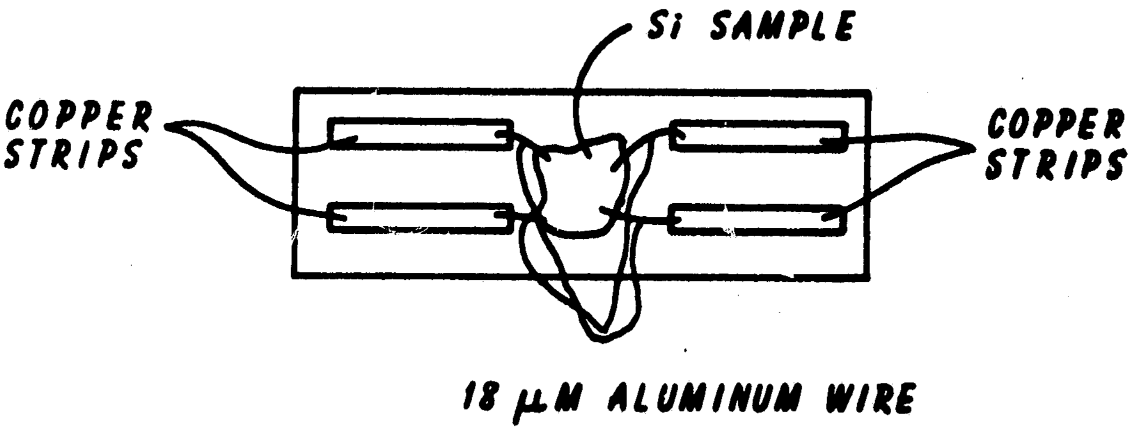

Fig. 37 Electrical Connections to Obtain a Small Contact Area and Reduce Contact Influence on Measurements

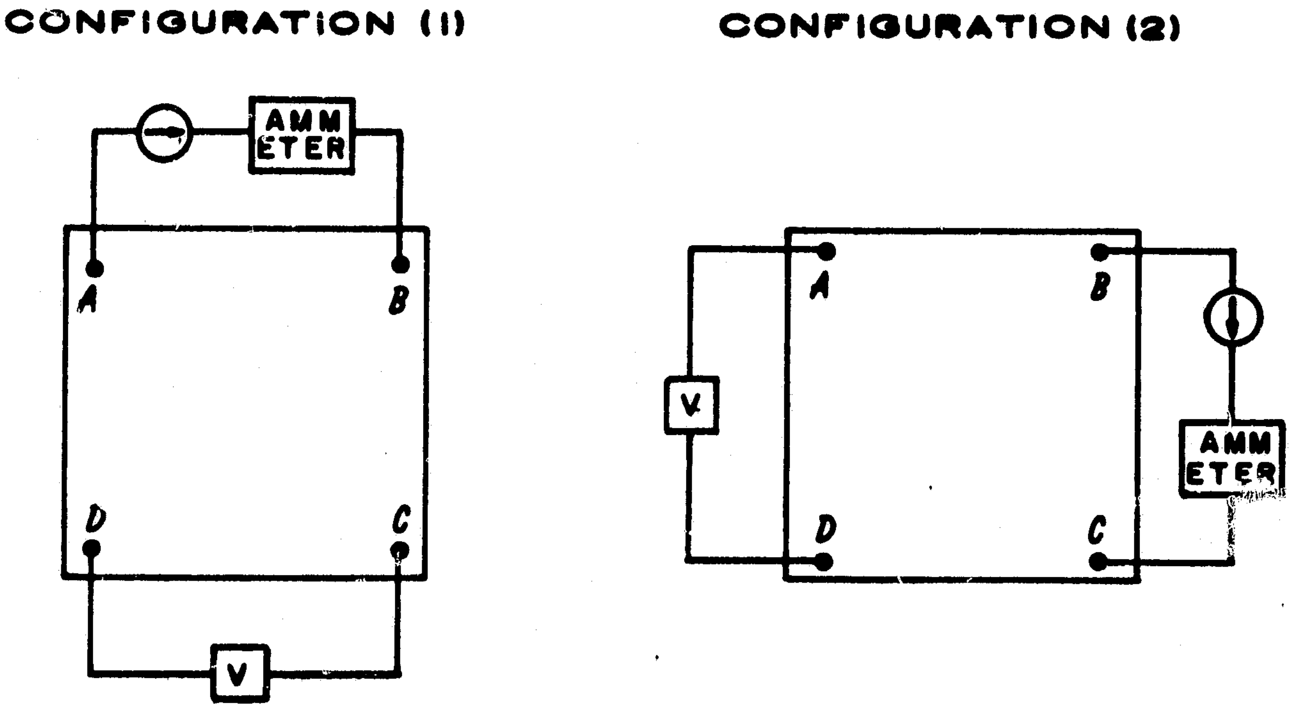

Fig. 38 Two Types of Configurations Used for Resistivity Measurements

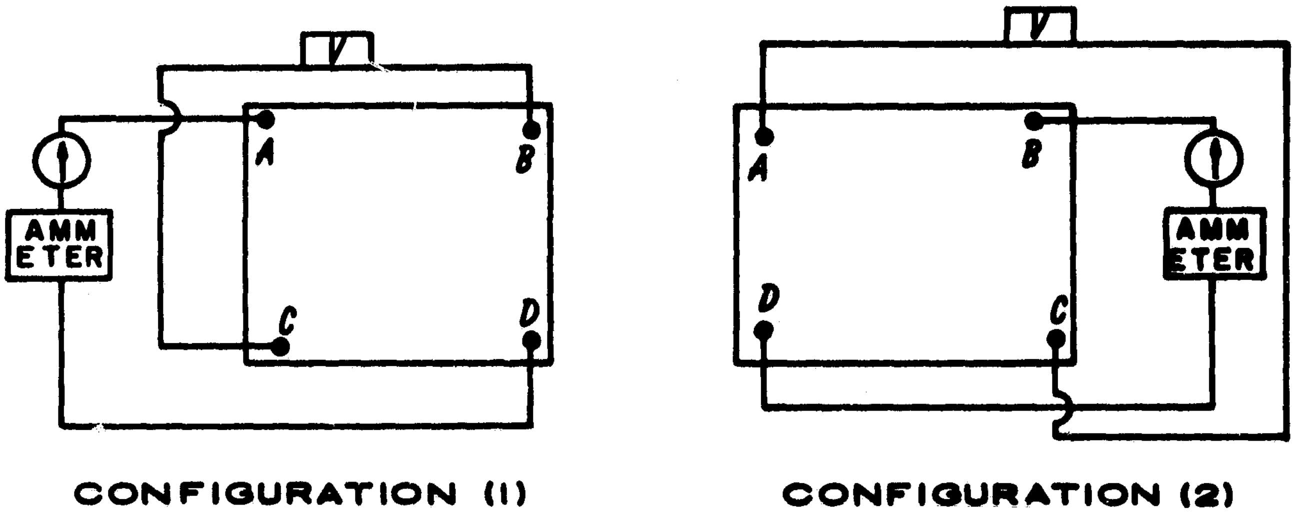

Fig. 39 Two Types of Configurations Used for Hall Voltage Measurements

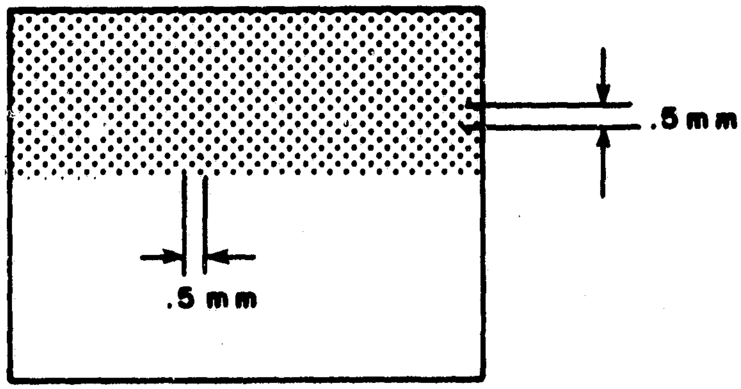

Fig. 40 Grid Used to Locate the Center of a Given Field

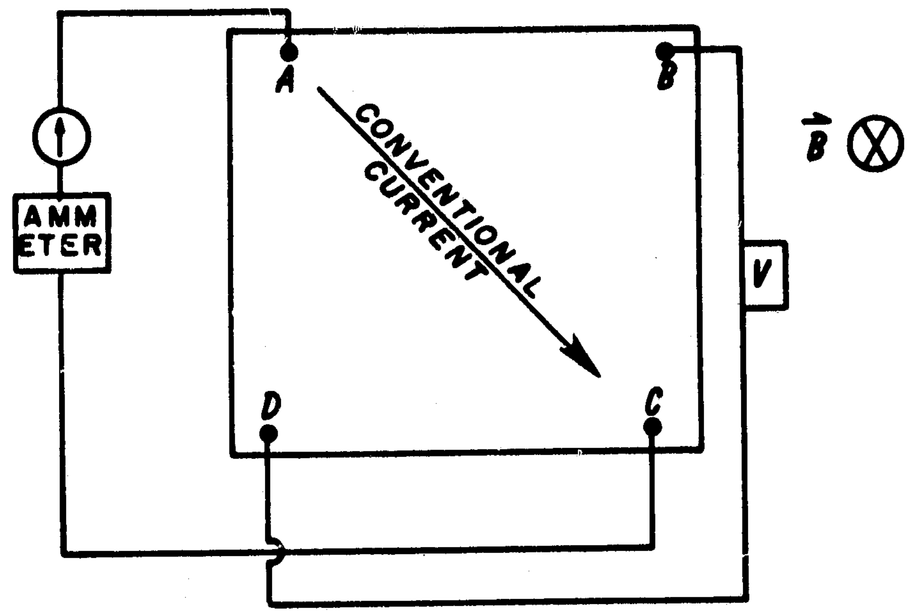

Fig. 41 Configuration Used to Determine Carrier Type

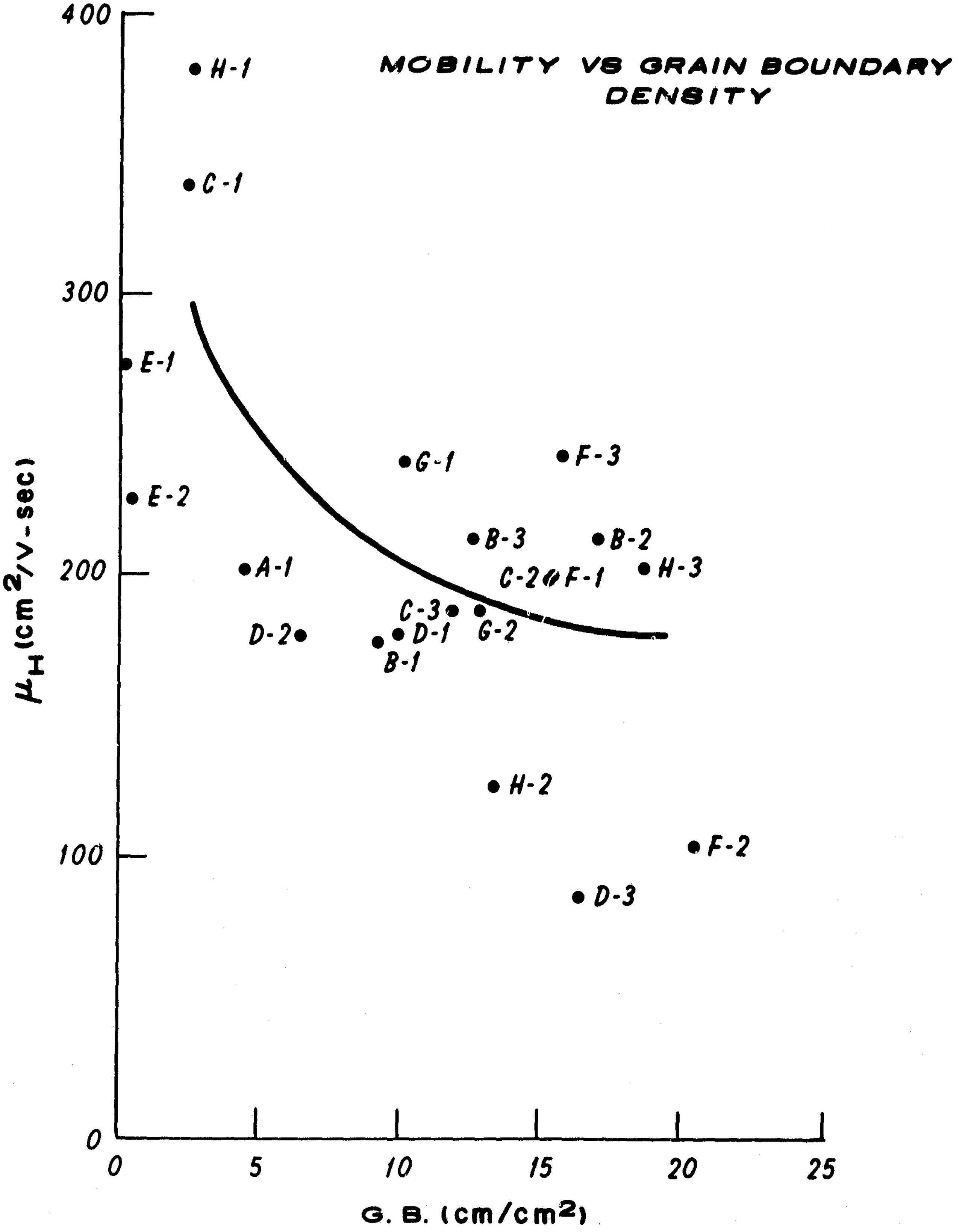
MOBILITY VS GRAIN BOUNDARY DENSITY
400
300
200
100
0
μ_H (cm²/V-sec)
H-1
C-1
E-1
E-2
A-1
D-2
G-1
F-3
B-3
B-2
C-2
F-1
H-3
C-3
D-1
G-2
B-1
H-2
F-2
D-3
0
5
10
15
20
25
G. B. (cm/cm²)

Figure 42

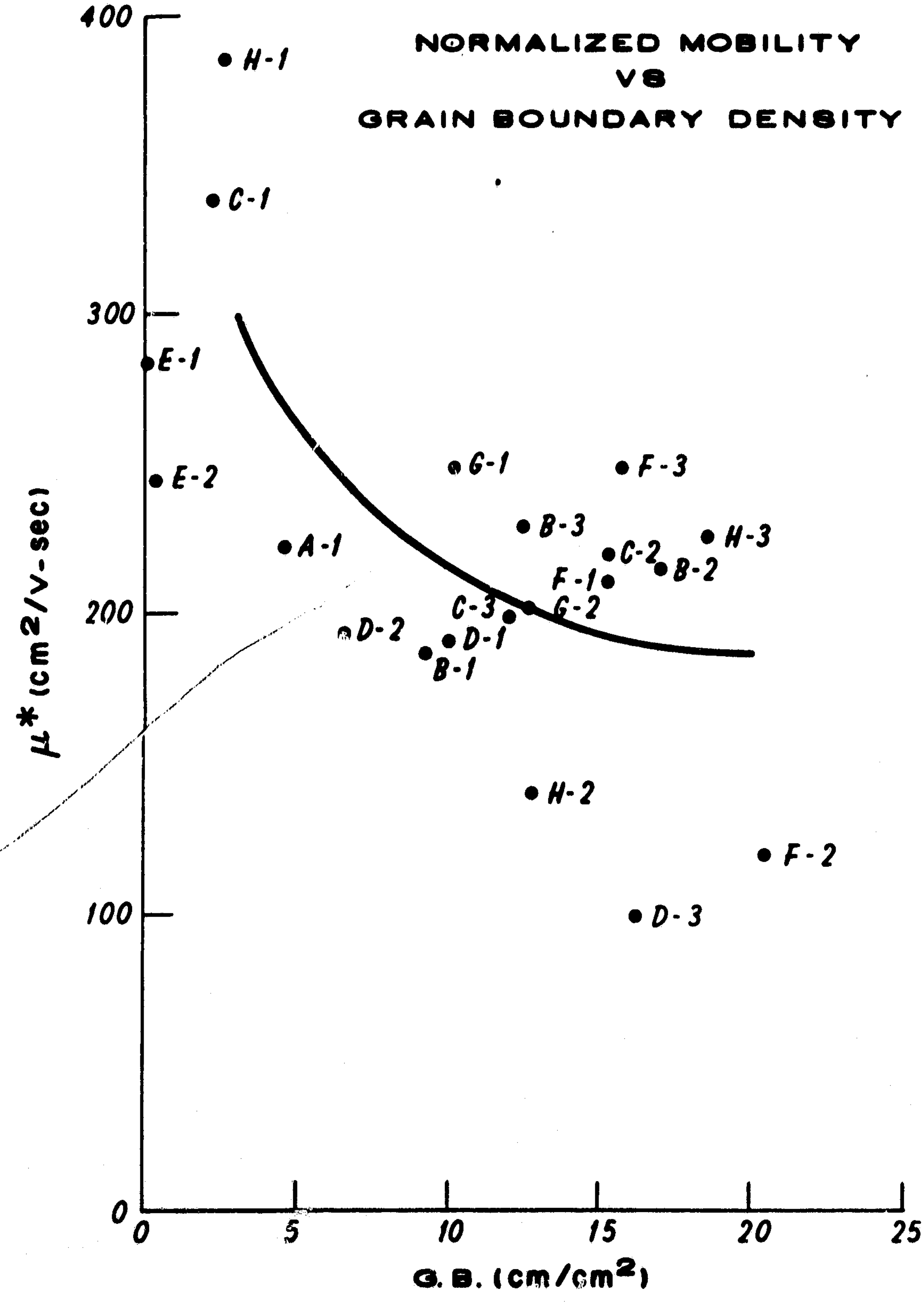

Fig. 43 Relationship Between Normalized Mobility and Grain Boundary

SECTION 6

APPENDIX

TABLES 1 THRU 45 LISTS ACTUAL DATA MEASURED

TABLE 1. Grain Boundary and Twin Boundary Density

SAMPLE SEMIX A-13 Sample in polished condition. Magnification 100X.

Field area = 0.0241 cm^2. Circumference of test circle = $\pi \cdot D$ = 0.55 cm.

A denotes No. of grain boundary intersections with circumference of test circle.

B denotes No. of twin boundary intersections with circumference of test circle.

X and Y denotes field location of the data measured.

FIELD Y	No.	X	A	No. of twins	B
12	1	33	7	33	24
12	2	35	7	28	37
12	3	37	2	137	201
12	4	39	4	12	23
12	5	41	2	113	119
12	6	43	2	9	14
12	7	45	3	15	10
12	8	47	6	26	31
12	9	49	0	0	0
12	10	51	0	0	0
14	11	50	2	0	0
14	12	47	2	12	12
14	13	44	0	2	4
14	14	41	2	124	196
14	15	38	2	19	33
14	16	35	7	40	47
16	17	34	0	0	0
16	18	36	3	27	28
16	19	38	3	12	15
16	20	40	5	50	47
16	21	42	2	1	2
16	22	44	2	8	8
16	23	46	4	9	8
16	24	48	0	0	0
16	25	50	2	0	0
18	26	49	3	20	6
18	27	46	5	14	9
18	28	43	2	4	6
18	29	40	4	6	11
18	30	37	6	8	4
20	31	37	4	39	19
20	32	39	2	10	8
20	33	41	3	3	3
20	34	43	2	2	2
20	35	45	0	1	2
20	36	47	2	0	0
10	37	50	8	32	3
10	38	47	5	24	25
10	39	44	2	9	9
10	40	41	4	14	12
10	41	38	2	112	198
10	42	35	6	21	24
8	43	34	5	33	42
8	44	36	2	29	41
8	45	38	4	144	257
8	46	40	2	12	22
8	47	42	2	20	9
8	48	44	2	0	0
8	49	46	0	15	30
8	50	48	4	63	29
8	51	50	2	7	11
6	52	49	4	29	33
6	53	46	0	13	23
6	54	43	2	5	9
6	55	40	4	20	24
6	56	37	4	38	62
4	57	37	6	117	148
4	58	39	2	100	160
4	59	41	3	42	37
4	60	43	2	3	4
4	61	45	0	0	0
4	62	47	0	2	4
Total for 62 fields:			179	1688	2145

L_A for grain boundary $= \frac{\pi}{2} \cdot P_L = \frac{\pi \cdot 179}{(2)(62)(0.55)} = 8.2 \ \frac{cm}{cm^2}$

L_A for twin boundary $= \frac{\pi \cdot 2145}{(2)(62)(0.55)} = 99 \ cm/cm^2$

$\overline{X}$ for grain boundary = 2.9

σ for grain boundary = 2.0

$\overline{X}$ for twin boundary = 34.6

σ for twin boundary = 56.5

$\frac{\pi}{2 \times 62 \times 0.55} = 0.0460644084$, to be used for next seven tables for grain boundary & twin boundary density calculation

TABLE 2 Precipitate Particle Density

SAMPLE SEMIX A-13 Sample in polished condition. Magnification 400X

Field area = 0.00149 cm^2

A denotes No. of Large precipitates observed in field of view.

B denotes No. of Small precipitates observed in field of view.

X and Y denotes location of microscope stage for the data measured.

FIELD			A		B
Y	No.	X			
12	1	33	1		15
12	2	34	1		7
12	3	35	0		67
12	4	36	0		42
12	5	37	2		32
12	6	38	2		89
12	7	39	1		15
12	8	40	0		18
12	9	41	0		19
12	10	42	0		19
12	11	43	0		9
12	12	44	0		26
12	13	45	1		9
12	14	46	0		118
12	15	47	1		187
12	16	48	7		98
12	17	49	2		136
12	18	50	2		28
12	19	51	0		40
16	20	34	2		35
16	21	35	0		30
16	22	36	1		11
16	23	37	5		3
16	24	38	0		20
16	25	39	1		24
16	26	40	0		46
16	27	41	1		60
16	28	42	1		21
16	29	43	1		11
16	30	44	3		24
16	31	45	1		32
16	32	46	0		5
16	33	47	1		102
16	34	48	1		23
16	35	49	4		17
16	36	50	6		9
16	37	51	1		14
8	38	35	0		27
8	39	36	0		12
20	63	44	3		8
20	64	46	2		18

FIELD			A		B
Y	No.	X			
8	40	37	0		9
8	41	38	2		22
8	42	39	0		69
8	43	40	0		124
8	44	41	0		69
8	45	42	2		38
8	46	43	0		11
8	47	44	0		1
8	48	45	1		3
8	49	46	0		2
8	50	47	0		9
8	51	48	0		13
8	52	49	3		3
8	53	50	3		7
8	54	51	1		6
4	55	38	1		32
4	56	40	0		21
4	57	42	0		25
4	58	44	1		40
4	59	46	2		14
20	60	38	0		11
20	61	40	0		46
20	62	42	1		6
Total for 64 fields:			71		2107

Area of 64 fields = 0.09536 cm^2

No. of large ppt. = 71/0.09536

= 745/ cm^2

$\bar{X}$ for large ppt. = 1.1

σ for large ppt. = 1.5

No. of small ppt. = 2107/0.09536

= 22095 / cm^2

$\bar{X}$ for small ppt. = 33.0

σ for small ppt. = 36.5

TABLE 3 DISLOCATION DENSITY

SAMPLE SEMIX A-13. Sample in etched condition

Magnification 1000X, Area of field = 0.000238 cm^2

X and Y denote the location of microscope stage (field of view)for the data measured.

FIELD Y	FIELD No.	FIELD X	No. of Dislocation Pits
12	1	34	45
12	2	35	46
12	3	37	6
12	4	39	5
12	5	41	1
12	6	43	6
12	7	45	3
12	8	47	5
12	9	49	8
12	10	50	4
14	11	49	2
14	12	47	6
14	13	44	4
14	14	41	104
14	15	38	118
14	16	35	26
16	17	35	14
16	18	36	5
16	19	38	1
16	20	40	22
16	21	42	4
16	22	44	3
16	23	46	3
16	24	48	2
16	25	49	19
18	26	47	5
18	27	46	5
18	28	43	0
18	29	40	9
18	30	37	5
19	32	39	16
19	33	41	6
19	34	43	15
19	35	45	3
19	36	47	8
10	37	50	3
10	38	47	3
10	39	44	0

FIELD Y	FIELD No.	FIELD X	No. of Dislocation Pits
10	40	41	1
10	41	38	75
10	42	35	2
8	44	36	4
8	45	38	5
8	46	40	8
8	47	42	1
8	48	44	5
8	49	46	2
8	50	48	1
8	51	49	0
6	52	49	1
6	53	46	4
6	54	43	6
6	55	40	7
6	56	37	6
5	58	39	2
5	59	41	4
5	60	43	3
5	61	45	4

Total for fields: 58 681

Dislocation density

$= 681/(58)(0.000238)$ pits/cm^2

$= 4.9 \times 10^4$ pits/cm^2

$\overline{X} = 12$

$\sigma = 23$

TABLE 4 Grain Boundary and Twin Boundary Density

SAMPLE SEMIX B-2, Sample in polished condition. Magnification 100X.

Field area = 0.0241 cm^2. Circumference of test circle = $\pi \cdot D$ = 0.55 cm.

A denotes No. of grain boundary intersections with circumference of test circle.

B denotes No. of twin boundary intersections with circumference of test circle.

X and Y denotes field location of the data measured.

FIELD			A	No. of twins	B
Y	No.	X			
12	1	33	7		15
12	2	35	3		25
12	3	37	0		0
12	4	39	0		4
12	5	41	0		2
12	6	43	0		0
12	7	45	0		0
12	8	47	0		0
12	9	49	0		0
12	10	51	4		29
14	11	50	0		0
14	12	47	0		0
14	13	44	0		0
14	14	41	0		4
14	15	38	0		0
14	16	35	6		1
16	17	34	8		3
16	18	36	3		6
16	19	38	2		4
16	20	40	0		0
16	21	42	0		0
16	22	44	0		4
16	23	46	0		0
16	24	48	0		[illegible]
16	25	50	0		0
18	26	49	0		0
18	27	46	0		7
18	28	43	0		0
18	29	40	2		4
18	30	37	2		3
20	31	37	2		8
20	32	39	2		30
20	33	41	2		8
20	34	43	1		6
20	35	45	0		0
20	36	47	0		0
10	37	50	6		50
10	38	47	0		2
10	39	44	0		0
10	40	41	2		0
10	41	38	2		4
10	42	35	4		17
8	43	34	7		16
8	44	36	6		25
8	45	38	4		7
8	46	40	2		0
8	47	42	0		0
8	48	44	0		0
8	49	46	0		7
8	50	48	0		17
8	51	50	3		7
6	52	49	0		3
6	53	46	0		0
6	54	43	0		0
6	55	40	5		3
6	56	37	2		0
4	57	37	5		10
4	58	39	4		6
4	59	41	2		7
4	60	43	0		0
4	61	45	0		1
4	62	47	0		2
Total for 62 fields:			98		347

L_A for grain boundary $= \frac{\pi}{2} \times P_L = \frac{\pi \times 98}{2 \times 62 \times 0.55} = 4.51 \frac{cm}{cm^2}$

L_A for twin boundary $= \frac{\pi \times 342}{2 \times 62 \times 0.55} = 15.75 \frac{cm}{cm^2}$

$\overline{X}$ for grain boundary = 1.6

σ for grain boundary = 2.2

$\overline{X}$ for twin boundary = 5.6

σ for twin boundary = 9.3

TABLE 5 Precipitate Particle Density

SAMPLE SEMIX B-2. Sample in polished condition. Magnification 400X.

Field area = 0.00149 cm^2

A denotes No. of Large precipitates observed in field of view.

B denotes No. of Small precipitates observed in field of view.

X and Y denotes location of microscope stage for the data measured.

FIELD			A		B
Y	No.	X			
12	1	33	2		14
12	2	35	0		24
12	3	37	0		18
12	4	39	1		18
12	5	41	0		25
12	6	43	0		22
12	7	45	1		11
12	8	47	0		71
12	9	49	0		31
12	10	51	0		27
14	11	50	0		34
14	12	47	3		86
14	13	44	2		23
14	14	41	1		32
14	15	38	0		44
14	16	35	0		38
16	17	34	1		13
16	18	36	0		14
16	19	38	0		35
16	20	40	2		13
16	21	42	0		23
16	22	44	0		17
16	23	46	0		38
16	24	48	0		15
16	25	50	1		36
18	26	49	3		13
18	27	46	3		48
18	28	43	2		23
18	29	40	0		9
18	30	37	2		27
20	31	37	4		34
20	32	39	0		28
20	33	41	0		20
20	34	43	1		39
20	35	45	0		14
20	36	47	1		13
10	37	50	1		27
10	38	47	1		14
10	39	44	0		17

FIELD			A		B
Y	No.	X			
10	40	41	0		9
10	41	38	1		22
10	42	35	0		31
8	43	34	0		19
8	44	36	1		17
8	45	38	0		22
8	46	40	1		16
8	47	42	0		33
8	48	44	1		16
8	49	46	0		66
8	50	48	0		59
8	51	50	0		59
6	52	49	0		27
6	53	46	0		22
6	54	43	0		18
6	55	40	1		14
6	56	37	1		15
4	57	37	0		25
4	58	39	2		95
4	59	41	0		36
4	60	43	1		64
4	61	45	0		40
4	62	47	0		29
Total for 62 fields:			41		1802

Area of 62 fields = 0.09238 cm^2

No. of large ppt. = 41 /0.09238 = 444/ cm^2

$\bar{X}$ for large ppt. = 0.66

σ for large ppt. = 0.95

No. of small ppt. = 1802 /0.09238 = 19506 / cm^2

$\bar{X}$ for small ppt. = 29.1

σ for small ppt. = 18.1

C-2

TABLE 6 DISLOCATION DENSITY

SAMPLE SEMIX B-2. Sample in etched condition

Magnification 1000X, Area of field = 0.000238 cm^2

X and Y denote the location of microscope stage (field of view)for the data measured.

FIELD			No. of Dislocation Pits		
Y	No.	X		↓	
12	1	34		10	
12	2	35		7	
12	3	37		30	
12	4	39		10	
12	5	41		7	
12	6	43		8	
12	7	45		22	
12	8	47		8	
12	9	49		69	
12	10	50		61	
14	11	49		47	
14	12	47		48	
14	13	44		10	
14	14	41		6	
14	15	38		13	
14	16	35		1	
16	17	35		1	
16	18	36		0	
16	19	38		28	
16	20	40		2	
16	21	42		16	
16	22	44		7	
16	23	46		16	
16	24	48		6	
16	25	49		13	
18	26	47		17	
18	27	46		24	
18	28	43		2	
18	29	40		5	
18	30	37		0	
19	31	37			
19	32	39			
19	33	41		9	
19	34	43		52	
19	35	45		20	
19	36	47			
10	37	50		294	
10	38	47		5	
10	39	44		4	

FIELD			No. of Dislocation Pits		
Y	No.	X		↓	
10	40	41		21	
10	41	38		1	
10	42	35		6	
8	43	35			
8	44	36		3	
8	45	38		34	
8	46	40		183	
8	47	42		13	
8	48	44		25	
8	49	46		18	
8	50	48		14	
8	51	49			
6	52	49		2	
6	53	46		5	
6	54	43		1	
6	55	40		3	
6	56	37		5	
5	57	38			
5	58	39		7	
5	59	41		6	
5	60	43		14	
5	61	45		12	
5	62	47		15	

Total for 56 fields: 1266

Dislocation density

= 1266 /(56)(0.000238) pits /cm^2

= 0.95×10^5 pits /cm^2

$\overline{X}$ = 23

σ = 45

TABLE 7 Grain Boundary and Twin Boundary Density

SAMPLE SEMIX C-12. Sample in polished condition. Magnification 100X.

Field area = 0.0241 cm^2. Circumference of test circle = $\pi \cdot D$ = 0.55 cm.

A denotes No. of grain boundary intersections with circumference of test circle.

B denotes No. of twin boundary intersections with circumference of test circle.

X and Y denotes field location of the data measured.

FIELD Y	FIELD No.	FIELD X	A	No. of twins	B
12	1	33	8	17	11
12	2	35	10	20	24
12	3	37	3	14	19
12	4	39	2	24	30
12	5	41	4	25	32
12	6	43	4	2	2
12	7	45	8	1	1
12	8	47	0	0	0
12	9	49	4	5	5
12	10	51	6	9	8
14	11	50	10	29	11
14	12	47	7	11	4
14	13	44	5	6	5
14	14	41	2	9	10
14	15	38	5	11	18
14	16	35	9	22	16
16	17	34	3	2	2
16	18	36	3	7	6
16	19	38	7	6	6
16	20	40	8	8	6
16	21	42	4	3	6
16	22	44	2	2	4
16	23	46	3	1	1
16	24	48	7	5	4
16	25	50	4	28	25
18	26	49	8	20	15
18	27	46	9	3	2
18	28	43	4	1	1
18	29	40	3	2	1
18	30	37	3	11	10
20	31	37	7	3	3
20	32	39	3	6	6
20	33	41	5	0	0
20	34	43	5	2	4
20	35	45	7	0	0
20	36	47	5	1	1
10	37	50	2	5	4
10	38	47	4	6	5
10	39	44	7	5	5
10	40	41	4	45	57
10	41	38	10	9	8
10	42	35	2	19	22
8	43	34	7	17	15
8	44	36	0	13	26
8	45	38	6	19	22
8	46	40	8	15	12
8	47	42	0	8	9
8	48	44	4	28	15
8	49	46	4	6	3
8	50	48	6	11	11
8	51	50	2	3	6
6	52	49	5	9	12
6	53	46	7	12	7
6	54	43	0	22	25
6	55	[illegible]	3	38	43
6	56	37	0	8	10
4	57	37	0	3	6
4	58	39	3	11	14
4	59	41	8	59	29
4	60	43	3	22	22
4	61	45	4	11	4
4	62	47	4	3	2
Total for 62 fields:			290	723	693

L_A for grain boundary $= \frac{\pi}{2} \cdot P_L = \frac{\pi}{2} \frac{290}{\times 62 \times 0.55} = 13.36 \frac{cm}{cm^2}$

L_A for twin boundary $= \frac{\pi \times 693}{2 \times 62 \times 0.55} = 31.92 \frac{cm}{cm^2}$

$\overline{X}$ for grain boundary = 4.7

σ for grain boundary = 2.7

$\overline{X}$ for twin boundary = 11.2

σ for twin boundary = 11.1

TABLE 8 Precipitate Particle Density

SAMPLE SEMIX C-12 Sample in polished condition. Magnification 400X.

Field area = 0.00149 cm^2

A denotes No. of Large precipitates observed in field of view.

B denotes No. of Small precipitates observed in field of view.

X and Y denotes location of microscope stage for the data measured.

FIELD			A		B
Y	No.	X			
12	1	33	4		0
12	2	35	11		0
12	3	37	8		0
12	4	39	7		0
12	5	41	7		0
12	6	43	12		0
12	7	45	15		0
12	8	47	4		0
12	9	49	10		0
12	10	51	14		0
14	11	50	8		0
14	12	47	10		0
14	13	44	15		0
14	14	41	5		0
14	15	38	14		0
14	16	35	12		0
16	17	34	19		0
16	18	36	4		0
16	19	38	6		0
16	20	40	0		0
16	21	42	2		0
16	22	44	0		0
16	23	46	17		0
16	24	48	27		0
16	25	50	10		0
18	26	49	18		0
18	27	46	13		0
18	28	43	7		0
18	29	40	29		0
18	30	37	8		0
20	31	37	4		0
20	32	39	8		1
20	33	41	3		0
20	34	43	3		0
20	35	45	2		0
20	36	47	0		0
10	37	50	3		0
10	38	47	9		0
10	39	44	2		0
10	40	41	1		0
10	41	38	0		0
10	42	35	3		0
8	43	34	6		0
8	44	36	7		0
8	45	38	0		0
8	46	40	3		0
8	47	42	0		0
8	48	44	5		0
8	49	46	6		0
8	50	48	10		0
8	51	50	7		0
6	52	49	20		0
6	53	46	17		1
6	54	43	5		0
6	55	40	12		2
6	56	37	8		0
4	57	37	18		0
4	58	39	16		0
4	59	41	26		0
4	60	43	5		0
4	61	45	22		2
4	62	47	35		0
Total for 62 fields:			572		6

Area of 62 fields = 0.09238 cm^2

No. of large ppt. = 6 /0.09238

= 65 / cm^2

$\bar{X}$ for large ppt. = 0.1

σ for large ppt. = 0.4

No. of small ppt. = 572 /0.09238

= 6192 / cm^2

$\bar{X}$ for small ppt. = 9.2

σ for small ppt. = 7.7

TABLE 9 DISLOCATION DENSITY

SAMPLE SEMIX C-12. Sample in etched condition

Magnification 1000X, Area of field = 0.000238 cm^2

X and Y denote the location of microscope stage (field of view)for the data measured.

FIELD Y	No.	X	No. of Dislocation Pits
12	1	34	26
12	2	35	187
12	3	37	114
12	4	39	58
12	5	41	17
12	6	43	33
12	7	45	29
12	8	47	101
12	9	49	15
12	10	50	11
14	11	49	55
14	12	47	162
14	13	44	11
14	14	41	20
14	15	38	185
14	16	35	253
16	17	35	136
16	18	36	82
16	19	38	205
16	20	40	37
16	21	42	52
16	22	44	52
16	23	46	47
16	24	48	44
16	25	49	177
18	26	47	265
18	27	46	34
18	28	43	90
18	29	40	43
18	30	37	31
19	31	37	
19	32	39	
19	33	41	10
19	34	43	8
19	35	45	
19	36	47	
10	37	50	165
10	38	47	82
10	39	44	48

FIELD Y	No.	X	No. of Dislocation Pits
10	40	41	104
10	41	38	149
10	42	35	132
8	43	35	89
8	44	36	170
8	45	38	97
8	46	40	59
8	47	42	75
8	48	44	99
8	49	46	143
8	50	48	35
8	51	49	83
6	52	49	
6	53	46	81
6	54	43	121
6	55	40	108
6	56	37	133
5	57	38	66
5	58	39	96
5	59	41	152
5	60	43	73
5	61	45	45
5	62	47	

Total for 56 fields: 4989

Dislocation density

= 4989/(56)(0.000238 pits/cm^2

= 3.7×10^5 pits/cm^2

$\overline{X}$ = 89

σ = 62

TABLE 10 Grain Boundary and Twin Boundary Density

SAMPLE SEMIX D-8. Sample in polished condition. Magnification 100X.

Field area = 0.0241 cm^2. Circumference of test circle = $\pi \cdot D$ = 0.55 cm.

A denotes No. of grain boundary intersections with circumference of test circle.

B denotes No. of twin boundary intersections with circumference of test circle.

X and Y denotes field location of the data measured.

FIELD Y	FIELD No.	FIELD X	A	No. of twins	B
12	1	33	10	89	23
12	2	35	3	3	6
12	3	37	4	9	8
12	4	39	4	2	1
12	5	41	4	8	8
12	6	43	2	14	22
12	7	45	2	3	6
12	8	47	0	0	0
12	9	49	4	22	24
12	10	51	3	0	0
14	11	50	4	6	6
14	12	47	2	1	1
14	13	44	4	5	6
14	14	41	11	5	3
14	15	38	4	13	13
14	16	35	6	9	11
16	17	34	6	24	19
16	18	36	2	11	12
16	19	38	3	7	7
16	20	40	7	23	29
16	21	42	5	48	21
16	22	44	2	0	0
16	23	46	2	0	0
16	24	48	2	1	1
16	25	50	5	16	15
18	26	49	4	1	1
18	27	46	0	0	0
18	28	43	4	0	0
18	29	40	8	57	56
18	30	37	7	16	16
20	31	37	9	31	28
20	32	39	10	26	17
20	33	41	6	68	51
20	34	43	2	72	57
20	35	45	2	4	11
20	36	47	0	0	0
10	37	50	2	6	9
10	38	47	2	3	3
10	39	44	4	24	10
10	40	41	6	22	10
10	41	38	6	0	0
10	42	35	5	24	17
8	43	34	8	58	37
8	44	36	11	38	37
8	45	38	17	35	8
8	46	40	12	1	2
8	47	42	6	17	15
8	48	44	10	92	75
8	49	46	2	47	61
8	50	48	3	26	36
8	51	50	2	10	10
6	52	49	5	2	2
6	53	46	8	52	40
6	54	43	6	0	0
6	55	40	7	17	14
6	56	37	4	127	35
4	57	37	5	29	25
4	58	39	4	13	16
4	59	41	3	4	5
4	60	43	0	0	0
4	61	45	4	33	11
4	62	47	4	12	10
Total for 62 fields:			299	1295	967

L_A for grain boundary $= \frac{\pi}{2} \cdot P_L = \frac{\pi \times 299}{2 \times 62 \times 0.55} = 13.77 \frac{cm}{cm^2}$

L_A for twin boundary $= \frac{\pi \times 967}{2 \times 62 \times 0.55} = 44.54 \frac{cm}{cm^2}$

$\overline{X}$ for grain boundary = 4.8

σ for grain boundary = 3.2

$\overline{X}$ for twin boundary = 15.6

σ for twin boundary = 17.1

TABLE 11 Precipitate Particle Density

SAMPLE SEMIX D-8. Sample in polished condition. Magnification 400X.

Field area = 0.00149 cm^2

A denotes No. of Large precipitates observed in field of view.

B denotes No. of Small precipitates observed in field of view.

X and Y denotes location of microscope stage for the data measured.

FIELD			A		B
Y	No.	X			
12	1	33	0		9
12	2	35	0		10
12	3	37	0		2
12	4	39	0		5
12	5	41	1		0
12	6	43	0		7
12	7	45	0		17
12	8	47	0		3
12	9	49	0		4
12	10	51	2		6
14	11	50	0		2
14	12	47	0		3
14	13	44	0		1
14	14	41	1		2
14	15	38	0		0
14	16	35	0		9
16	17	34	1		1
16	18	36	0		0
16	19	38	0		4
16	20	40	1		3
16	21	42	0		7
16	22	41	1		0
16	23	46	0		5
16	24	48	0		7
16	25	50	0		8
18	26	49	1		2
18	27	46	0		1
18	28	43	1		3
18	29	40	0		0
18	30	37	0		3
20	31	37	0		6
20	32	39	0		3
20	33	41	0		3
20	34	43	0		2
20	35	45	1		2
20	36	47	1		7
10	37	50	0		1
10	38	47	0		0
10	39	44	0		1
10	40	41	0		0
10	41	38	1		0
10	42	35	0		11
8	43	34	0		4
8	44	36	0		1
8	45	38	0		0
8	46	40	1		1
8	47	42	0		0
8	48	44	1		0
8	49	46	0		2
8	50	48	0		2
8	51	50	0		1
6	52	49	0		8
6	53	46	0		2
6	54	43	0		0
6	55	40	0		0
6	56	37	0		7
4	57	37	0		16
4	58	39	0		6
4	59	41	0		2
4	60	43	0		4
4	61	45	0		16
4	62	47	0		3

Total for 62 fields: 14 235

Area of 62 fields = 0.09238 cm^2

No. of large ppt. = 14/0.09238

= 152/ cm^2

$\bar{X}$ for large ppt. = 0.23

σ for large ppt. = 0.46

No. of small ppt. = 235/0.09238

= 2544 / cm^2

$\bar{X}$ for small ppt. = 3.8

σ for small ppt. = 4.0

TABLE 12 DISLOCATION DENSITY

SAMPLE SEMIX D-8, Sample in etched condition

Magnification 1000X, Area of field = 0.000238 cm^2

X and Y denote the location of microscope stage (field of view)for the data measured.

FIELD Y	No.	X	No. of Dislocation Pits
12	1	34	7
12	2	35	5
12	3	37	0
12	4	39	9
12	5	41	64
12	6	43	7
12	7	45	2
12	8	47	8
12	9	49	3
12	10	50	
14	11	49	14
14	12	47	6
14	13	44	2
14	14	41	3
14	15	38	2
14	16	35	4
16	17	35	
16	18	36	29
16	19	38	5
16	20	40	10
16	21	42	2
16	22	44	9
16	23	46	5
16	24	48	7
16	25	49	6
18	26	47	7
18	27	46	8
18	28	43	142
18	29	40	49
18	30	37	5
19	31	37	6
19	32	39	196
19	33	41	20
19	34	43	6
19	35	45	7
19	36	47	
10	37	50	12
10	38	47	19
10	39	44	15
10	40	41	12
10	41	38	7
10	42	35	5
8	43	35	2
8	44	36	2
8	45	38	15
8	46	40	11
8	47	42	304
8	48	44	7
8	49	46	2
8	50	48	8
8	51	49	
6	52	49	5
6	53	46	34
6	54	43	3
6	55	40	48
6	56	37	2
5	57	38	
5	58	39	95
5	59	41	6
5	60	43	5
5	61	45	14
5	62	47	89

Total for 57 fields: 1377

Dislocation density

$= 1377/(57)(0.000238)$ pits/cm^2

$= 1.0 \times 10^5$ pits/cm^2

$\bar{X} = 24$

$\sigma = 51$

TABLE 13 Grain Boundary and Twin Boundary Density

SAMPLE SEMIX E-13. Sample in polished condition. Magnification 100X.

Field area = 0.0241 cm^2. Circumference of test circle = $\pi \cdot D$ = 0.55 cm.

A denotes No. of grain boundary intersections with circumference of test circle.

B denotes No. of twin boundary intersections with circumference of test circle.

X and Y denotes field location of the data measured.

FIELD Y	No.	X	A	No. of twins	B
12	1	33	4	7	7
12	2	35	2	5	7
12	3	37	0	4	6
12	4	39	0	1	2
12	5	41	2	38	35
12	6	43	0	0	0
12	7	45	2	0	0
12	8	47	0	0	0
12	9	49	0	0	0
12	10	51	0	0	0
14	11	50	0	0	0
14	12	47	0	1	1
14	13	44	0	0	0
14	14	41	0	0	0
14	15	38	2	13	13
14	16	35	0	4	7
16	17	34	0	0	0
16	18	36	4	6	3
16	19	38	0	0	0
16	20	40	2	15	15
16	21	42	7	18	10
16	22	44	6	20	17
16	23	46	4	51	51
16	24	48	6	33	39
16	25	50	6	53	74
18	26	49	3	69	57
18	27	46	2	10	11
18	28	43	0	0	0
18	29	40	0	0	0
18	30	37	2	0	0
20	31	37	0	0	0
20	32	39	0	0	0
20	33	41	0	0	0
20	34	43	0	0	0
20	35	45	2	1	1
20	36	47	2	8	7
10	37	50	3	21	17
10	38	47	2	4	4
10	39	44	3	4	3
10	40	41	2	170	124
10	41	38	5	27	29
10	42	35	3	3	2
8	43	34	5	0	0
8	44	36	7	12	8
8	45	38	6	8	6
8	46	40	3	12	20
8	47	42	2	8	15
8	48	44	2	16	24
8	49	46	6	34	50
8	50	48	4	86	94
8	51	50	3	102	161
6	52	49	2	71	132
6	53	46	4	92	152
6	54	43	4	43	71
6	55	40	4	26	38
6	56	37	2	0	0
4	57	37	3	2	2
4	58	39	3	25	24
4	59	41	3	33	45
4	60	43	3	24	38
4	61	45	7	17	24
4	62	47	4	26	42
Total for 62 fields:			153	1223	1488

L_A for grain boundary $= \frac{\pi}{2} \cdot P_L = \frac{\pi}{2} \frac{153}{\times 62 \times 0.55} = 7.05 \frac{cm}{cm^2}$

L_A for twin boundary $= \frac{\pi \times 1488}{2 \times 62 \times 0.55} = 68.54 \frac{cm}{cm^2}$

$\overline{X}$ for grain boundary = 2.5

σ for grain boundary = 2.1

$\overline{X}$ for twin boundary = 24

σ for twin boundary = 37.7

TABLE 14 Precipitate Particle Density

SAMPLE SEMIX E-13. Sample in polished condition. Magnification 400X.

Field area = 0.00149 cm^2

A denotes No. of Large precipitates observed in field of view.

B denotes No. of Small precipitates observed in field of view.

X and Y denotes location of microscope stage for the data measured.

FIELD			A		B
Y	No.	X			
12	1	33	1		22
12	2	35	0		13
12	3	37	0		7
12	4	39	0		18
12	5	41	2		15
12	6	43	2		12
12	7	45	2		15
12	8	47	1		4
12	9	49	1		19
12	10	51	0		30
14	11	50	0		48
14	12	47	2		12
14	13	44	0		4
14	14	41	0		12
14	15	38	1		12
14	16	35	1		16
16	17	34	0		8
16	18	36	0		5
16	19	38	1		13
16	20	40	0		8
16	21	42	1		9
16	22	44	1		7
16	23	46	0		19
16	24	48	1		10
16	25	50	0		15
18	26	49	1		11
18	27	46	1		6
18	28	43	0		17
18	29	40	1		11
18	30	37	0		21
20	31	37	0		9
20	32	39	0		10
20	33	41	0		59
20	34	43	1		19
20	35	45	1		9
20	36	47	1		4
10	37	50	0		27
10	38	47	1		21
10	39	44	2		3
10	40	41	1		5
10	41	38	0		10
10	42	35	0		4
8	43	34	0		48
8	44	36	0		13
8	45	38	0		4
8	46	40	0		8
8	47	42	0		20
8	48	44	1		5
8	49	46	2		7
8	50	48	2		6
8	51	50	1		23
6	52	49	1		7
6	53	46	1		6
6	54	43	0		19
6	55	40	1		16
6	56	37	0		8
4	57	37	0		5
4	58	39	0		5
4	59	41	0		7
4	60	43	0		10
4	61	45	0		7
4	62	47	1		17
Total for 62 fields:			37		840

Area of 62 fields = 0.09238 cm^2

No. of large ppt. = 37/0.09238 = 400 / cm^2

$\bar{X}$ for large ppt. = 0.6

σ for large ppt. = 0.7

No. of small ppt. = 840/0.09238 = 9090 / cm^2

$\bar{X}$ for small ppt. = 13.5

σ for small ppt. = 10.6

TABLE 15 DISLOCATION DENSITY

SAMPLE SEMIX E-13. Sample in etched condition

Magnification 1000X, Area of field = 0.000238 cm^2

X and Y denote the location of microscope stage (field of view)for the data measured.

FIELD Y	FIELD No.	FIELD X	No. of Dislocation Pits
12	1	34	175
12	2	35	141
12	3	37	245
12	4	39	56
12	5	41	39
12	6	43	19
12	7	45	4
12	8	47	140
12	9	49	141
12	10	50	285
14	11	49	74
14	12	47	106
14	13	44	6
14	14	41	19
14	15	38	9
14	16	35	14
16	17	35	2
16	18	36	4
16	19	38	24
16	20	40	2
16	21	42	32
16	22	44	6
16	23	46	38
16	24	48	21
16	25	49	
18	26	47	9
18	27	46	35
18	28	43	14
18	29	40	2
18	30	37	11
19	31	37	
19	32	39	34
19	33	41	11
19	34	43	52
19	35	45	2
19	36	47	
10	37	50	360
10	38	47	370
10	39	44	250
10	40	41	242
10	41	38	93
10	42	35	68
8	43	35	295
8	44	36	97
8	45	38	58
8	46	40	170
8	47	42	235
8	48	44	187
8	49	46	188
8	50	48	203
8	51	49	102
6	52	49	
6	53	46	70
6	54	43	39
6	55	40	78
6	56	37	62
5	57	38	
5	58	39	22
5	59	41	22
5	60	43	35
5	61	45	38
5	62	47	

Total for 56 fields: 4996

Dislocation density

$= 4996/(56)(0.000238)$ pits/cm^2

$= 3.7 \times 10^5$ pits/cm^2

$\overline{X} = 89$

$\sigma = 96$

TABLE 16 Grain Boundary and Twin Boundary Density

SAMPLE SEMIX F-2. Sample in polished condition. Magnification 100X.

Field area = 0.0241 cm^2. Circumference of test circle = $\pi \cdot D$ = 0.55 cm.

A denotes No. of grain boundary intersections with circumference of test circle.

B denotes No. of twin boundary intersections with circumference of test circle.

X and Y denotes field location of the data measured.

FIELD Y	FIELD No.	FIELD X	A	No. of twins	B
12	1	33	0	6	9
12	2	35	0	4	7
12	3	37	0	0	0
12	4	39	0	0	0
12	5	41	2	0	0
12	6	43	0	0	0
12	7	45	0	0	0
12	8	47	0	0	0
12	9	49	0	2	4
12	10	51	3	3	2
14	11	50	2	19	28
14	12	47	0	0	0
14	13	44	0	0	0
14	14	41	5	0	0
14	15	38	5	0	0
14	16	35	3	28	12
16	17	34	2	30	27
16	18	36	2	26	24
16	19	38	2	3	3
16	20	40	4	10	12
16	21	42	2	5	5
16	22	44	0	0	0
16	23	46	3	1	2
16	24	48	6	12	10
16	25	50	5	11	16
18	26	49	5	3	3
18	27	46	3	2	3
18	28	43	5	5	4
18	29	40	2	6	9
18	30	37	3	46	22
20	31	37	3	3	5
20	32	39	6	6	2
20	33	41	9	10	8
20	34	43	7	5	4
20	35	45	7	2	8
20	36	47	11	3	1
10	37	50	0	0	0
10	38	47	0	2	4
10	39	44	0	0	0
10	40	41	0	0	0
10	41	38	0	0	0
10	42	35	0	0	0
8	43	34	0	0	0
8	44	36	0	0	0
8	45	38	0	0	0
8	46	40	0	0	0
8	47	42	0	0	0
8	48	44	0	0	0
8	49	46	0	0	0
8	50	48	0	2	4
8	51	50	0	0	0
6	52	49	0	1	2
6	53	46	0	0	0
6	54	43	0	0	0
6	55	40	2	6	6
6	56	37	0	0	0
4	57	37	0	0	0
4	58	39	4	5	5
4	59	41	5	19	13
4	60	43	0	0	0
4	61	45	0	0	0
4	62	47	0	0	0
Total for 62 fields:			118	287	264

L_A for grain boundary $= \frac{\pi}{2} \cdot P_L = \frac{\pi \times 118}{2 \times 62 \times 0.55} = 5.44 \frac{cm}{cm^2}$

L_A for twin boundary $= \frac{\pi \times 264}{2 \times 62 \times 0.55} = 12.16 \frac{cm}{cm^2}$

$\overline{X}$ for grain boundary = 1.9

σ for grain boundary = 2.6

$\overline{X}$ for twin boundary = 4.3

σ for twin boundary = 6.8

TABLE 17 Precipitate Particle Density

SAMPLE SFMIX F-2. Sample in polished condition. Magnification 400X.

Field area = 0.00149 cm^2

A denotes No. of Large precipitates observed in field of view.

B denotes No. of Small precipitates observed in field of view.

X and Y denotes location of microscope stage for the data measured.

FIELD Y	No.	X	B		A
12	1	33	11		1
12	2	35	4		0
12	3	37	35		3
12	4	39	43		2
12	5	41	2		0
12	6	43	26		13
12	7	45	3		0
12	8	47	26		3
12	9	49	6		1
12	10	51	34		0
14	11	50	35		2
14	12	47	3		0
14	13	44	3		1
14	14	41	6		1
14	15	38	8		0
14	16	35	0		0
16	17	34	6		0
16	18	36	1		3
16	19	38	5		0
16	20	40	1		1
16	21	42	2		0
16	22	44	4		1
16	23	46	5		0
16	24	48	0		0
16	25	50	1		2
18	26	49	0		1
18	27	46	0		0
18	28	43	1		0
18	29	40	1		2
18	30	37	1		0
20	31	37	3		0
20	32	39	2		2
20	33	41	1		0
20	34	43	0		1
20	35	45	0		0
20	36	47	4		0
10	37	50	7		8
10	38	47	1		0
10	39	44	16		0
10	40	41	42		0
10	41	38	7		0
10	42	35	15		0
8	43	34	3		5
8	44	36	7		2
8	45	38	7		3
8	46	40	4		2
8	47	42	2		0
8	48	44	0		0
8	49	46	5		0
8	50	48	1		0
8	51	50	5		1
6	52	49	0		0
6	53	46	4		1
6	54	43	2		0
6	55	40	6		2
6	56	37	3		1
4	57	37	6		2
4	58	39	2		0
4	59	41	3		0
4	60	43	2		1
4	61	45	6		0
4	62	47	0		0
Total for 62 fields:			447		68

Area of 62 fields = 0.09238 cm^2

No. of large ppt. = 68 / 0.09238 = 736 / cm^2

$\bar{X}$ for large ppt. = 1.1

σ for large ppt. = 2.1

No. of small ppt. = 447 / 0.09238 = 4840 / cm^2

$\bar{X}$ for small ppt. = 7.2

σ for small ppt. = 10.5

TABLE 18 DISLOCATION DENSITY

SAMPLE SEMIX F-2. Sample in etched condition

Magnification 1000X, Area of field = 0.000238 cm^2

X and Y denote the location of microscope stage (field of view)for the data measured.

FIELD Y	FIELD No.	FIELD X	No. of Dislocation Pits
12	1	34	7
12	2	35	0
12	3	37	15
12	4	39	14
12	5	41	16
12	6	43	7
12	7	45	4
12	8	47	7
12	9	49	2
12	10	50	4
14	11	49	6
14	12	47	2
14	13	44	4
14	14	41	5
14	15	38	5
14	16	35	12
16	17	35	8
16	18	36	3
16	19	38	3
16	20	40	13
16	21	42	7
16	22	44	5
16	23	46	110
16	24	48	1
16	25	49	3
18	26	47	9
18	27	46	188
18	28	43	9
18	29	40	13
18	30	37	47
19	31	37	
19	32	39	36
19	33	41	850
19	34	43	44
19	35	45	
19	36	47	
10	37	50	23
10	38	47	36
10	39	44	31

FIELD Y	FIELD No.	FIELD X	No. of Dislocation Pits
10	40	41	41
10	41	38	47
10	42	35	34
8	43	35	22
8	44	36	18
8	45	38	22
8	46	40	37
8	47	42	127
8	48	44	58
8	49	46	25
8	50	48	38
8	51	49	22
6	52	49	16
6	53	46	29
6	54	43	68
6	55	40	16
6	56	37	20
5	57	38	21
5	58	39	19
5	59	41	45
5	60	43	14
5	61	45	26
5	62	47	20
Total for fields:	59		2334

Dislocation density

$= 2334/(59)(0.000238 \text{ pits/cm}^2$

$= 1.7 \times 10^5 \text{ pits / cm}^2$

$\overline{X} = 40$

$\sigma = 111$

ORIGINAL PAGE IS OF POOR QUALITY

TABLE 19 Grain Boundary and Twin Boundary Density

SAMPLE SEMIX G-12. Sample in polished condition. Magnification 100X.

Field area = 0.0241 cm^2, Circumference of test circle = $\pi \cdot D$ = 0.55 cm.

A denotes No. of grain boundary intersections with circumference of test circle.

B denotes No. of twin boundary intersections with circumference of test circle.

X and Y denotes field location of the data measured.

FIELD Y	FIELD No.	FIELD X	A	No. of twins	B
12	1	33	2	6	9
12	2	35	5	2	4
12	3	37	2	3	3
12	4	39	5	13	16
12	5	41	2	4	3
12	6	43	8	30	38
12	7	45	8	74	100
12	8	47	4	52	38
12	9	49	4	44	9
12	10	51	6	79	42
14	11	50	2	25	16
14	12	47	3	7	7
14	13	44	5	0	0
14	14	41	10	5	2
14	15	38	2	4	2
14	16	35	0	0	0
16	17	34	2	0	0
16	18	36	5	6	3
16	19	38	4	10	3
16	20	40	8	10	5
16	21	42	10	8	3
16	22	44	4	1	1
16	23	46	6	69	15
16	24	48	3	12	2
16	25	50	4	16	16
18	26	49	4	30	8
18	27	46	4	19	15
18	28	43	0	0	0
18	29	40	5	15	6
18	30	37	7	20	5
20	31	37	9	11	13
20	32	39	8	27	22
20	33	41	3	12	10
20	34	43	5	16	8
20	35	45	0	2	3
20	36	47	2	6	11
10	37	50	0	18	28
10	38	47	9	22	11
10	39	44	4	32	24
10	40	41	6	39	11
10	41	38	3	24	24
10	42	35	3	6	2
8	43	34	3	6	6
8	44	36	2	22	22
8	45	38	3	16	19
8	46	40	8	26	17
8	47	42	3	14	18
8	48	44	6	19	26
8	49	46	3	45	34
8	50	48	2	15	26
8	51	50	0	5	10
6	52	49	0	7	5
6	53	46	2	19	24
6	54	43	8	38	40
6	55	40	7	24	18
6	56	37	2	0	0
4	57	37	8	13	6
4	58	39	2	3	4
4	59	41	6	16	9
4	60	43	4	38	20
4	61	45	5	33	22
4	62	47	2	19	20
Total for 62 fields:			262	1157	884

L_A for grain boundary $= \frac{\pi}{2} \cdot P_L = \frac{\pi \times 262}{2 \times 62 \times 0.55} = 12.07 \frac{cm}{cm^2}$

L_A for twin boundary $= \frac{\pi \times 884}{2 \times 62 \times 0.55} = 40.72 \frac{cm}{cm^2}$

$\overline{X}$ for grain boundary = 4.2

σ for grain boundary = 2.6

$\overline{X}$ for twin boundary = 14.3

σ for twin boundary = 15.5

TABLE 20 Precipitate Particle Density

SAMPLE SEMIX G-12. Sample in polished condition. Magnification 400X.

Field area = 0.00149 cm^2

A denotes No. of Large precipitates observed in field of view.

B denotes No. of Small precipitates observed in field of view.

X and Y denotes location of microscope stage for the data measured.

FIELD			A		B
Y	No.	X			
12	1	33	0		16
12	2	35	0		18
12	3	37	1		3
12	4	39	0		9
12	5	41	1		15
12	6	43	0		8
12	7	45	0		1
12	8	47	0		2
12	9	49	0		7
12	10	51	0		11
14	11	50	1		2
14	12	47	0		27
14	13	44	0		8
14	14	41	0		26
14	15	38	1		5
14	16	35	0		8
16	17	34	0		36
16	18	36	0		40
16	19	38	0		12
16	20	40	1		21
16	21	42	0		9
16	22	44	1		2
16	23	46	1		12
16	24	48	0		1
16	25	50	0		3
18	26	49	0		14
18	27	46	0		1
18	28	43	1		9
18	29	40	0		20
18	30	37	0		12
20	31	37	0		7
20	32	39	0		5
20	33	41	0		6
20	34	43	0		7
20	35	45	0		0
20	36	47	0		13
10	37	50	0		10
10	38	47	1		4
10	39	44	0		9
10	40	41	0		6
10	41	38	0		9
10	42	35	1		9
8	43	34	0		3
8	44	36	0		6
8	45	38	0		2
8	46	40	0		3
8	47	42	0		2
8	48	44	1		17
8	49	46	0		2
8	50	48	1		16
8	51	50	0		14
6	52	49	0		3
6	53	46	0		10
6	54	43	1		11
6	55	40	0		2
6	56	37	0		15
4	57	37	0		13
4	58	39	0		4
4	59	41	0		11
4	60	43	0		1
4	61	45	0		11
4	62	47	0		4
Total for 62 fields:			13		593

Area of 62 fields = 0.09238 cm^2

No. of large ppt. = 13 /0.09238 = 140 / cm^2

$\bar{X}$ for large ppt. = 0.21

σ for large ppt. = 0.41

No. of small ppt. = 593 /0.09238 = 6420/ cm^2

$\bar{X}$ for small ppt. = 9.6

σ for small ppt. = 8.0

TABLE 21 DISLOCATION DENSITY

SAMPLE SEMIX G-12. Sample in etched condition

Magnification 1000X, Area of field = 0.000238 cm^2

X and Y denote the location of microscope stage (field of view)for the data measured.

FIELD			No. of Dislocation Pits		
Y	No.	X		↓	
12	1	34			
12	2	35		1	
12	3	37		2	
12	4	39		25	
12	5	41		0	
12	6	43		27	
12	7	45		0	
12	8	47		106	
12	9	49		187	
12	10	50		182	
14	11	49		125	
14	12	47		158	
14	13	44		163	
14	14	41		6	
14	15	38		92	
14	16	35		23	
16	17	35		21	
16	18	36		49	
16	19	38		89	
16	20	40		63	
16	21	42		10	
16	22	44		480	
16	23	46		310	
16	24	48		1000	
16	25	49		92	
18	26	47		23	
18	27	46		122	
18	28	43		15	
18	29	40		99	
18	30	37		74	
19	31	37			
19	32	39		108	
19	33	41		230	
19	34	43		450	
19	35	45		20	
19	36	47			
10	37	50		320	
10	38	47		275	
10	39	44		16	

FIELD			No. of Dislocation Pits		
Y	No.	X		↓	
10	40	41		33	
10	41	38		3	
10	42	35		3	
8	43	35			
8	44	36		0	
8	45	38		58	
8	46	40		127	
8	47	42		112	
8	48	44		78	
8	49	46		135	
8	50	48		15	
8	51	49			
6	52	49		72	
6	53	46		63	
6	54	43		15	
6	55	40		2	
6	56	37		10	
5	57	38			
5	58	39		85	
5	59	41		41	
5	60	43		70	
5	61	45		47	
5	62	47			

Total for 55 fields: 5932

Dislocation density

$= 5932/(55)(0.000238)$ pits/cm^2

$= 4.5 \times 10^5$ pits/cm^2

$\overline{X} = 108$

$\sigma = 161$

TABLE 22 Grain Boundary and Twin Boundary Density

SAMPLE SEMIX H-8, Sample in polished condition. Magnification 100X .

Field area = 0.0241 cm^2. Circumference of test circle = $\pi \cdot D$ = 0.55 cm.

A denotes No. of grain boundary intersections with circumference of test circle.

B denotes No. of twin boundary intersections with circumference of test circle.

X and Y denotes field location of the data measured.

FIELD Y	FIELD No.	FIELD X	A	No. of twins	B
12	1	33	8	44	19
12	2	35	3	4	5
12	3	37	4	9	8
12	4	39	2	4	3
12	5	41	5	6	6
12	6	43	2	10	11
12	7	45	2	1	2
12	8	47	2	3	1
12	9	49	5	13	12
12	10	51	4	3	3
14	11	50	2	10	12
14	12	47	2	2	2
14	13	44	2	4	4
14	14	41	2	4	2
14	15	38	5	15	10
14	16	35	3	12	15
16	17	34	6	19	18
16	18	36	2	12	17
16	19	38	2	2	2
16	20	40	6	17	24
16	21	42	6	39	34
16	22	44	0	1	2
16	23	46	3	2	2
16	24	48	3	2	2
16	25	50	6	1	2
18	26	49	2	0	0
18	27	46	0	0	0
18	28	43	3	6	8
18	29	40	3	4	45
18	30	37	3	17	19
20	31	37	5	12	9
20	32	39	4	22	18
20	33	41	5	48	44
20	34	43	2	54	68
20	35	45	2	13	13
20	36	47	0	0	0
10	37	50	2	4	5
10	38	47	0	0	0
10	39	44	3	13	6
10	40	41	3	15	9
10	41	38	2	2	2
10	42	35	5	15	13
8	43	34	7	20	24
8	44	36	6	17	17
8	45	38	3	4	4
8	46	40	3	1	1
8	47	42	2	17	5
8	48	44	5	54	39
8	49	46	0	14	28
8	50	48	4	9	11
8	51	50	0	7	9
6	52	49	4	11	10
6	53	46	4	21	34
6	54	43	4	37	18
6	55	40	7	8	11
6	56	37	4	113	28
4	57	37	6	50	31
4	58	39	2	7	13
4	59	41	3	3	3
4	60	43	0	0	0
4	61	45	6	35	6
4	62	47	4	4	4
Total for 62 fields:			205	931	779

L_A for grain boundary $= \frac{\pi}{2} \cdot P_L = \frac{\pi \times 205}{2 \times 62 \times 0.55} = 9.44 \frac{cm}{cm^2}$

L_A for twin boundary $= \frac{\pi \times 779}{2 \times 62 \times 0.55} = 35.88 \frac{cm}{cm^2}$

$\overline{X}$ for grain boundary = 3.3

σ for grain boundary = 1.9

$\overline{X}$ for twin boundary = 12.6

σ for twin boundary = 13.3

TABLE 23 Precipitate Particle Density

SAMPLE SEMIX H-8. Sample in polished condition. Magnification 400X.

Field area = 0.00149 cm^2

A denotes No. of Large precipitates observed in field of view.

B denotes No. of Small precipitates observed in field of view.

X and Y denotes location of microscope stage for the data measured.

FIELD Y	No.	X	A		B	FIELD Y	No.	X	A		B
12	1	33	2		48	10	40	41	0		10
12	2	35	2		3	10	41	38	4		10
12	3	37	0		13	10	42	35	0		38
12	4	39	0		7	8	43	34	0		41
12	5	41	0		9	8	44	36	0		19
12	6	43	1		14	8	45	38	0		25
12	7	45	0		8	8	46	40	0		12
12	8	47	0		5	8	47	42	1		7
12	9	49	1		6	8	48	44	0		11
12	10	51	1		9	8	49	46	0		23
14	11	50	0		17	8	50	48	1		14
14	12	47	0		9	8	51	50	0		18
14	13	44	1		14	6	52	49	0		19
14	14	41	0		19	6	53	46	0		34
14	15	38	0		11	6	54	43	0		8
14	16	35	0		28	6	55	40	0		4
16	17	34	1		14	6	56	37	0		9
16	18	36	0		5	4	57	37	1		13
16	19	38	0		3	4	58	39	0		9
16	20	40	0		4	4	59	41	0		6
16	21	42	0		11	4	60	43	0		16
16	22	44	0		1	4	61	45	0		17
16	23	46	0		5	4	62	47	0		15
16	24	48	0		7	Total for 62 fields:			23		875
16	25	50	0		8						
18	26	49	0		3						
18	27	46	0		10						
18	28	43	3		18						
18	29	40	0		3						
18	30	37	0		14						
20	31	37	0		37						
20	32	39	2		52						
20	33	41	0		11						
20	34	43	0		22						
20	35	45	1		9						
20	36	47	0		15						
10	37	50	0		7						
10	38	47	0		3						
10	39	44	1		15						

Area of 62 fields = 0.09238 cm^2

No. of large ppt. = 23/0.09238 = 250/ cm^2

$\bar{X}$ for large ppt. = 0.4

σ for large ppt. = 0.8

No. of small ppt. = 875 /0.09238 = 9470 / cm^2.

$\bar{X}$ for small ppt. = 14.1

σ for small ppt. = 10.9

TABLE 24 DISLOCATION DENSITY

SAMPLE SEMIX H-8. Sample in etched condition

Magnification 1000X, Area of field = 0.000238 cm^2

X and Y denote the location of microscope stage (field of view)for the data measured.

FIELD Y	No.	X	No. of Dislocation Pits
12	1	34	138
12	2	35	103
12	3	37	4
12	4	39	71
12	5	41	197
12	6	43	215
12	7	45	360
12	8	47	222
12	9	49	172
12	10	50	155
14	11	49	19
14	12	47	3
14	13	44	78
14	14	41	6
14	15	38	69
14	16	35	125
16	17	35	
16	18	36	320
16	19	38	24
16	20	40	248
16	21	42	127
16	22	44	17
16	23	46	16
16	24	48	2
16	25	49	2
18	26	47	310
18	27	46	189
18	28	43	271
18	29	40	425
18	30	37	219
19	31	37	111
19	32	39	303
19	33	41	82
19	34	43	300
19	35	45	180
19	36	47	
10	37	50	6
10	38	47	307
10	39	44	226

FIELD Y	No.	X	No. of Dislocation Pits
10	40	41	164
10	41	38	960
10	42	35	72
8	43	35	
8	44	36	49
8	45	38	1050
8	46	40	23
8	47	42	725
8	48	44	119
8	49	46	325
8	50	48	213
8	51	49	
6	52	49	255
6	53	46	32
6	54	43	83
6	55	40	1030
6	56	37	3
5	57	38	
5	58	39	21
5	59	41	184
5	60	43	228
5	61	45	270
5	62	47	

Total for fields: 56 11428

Dislocation density

$= 11428/(56)(0.000238)$ pits/cm^2

$= 8.6 \times 10^5$ pits/cm^2

$\bar{X} = 204$

$\sigma = 235$

TABLE 25 Grain Boundary and Twin Boundary Density

SAMPLE: Semix 1-10-13(T) Sample in polished condition. Magnification 100X .
Field area = 0.0241 cm^2. Circumference of test circle = $\pi \cdot D$ = 0.55 cm.
A denotes No. of grain boundary intersections with circumference of test circle.
B denotes No. of twin boundary intersections with circumference of test circle.
X and Y denotes field location of the data measured.

FIELD			A	No. of twins	B
Y	No.	X	GB		Twin
12	1	33	0		9
12	2	35	2		3
12	3	37	5		38
12	4	39	4		67
12	5	41	0		0
12	6	43	3		17
12	7	45	0		40
12	8	47	2		35
12	9	49	2		10
12	10	51	2		13
14	11	50	0		3
14	12	47	0		6
14	13	44	2		1
14	14	41	0		0
14	15	38	0		3
14	16	35	2		5
16	17	34	3		12
16	18	36	3		4
16	19	38	2		10
16	20	40	5		6
16	21	42	3		9
16	22	44	2		2
16	23	46	0		8
16	24	48	0		1
16	25	50	0		0
18	26	49	4		36
18	27	46	4		33
18	28	43	4		36
18	29	40	4		30
18	30	37	0		1
20	31	37	0		0
20	32	39	4		0
20	33	41	0		15
20	34	43	0		32
20	35	45	2		26
20	36	47	5		80
10	37	50	2		84
10	38	47	5		70
10	39	44			
10	40	41	2		37
10	41	38	6		78
10	42	35	4		7
8	43	34	3		30
8	44	36	2		29
8	45	38	2		32
8	46	40	4		32
8	47	42	3		21
8	48	44	2		62
8	49	46	2		73
8	50	48	6		76
8	51	50	3		59
6	52	49	8		61
6	53	46	2		24
6	54	43	5		25
6	55	40	4		34
6	56	37	8		7
4	57	37	10		7
4	58	39	7		8
4	59	41	4		43
4	60	43	0		50
4	61	45	3		71
4	62	47	5		76
Total for 62 fields:			171		1720

L_A for grain boundary $= \frac{\pi}{2} \cdot P_L = \frac{\pi}{2} \frac{2.76}{0.55} = 7.88$ cm/cm^2

L_A for twin boundary $= \frac{\pi}{2} \frac{27.7}{0.55} = 79.2$ cm/cm^2

$\overline{X}$ for grain boundary = 2.76
σ for grain boundary = 2.28

$\overline{X}$ for twin boundary = 27.7
σ for twin boundary = 25.3

TABLE 26 Precipitate Particle Density

SAMPLE: Semix 1-10-13 (T) Sample in polished condition. Magnification 400X.

Field area = 0.00149 cm^2

A denotes No. of Large precipitates observed in field of view.

B denotes No. of Small precipitates observed in field of view.

X and Y denotes location of microscope stage for the data measured.

FIELD Y	No.	X	A Large		B Small
12	1	33	0		23
12	2	35	2		94
12	3	37	8		208
12	4	39	1		24
12	5	41	3		36
12	6	43	4		10
12	7	45	2		9
12	8	47	1		60
12	9	49	3		137
12	10	51	2		15
14	11	50	1		6
14	12	47	0		13
14	13	44	1		10
14	14	41	3		6
14	15	38	5		83
14	16	35	3		39
16	17	34	4		30
16	18	36	3		39
16	19	38	4		195
16	20	40	5		241
16	21	42	4		56
16	22	44	3		80
16	23	46	1		19
16	24	48	0		5
16	25	50	4		161
18	26	49	1		46
18	27	46	3		45
18	28	43	2		21
18	29	40	2		73
18	30	37	0		35
20	31	37	1		48
20	32	39	1		45
20	33	41	2		70
20	34	43	3		48
20	35	45	1		5
20	36	47	4		114
10	37	50	2		61
10	38	47	2		11
10	39	44	1		2

FIELD Y	No.	X	A		B
10	40	41	12		120
10	41	38	6		38
10	42	35	1		115
8	43	34	11		229
8	44	36	3		6
8	45	38	1		105
8	46	40	0		40
8	47	42	1		7
8	48	44	4		128
8	49	46	1		1
8	50	48	4		139
8	51	50	1		20
6	52	49	7		336
6	53	46	8		54
6	54	43	5		11
6	55	40	1		12
6	56	37	2		92
4	57	37	4		43
4	58	39	2		48
4	59	41	11		140
4	60	43	3		90
4	61	45	3		51
4	62	47	5		35

Total for 62 fields: 188 4083

Area of 62 fields = 0.09238 cm^2

No. of large ppt. = 188/0.09238 = 2035 / cm^2

$\bar{X}$ for large ppt. = 3.0

σ for large ppt. = 2.6

No. of small ppt. = 4083 /0.09238 = 44200 / cm^2

$\bar{X}$ for small ppt. = 66

σ for small ppt. = 67

TABLE 26 Precipitate Particle Density

SAMPLE: Semix 1-10-13 (T) Sample in polished condition. Magnification 400X.

Field area = 0.00149 cm^2

A denotes No. of Large precipitates observed in field of view.

B denotes No. of Small precipitates observed in field of view.

X and Y denotes location of microscope stage for the data measured.

FIELD			A		B
Y	No.	X	Large		Small
12	1	33	0		23
12	2	35	2		94
12	3	37	8		208
12	4	39	1		24
12	5	41	3		36
12	6	43	4		10
12	7	45	2		9
12	8	47	1		60
12	9	49	3		137
12	10	51	2		15
14	11	50	1		6
14	12	47	0		13
14	13	44	1		10
14	14	41	3		6
14	15	38	5		83
14	16	35	3		39
16	17	34	4		30
16	18	36	3		39
16	19	38	4		195
16	20	40	5		241
16	21	42	4		56
16	22	44	3		80
16	23	46	1		19
16	24	48	0		5
16	25	50	4		161
18	26	49	1		46
18	27	46	3		45
18	28	43	2		21
18	29	40	2		73
18	30	37	0		35
20	31	37	1		48
20	32	39	1		45
20	33	41	2		70
20	34	43	3		48
20	35	45	1		5
20	36	47	4		114
10	37	50	2		61
10	38	47	2		11
10	39	44	1		2
10	40	41	12		120
10	41	38	6		38
10	42	35	1		115
8	43	34	11		229
8	44	36	3		6
8	45	38	1		105
8	46	40	0		40
8	47	42	1		7
8	48	44	4		128
8	49	46	1		1
8	50	48	4		139
8	51	50	1		20
6	52	49	7		336
6	53	46	8		54
6	54	43	5		11
6	55	40	1		12
6	56	37	2		92
4	57	37	4		43
4	58	39	2		48
4	59	41	11		140
4	60	43	3		90
4	61	45	3		51
4	62	47	5		35
Total for 62 fields:			188		4083

Area of 62 fields = 0.09238 cm^2

No. of large ppt. = 188/0.09238 = 2035 / cm^2

$\bar{X}$ for large ppt. = 3.0

σ for large ppt. = 2.6

No. of small ppt. = 4083 /0.09238 = 44200 / cm^2

$\bar{X}$ for small ppt. = 66

σ for small ppt. = 67

TABLE 27 **DISLOCATION DENSITY**

SAMPLE: Semix 1-10-13 (T) **Sample in etched condition**

Magnification 1000X, Area of field = 0.000238 cm^2

X and Y denote the location of microscope stage (field of view)for the data measured.

FIELD			No. of Dislocation Pits
Y	No.	X	↓
12	1	34	1
12	2	35	5
12	3	37	4
12	4	39	0
12	5	41	2
12	6	43	2
12	7	45	4
12	8	47	4
12	9	49	6
12	10	50	4
14	11	49	0
14	12	47	0
14	13	44	8
14	14	41	2
14	15	38	4
14	16	35	3
16	17	35	2
16	18	36	1
16	19	38	2
16	20	40	7
16	21	42	5
16	22	44	0
16	23	46	4
16	24	48	5
16	25	49	0
18	26	47	73
18	27	46	5
18	28	43	6
18	29	40	6
18	30	37	1
19	31	37	1
19	32	39	4
19	33	41	4
19	34	43	0
19	35	45	32
19	36	47	17
10	37	50	3
10	38	47	8
10	39	44	0

FIELD			No. of Dislocation Pits
Y	No.	X	↓
10	40	41	1
10	41	38	83
10	42	35	6
8	43	35	1
8	44	36	6
8	45	38	4
8	46	40	3
8	47	42	16
8	48	44	7
8	49	46	10
8	50	48	20
8	51	49	13
6	52	49	12
6	53	46	13
6	54	43	7
6	55	40	136
6	56	37	137
5	57	38	27
5	58	39	4
5	59	41	20
5	60	43	13
5	61	45	14
5	62	47	97

Total for fields: 62 885

Dislocation density = $6.0 \times 10^4 /cm^2$

$\overline{X}$ = 14.3

σ = 28.7

TABLE 28 Grain Boundary and Twin Boundary Density

SAMPLE: Semix 1-12-14(U) Sample in polished condition. Magnification 100X.
Field area = 0.0241 cm^2. Circumference of test circle = $\pi \cdot D$ = 0.55 cm.
A denotes No. of grain boundary intersections with circumference of test circle.
B denotes No. of twin boundary intersections with circumference of test circle.
X and Y denotes field location of the data measured.

FIELD Y	FIELD No.	FIELD X	A GB	No. of twins	B Twin
12	1	33	0		0
12	2	35	0		0
12	3	37	0		4
12	4	39	0		0
12	5	41	0		11
12	6	43	0		11
12	7	45	0		5
12	8	47	0		2
12	9	49	4		14
12	10	51	0		8
14	11	50	2		11
14	12	47	4		7
14	13	44	2		2
14	14	41	0		5
14	15	38	0		5
14	16	35	0		0
16	17	34	-		-
16	18	36	0		0
16	19	38	0		6
16	20	40	2		2
16	21	42	2		2
16	22	44	2		8
16	23	46	2		5
16	24	48	0		0
16	25	50	0		0
18	26	49	4		5
18	27	46	0		2
18	28	43	0		5
18	29	40	0		3
18	30	37	0		5
20	31	37	0		10
20	32	39	3		9
20	33	41	0		8
20	34	43	2		7
20	35	45	3		6
20	36	47	5		4
10	37	50	2		9
10	38	47	3		3
10	39	44	2		36

FIELD Y	FIELD No.	FIELD X	A	No. of twins	B
10	40	41	0		9
10	41	38	0		1
10	42	35	0		0
8	43	34	2		8
8	44	36	0		4
8	45	38	0		6
8	46	40	0		2
8	47	42	0		13
8	48	44	0		34
8	49	46	0		9
8	50	48	2		28
8	51	50	2		6
6	52	49	2		35
6	53	46	2		52
6	54	43	0		18
6	55	40	2		24
6	56	37	4		6
4	57	37	0		0
4	58	39	0		16
4	59	41	3		14
4	60	43	0		19
4	61	45	2		31
4	62	47	2		68
Total for 61 fields:			67		623

L_A for grain boundary $= \frac{\pi}{2} \cdot P_L = \frac{\pi}{2} \frac{1.1}{0.55} = 3.14$ cm/cm^2

L_A for twin boundary $= \frac{\pi}{2} \frac{10.21}{0.55} = 29.2$ cm/cm^2

$\overline{X}$ for grain boundary = 1.1
σ for grain boundary = 1.4

$\overline{X}$ for twin boundary = 10.2
σ for twin boundary = 12.8

ORIGINAL PAGE IS OF POOR QUALITY

TABLE 29 Precipitate Particle Density

SAMPLE: Semixl-12-14 (U) Sample in polished condition. Magnification 400X.

Field area = 0.00149 cm^2

A denotes No. of Large precipitates observed in field of view.

B denotes No. of Small precipitates observed in field of view.

X and Y denotes location of microscope stage for the data measured.

FIELD			A		B	FIELD			A		B
Y	No.	X	Large		Small	Y	No.	X			
12	1	33	5		129	10	40	41	2		38
12	2	35	3		14	10	41	38	0		32
12	3	37	2		20	10	42	35	2		25
12	4	39	2		44	8	43	34	4		46
12	5	41	5		42	8	44	36	2		30
12	6	43	2		25	8	45	38	1		34
12	7	45	6		104	8	46	40	2		41
12	8	47	3		39	8	47	42	1		17
12	9	49	4		43	8	48	44	3		62
12	10	51	11		175	8	49	46	7		75
14	11	50	4		70	8	50	48	1		43
14	12	47	2		20	8	51	50	1		60
14	13	44	4		8	6	52	49	3		92
14	14	41	3		11	6	53	46	1		67
14	15	38	6		30	6	54	43	2		41
14	16	35	2		13	6	55	40	0		60
16	17	34	-		-	6	56	37	2		56
16	18	36	1		41	4	57	37	0		8
16	19	38	2		27	4	58	39	1		59
16	20	40	1		30	4	59	41	0		41
16	21	42	2		19	4	60	43	2		24
16	22	44	4		40	4	61	45	2		45
16	23	46	1		33	4	62	47	3		31
16	24	48	2		54						
16	25	50	3		99						
18	26	49	7		49						
18	27	46	1		36						
18	28	43	1		47						
18	29	40	2		45						
18	30	37	3		36						
20	31	37	0		7						
20	32	39	2		26						
20	33	41	5		20						
20	34	43	3		37						
20	35	45	2		39						
20	36	47	3		67						
10	37	50	2		55						
10	38	47	1		75						
10	39	44	1		26						

Total for 61 fields: 155 2724

Area of 62 fields = 0.09089 cm^2

No. of large ppt. = 155/0.09089 = 1705 / cm^2

$\bar{X}$ for large ppt. = 2.54

σ for large ppt. = 1.96

No. of small ppt. = 2724 /0.09089 = 29970 / cm^2

$\bar{X}$ for small ppt. = 44.7

σ for small ppt. = 29.1

TABLE 30 DISLOCATION DENSITY

SAMPLE: Semix 1-12-14 (U) Sample in etched condition

Magnification 1000X, Area of field = 0.000238 cm^2

X and Y denote the location of microscope stage (field of view)for the data measured.

FIELD Y	No.	X	No. of Dislocation Pits
12	1	34	7
12	2	35	6
12	3	37	17
12	4	39	5
12	5	41	7
12	6	43	9
12	7	45	2
12	8	47	5
12	9	49	4
12	10	50	4
14	11	49	0
14	12	47	2
14	13	44	7
14	14	41	2
14	15	38	2
14	16	35	0
16	17	35	4
16	18	36	0
16	19	38	3
16	20	40	0
16	21	42	1
16	22	44	0
16	23	46	1
16	24	48	0
16	25	49	15
18	26	47	1
18	27	46	0
18	28	43	4
18	29	40	1
18	30	37	3
19	31	37	5
19	32	39	1
19	33	41	0
19	34	43	2
19	35	45	0
19	36	47	0
10	37	50	3
10	38	47	3
10	39	44	1

FIELD Y	No.	X	No. of Dislocation Pits
10	40	41	4
10	41	38	4
10	42	35	2
8	43	35	3
8	44	36	1
8	45	38	8
8	46	40	2
8	47	42	0
8	48	44	0
8	49	46	2
8	50	48	1
8	51	49	1
6	52	49	0
6	53	46	3
6	54	43	0
6	55	40	0
6	56	37	1
5	57	38	0
5	58	39	2
5	59	41	0
5	60	43	0
5	61	45	5
5	62	47	0

Total for fields: 62 166

Dislocation density = $1.1 \times 10^4 /cm^2$

$\overline{X} = 2.68$

$\sigma = 3.34$

TABLE 31 Grain Boundary and Twin Boundary Density

SAMPLE: Semix 2-5-1 (V_2) Sample in polished condition. Magnification 100X.
Field area = 0.0241 cm^2. Circumference of test circle = $\pi \cdot D$ = 0.55 cm.
A denotes No. of grain boundary intersections with circumference of test circle.
B denotes No. of twin boundary intersections with circumference of test circle.
X and Y denotes field location of the data measured.

FIELD Y	No.	X	A GB	No. of twins	B Twin
12	1	33	2		0
12	2	35	8		0
12	3	37	23		0
12	4	39	22		0
12	5	41	17		1
12	6	43	5		0
12	7	45	5		15
12	8	47	5		8
12	9	49	4		9
12	10	51	2		26
[illegible]	11	50	2		11
14	12	47	3		36
14	13	44	10		13
14	14	41	6		9
14	15	38	8		3
14	16	35	10		1
16	17	34	3		10
16	18	36	7		40
16	19	38	14		40
16	20	40	22		17
16	21	42	11		13
16	22	44	5		29
16	23	46	12		46
16	24	48	9		15
16	25	50	15		5
18	26	49	3		1
18	27	46	11		24
18	28	43	14		26
18	29	40	13		13
18	30	37	12		43
20	31	37	19		25
20	32	39	22		11
20	33	41	17		26
20	34	43	19		23
20	35	45	12		52
20	36	47	4		14
10	37	50	3		0
10	38	47	23		5
10	39	44	26		8
10	40	41	12		8
10	41	38	2		0
10	42	35	0		0
8	43	34	0		0
8	44	36	0		0
8	45	38	5		0
8	46	40	6		1
8	47	42	13		0
8	48	44	19		8
8	49	46	29		1
8	50	48	21		0
8	51	50	17		0
6	52	49	15		2
6	53	46	22		0
6	54	43	23		10
6	55	40	13		3
6	56	37	0		0
4	57	37	6		50
4	58	39	11		39
4	59	41	13		41
4	60	43	13		8
4	61	45	12		0
4	62	47	14		0
Total for 62 fields:			694		789

$$L_A \text{ for grain boundary} = \frac{\pi}{2} \cdot P_L = \frac{\pi}{2} \frac{11.2}{0.55} = 32 \text{ cm/cm}^2$$

$$L_A \text{ for twin boundary} = \frac{\pi}{2} \frac{12.7}{0.55} = 36.3 \text{ cm/cm}^2$$

$\overline{X}$ for grain boundary = 11.2
σ for grain boundary = 7.4

$\overline{X}$ for twin boundary = 12.7
σ for twin boundary = 15.0

TABLE 32 Precipitate Particle Density

SAMPLE: Semix 2-5-1 (V) Sample in polished condition. Magnification 400X.

Field area = 0.00149 cm^2

A denotes No. of Large precipitates observed in field of view.

B denotes No. of Small precipitates observed in field of view.

X and Y denotes location of microscope stage for the data measured.

FIELD Y	No.	X	A Large	B Small
12	1	33	2	93
12	2	35	5	22
12	3	37	0	8
12	4	39	1	31
12	5	41	3	27
12	6	43	1	38
12	7	45	1	57
12	8	47	1	25
12	9	49	0	17
12	10	51	0	11
14	11	50	0	34
14	12	47	0	117
14	13	44	0	26
14	14	41	1	10
14	15	38	0	31
14	16	35	0	123
16	17	34	2	52
16	18	36	29	53
16	19	38	2	58
16	20	40	1	13
16	21	42	1	60
16	22	44	0	43
16	23	46	1	253
16	24	48	0	85
16	25	50	1	38
18	26	49	1	148
18	27	46	0	36
18	28	43	2	92
18	29	40	2	36
18	30	37	0	19
20	31	37	3	20
20	32	39	2	49
20	33	41	0	33
20	34	43	1	34
20	35	45	0	52
20	36	47	0	40
10	37	50	0	28
10	38	47	0	57
10	39	44	0	60
10	40	41	0	7
10	41	38	1	16
10	42	35	0	10
8	43	34	1	53
8	44	36	2	51
8	45	38	0	20
8	46	40	0	18
8	47	42	0	9
8	48	44	0	27
8	49	46	0	11
8	50	48	0	20
8	51	50	1	4
6	52	49	0	12
6	53	46	0	3
6	54	43	1	16
6	55	40	0	9
6	56	37	1	4
4	57	37	1	12
4	58	39	2	34
4	59	41	2	18
4	60	43	0	12
4	61	45	0	14
4	62	47	0	14
Total for 62 fields:			75	2425

Area of 62 fields = 0.09238 cm^2

No. of large ppt. = 75 /0.09238
= 812 / cm^2

$\bar{X}$ for large ppt. = 1.2

σ for large ppt. = 3.7

No. of small ppt. = 2425 /0.09238
= 26250 / cm^2

$\bar{X}$ for small ppt. = 39

σ for small ppt. = 40

TABLE 33 DISLOCATION DENSITY

SAMPLE: Semix 2-5-1 (V) Sample in etched condition

Magnification 1000X, Area of field = 0.000238 cm^2

X and Y denote the location of microscope stage (field of view)for the data measured.

FIELD Y	FIELD No.	FIELD X	No. of Dislocation Pits
12	1	34	7
12	2	35	19
12	3	37	5
12	4	39	32
12	5	41	3
12	6	43	9
12	7	45	8
12	8	47	5
12	9	49	7
12	10	50	4
14	11	49	26
14	12	47	62
14	13	44	27
14	14	41	325
14	15	38	22
14	16	35	58
16	17	35	17
16	18	36	21
16	19	38	50
16	20	40	148
16	21	42	0
16	22	44	5
16	23	46	14
16	24	48	6
16	25	49	7
18	26	47	6
18	27	46	15
18	28	43	138
18	29	40	56
18	30	37	196
19	31	37	430
19	32	39	16
19	33	41	95
19	34	43	210
19	35	45	650
19	36	47	43
10	37	50	4
10	38	47	3
10	39	44	45
10	40	41	28
10	41	38	7
10	42	35	9
8	43	35	1
8	44	36	2
8	45	38	7
8	46	40	3
8	47	42	5
8	48	44	9
8	49	46	12
8	50	48	8
8	51	49	5
6	52	49	7
6	53	46	19
6	54	43	27
6	55	40	7
6	56	37	5
5	57	38	10
5	58	39	15
5	59	41	8
5	60	43	13
5	61	45	15
5	62	47	18

Total for 62 fields: 3034

Dislocation density = 20.6 x $10^4/cm^2$

$\overline{X}$ = 48.9

σ = 108

TABLE 34 Grain Boundary and Twin Boundary Density

SAMPLE: Semix 3-4-12 (W) Sample in polished condition. Magnification 100X.

Field area = 0.0241 cm^2. Circumference of test circle = $\pi \cdot D$ = 0.55 cm.

A denotes No. of grain boundary intersections with circumference of test circle.

B denotes No. of twin boundary intersections with circumference of test circle.

X and Y denotes field location of the data measured.

FIELD			A	No. of twins	B
Y	No.	X	GB		Twin
12	1	33	2		5
12	2	35	4		5
12	3	37	4		0
12	4	39	9		8
12	5	41	14		5
12	6	43	8		27
12	7	45	5		48
12	8	47	0		14
12	9	49	3		23
12	10	51	0		18
14	11	50	2		4
14	12	47	0		5
14	13	44	12		10
14	14	41	8		3
14	15	38	5		12
14	16	35	8		13
16	17	34	7		6
16	18	36	7		0
16	19	38	4		11
16	20	40	5		8
16	21	42	10		7
16	22	44	2		0
16	23	46	5		0
16	24	48	5		6
16	25	50	14		11
18	26	49	7		22
18	27	46	2		5
18	28	43	5		17
18	29	40	3		10
18	30	37	14		5
20	31	37	3		4
20	32	39	10		17
20	33	41	1[illegible]		14
20	34	43	1[illegible]		18
20	35	45	4		1
20	36	47	0		1
10	37	50	6		0
10	38	47	6		15
10	39	44	7		4

FIELD			A	No. of twins	B
Y	No.	X			
10	40	41	7		53
10	41	38	3		14
10	42	35	2		32
8	43	34	6		16
8	44	36	7		29
8	45	38	6		27
8	46	40	10		19
8	47	42	4		45
8	48	44	9		39
8	49	46	6		15
8	50	48	9		3
8	51	50	4		5
6	52	49	2		41
6	53	46	3		13
6	54	43	8		21
6	55	40	5		17
6	56	37			
4	57	37			
4	58	39			
4	59	41			
4	60	43			
4	61	45			
4	62	47			
Total for 55 fields:			325		770

L_A for grain boundary $= \frac{\pi}{2} \cdot P_L = \frac{\pi}{2} \frac{5.9}{0.55} = 16.9$ cm/cm^2

L_A for twin boundary $= \frac{\pi}{2} \frac{14}{0.55} = 40$ cm/cm^2

$\overline{X}$ for grain boundary = 5.9

σ for grain boundary = 3.6

$\overline{X}$ for twin boundary = 14

σ for twin boundary = 12.7

TABLE 35 Precipitate Particle Density

SAMPLE: Semix 3-4-12 (W) Sample in polished condition. Magnification 400X.

Field area = 0.00149 cm^2

A denotes No. of Large precipitates observed in field of view.

B denotes No. of Small precipitates observed in field of view.

X and Y denotes location of microscope stage for the data measured.

FIELD			A		B
Y	No.	X	Large		Small
12	1	33	-		-
12	2	35	0		55
12	3	37	0		22
12	4	39	5		27
12	5	41	1		10
12	6	43	2		16
12	7	45	3		39
12	8	47	2		51
12	9	49	2		13
12	10	51	4		79
14	11	50	5		24
14	12	47	1		34
14	13	44	2		47
14	14	41	2		20
14	15	38	1		58
14	16	35	1		17
16	17	34	5		43
16	18	36	3		98
16	19	38	6		39
16	20	40	2		65
16	21	42	1		7
16	22	44	4		89
16	23	46	5		83
16	24	48	5		460
16	25	50	3		79
18	26	49	10		420
18	27	46	1		93
18	28	43	5		65
18	29	40	9		163
18	30	37	7		290
20	31	37	7		30
20	32	39	4		29
20	33	41	4		95
20	34	43	0		11
20	35	45	3		54
20	36	47	3		119
10	37	50	2		37
10	38	47	1		25
10	39	44	1		14

FIELD			A		B
Y	No.	X			
10	40	41	5		24
10	41	38	5		13
10	42	35	1		5
8	43	34	3		38
8	44	36	2		23
8	45	38	1		47
8	46	40	4		84
8	47	42	0		28
8	48	44	3		41
8	49	46	3		9
8	50	48	2		9
8	51	50	4		12
6	52	49	2		60
6	53	46	9		75
6	54	43	5		34
6	55	40	2		12
6	56	37	3		43
4	57	37	1		6
4	58	39	2		3
4	59	41	1		8
4	60	43	5		94
4	61	45	2		21
4	62	47	-		-
Total for 60 fields:			187		3609

Area of 62 fields = 0.0894 cm^2

No. of large ppt. = 187 /0.0894 = 2092 / cm^2

$\bar{X}$ for large ppt. = 3.1

σ for large ppt. = 2.3

No. of small ppt. = 3609 /0.0894 = 40370 / cm^2

$\bar{X}$ for small ppt. = 60

σ for small ppt. = 84

TABLE 36 DISLOCATION DENSITY

SAMPLE: Semix 3-4-12 (W) Sample in etched condition

Magnification 1000X, Area of field = 0.000238 cm^2

X and Y denote the location of microscope stage (field of view)for the data measured.

FIELD			No. of Dislocation Pits
Y	No.	X	↓
12	1	34	0
12	2	35	0
12	3	37	3
12	4	39	1
12	5	41	173
12	6	43	0
12	7	45	1
12	8	47	0
12	9	49	2
12	10	50	28
14	11	49	0
14	12	47	5
14	13	44	0
14	14	41	25
14	15	38	0
14	16	35	1
16	17	35	66
16	18	36	1
16	19	38	1
16	20	40	0
16	21	42	1
16	22	44	0
16	23	46	101
16	24	48	1
16	25	49	0
18	26	47	27
18	27	46	0
18	28	43	0
18	29	40	1
18	30	37	20
19	31	37	42
19	32	39	0
19	33	41	0
19	34	43	0
19	35	45	11
19	36	47	91
10	37	50	0
10	38	47	1
10	39	44	217
10	40	41	0
10	41	38	2
10	42	35	0
8	43	35	1
8	44	36	0
8	45	38	0
8	46	40	0
8	47	42	0
8	48	44	183
8	49	46	5
8	50	48	18
8	51	49	15
6	52	49	0
6	53	46	45
6	54	43	0
6	55	40	127
6	56	37	2
5	57	38	249
5	58	39	19
5	59	41	2
5	60	43	73
5	61	45	-
5	62	47	-

Total for 60 fields: 1561

Dislocation density = $10.9 \times 10^4/cm^2$

$\overline{X} = 26$

$\sigma = 55$

TABLE 37 Grain Boundary and Twin Boundary Density

SAMPLE: Semix 3-4-16 (X) **Sample in polished condition. Magnification 100X.**

Field area = 0.0241 cm^2. **Circumference of test circle** = $\pi \cdot D$ = **0.55 cm.**

A denotes No. of grain boundary intersections with circumference of **test circle.**

B denotes No. of twin boundary intersections with circumference of **test circle.**

X and Y denotes field location of the data measured.

FIELD Y	No.	X	A GB	No. of twins	B Twin
12	1	33	4		27
12	2	35	4		24
12	3	37	9		13
12	4	39	9		7
12	5	41	20		17
12	6	43	16		10
12	7	45	13		1
12	8	47	12		7
12	9	49	16		2
12	10	51	15		3
14	11	50	13		14
14	12	47	14		5
14	13	44	18		0
14	14	41	11		38
14	15	38	4		5
14	16	35	4		20
16	17	34	9		5
16	18	36	7		6
16	19	38	2		4
16	20	40	9		3
16	21	42	16		4
16	22	44	13		0
16	23	46	12		3
16	24	48	8		4
16	25	50	8		2
18	26	49	18		0
18	27	46	14		0
18	28	43	20		1
18	29	40	17		1
18	30	37	0		4
20	31	37	2		11
20	32	39	11		11
20	33	41	14		0
20	34	43	7		1
20	35	45	16		0
20	36	47	15		1
10	37	50	7		5
10	38	47	18		1
10	39	44	16		2

FIELD Y	No.	X	A	No. of twins	B
10	40	41	15		6
10	41	38	7		13
10	42	35	5		11
8	43	34	5		61
8	44	36	9		6
8	45	38	9		22
8	46	40	14		3
8	47	42	16		7
8	48	44	16		0
8	49	46	3		14
8	50	48	0		18
8	51	50	0		6
6	52	49	0		29
6	53	46	0		21
6	54	43	14		0
6	55	40	9		16
6	56	37	8		16
4	57	37	8		25
4	58	39	11		13
4	59	41	-		-
4	60	43	11		5
4	61	45	4		13
4	62	47	-		-
Total for 60 fields:			605		567

L_A for grain boundary $= \frac{\pi}{2} \cdot P_L = \frac{\pi}{2} \frac{10.1}{0.55} = 28.8$ cm/cm^2

L_A for twin boundary $= \frac{\pi}{2} \frac{9.45}{0.55} = 27.0$ cm/cm^2

$\overline{X}$ for grain boundary = 10.1

σ for grain boundary = 5.6

$\overline{X}$ for twin boundary = 9.45

σ for twin boundary = 10.9

TABLE 38 Precipitate Particle Density

SAMPLE: Semix 3-4-16 (X) Sample in polished condition. Magnification 400X.

Field area = 0.00149 cm^2

A denotes No. of Large precipitates observed in field of view.

B denotes No. of Small precipitates observed in field of view.

X and Y denotes location of microscope stage for the data measured.

FIELD			A		B
Y	No.	X	Large		Small
12	1	33	4		85
12	2	35	6		193
12	3	37	4		41
12	4	39	1		58
12	5	41	8		27
12	6	43	5		8
12	7	45	3		6
12	8	47	6		5
12	9	49	3		63
12	10	51	4		160
14	11	50	9		39
14	12	47	2		19
14	13	44	5		9
14	14	41	2		38
14	15	38	0		4
14	16	35	2		32
16	17	34	0		144
16	18	36	2		26
16	19	38	3		3
16	20	40	5		14
16	21	42	4		18
16	22	44	0		14
16	23	46	5		16
16	24	48	25		37
16	25	50	6		54
18	26	49	1		44
18	27	46	1		21
18	28	43	6		8
18	29	40	4		6
18	30	37	3		12
20	31	37	4		19
20	32	39	2		37
20	33	41	3		13
20	34	43	3		65
20	35	45	4		20
20	36	47	0		15
10	37	50	2		20
10	38	47	5		18
10	39	44	1		18

FIELD			A		B
Y	No.	X			
10	40	41	4		69
10	41	38	1		149
10	42	35	0		280
8	43	34	3		265
8	44	36	1		167
8	45	38	1		216
8	46	40	2		13
8	47	42	0		104
8	48	44	2		18
8	49	46	5		21
8	50	48	8		80
8	51	50	6		71
6	52	49	4		68
6	53	46	2		38
6	54	43	2		23
6	55	40	3		152
6	56	37	3		55
4	57	37	2		103
4	58	39	1		56
4	59	41	-		-
4	60	43	3		31
4	61	45	9		82
4	62	47	-		-
Total for 60 fields:			215		3491

Area of 62 fields = 0.0894 cm^2

No. of large ppt. = 215 /0.0894 = 2405 / cm^2

$\bar{X}$ for large ppt. = 3.6

σ for large ppt. = 3.6

No. of small ppt. = 3491/0.0894 =39050 / cm^2

$\bar{X}$ for small ppt. = 58.2

σ for small ppt. = 64.0

TABLE 39 DISLOCATION DENSITY

SAMPLE: Semix 3-4-16 (X) Sample in etched condition

Magnification 1000X, Area of field = 0.000238 cm^2

X and Y denote the location of microscope stage (field of view)for the data measured.

FIELD Y	FIELD No.	FIELD X	No. of Dislocation Pits
12	1	34	45
12	2	35	2
12	3	37	44
12	4	39	58
12	5	41	8
12	6	43	73
12	7	45	96
12	8	47	0
12	9	49	53
12	10	50	34
14	11	49	45
14	12	47	0
14	13	44	1
14	14	41	146
14	15	38	0
14	16	35	0
16	17	35	5
16	18	36	0
16	19	38	5
16	20	40	190
16	21	42	170
16	22	44	2
16	23	46	200
16	24	48	22
16	25	49	0
18	26	47	114
18	27	46	71
18	28	43	0
18	29	40	0
18	30	37	0
19	31	37	35
19	32	39	28
19	33	41	65
19	34	43	84
19	35	45	13
19	36	47	83
10	37	50	65
10	38	47	89
10	39	44	3
10	40	41	49
10	41	38	0
10	42	35	19
8	43	35	3
8	44	36	26
8	45	38	23
8	46	40	4
8	47	42	30
8	48	44	83
8	49	46	3
8	50	48	10
8	51	49	0
6	52	49	4
6	53	46	3
6	54	43	54
6	55	40	2
6	56	37	46
5	57	38	9
5	58	39	7
5	59	41	13
5	60	43	0
5	61	45	1
5	62	47	0

Total for 62 fields: 2244

Dislocation density = $15.2 \times 10^4/cm^2$

$\bar{X}$ = 36.2

σ = 47.75

ORIGINAL PAGE IS
OF POOR QUALITY

TABLE 40 Grain Boundary and Twin Boundary Density

SAMPLE: Semix 4-2-4 (Y_2) Sample in polished condition. Magnification 100X .
Field area = 0.0241 cm^2. Circumference of test circle = $\pi \cdot D$ = 0.55 cm.
A denotes No. of grain boundary intersections with circumference of test circle.
B denotes No. of twin boundary intersections with circumference of test circle.
X and Y denotes field location of the data measured.

FIELD			A	No. of twins	B
Y	No.	X	GB		Twin
12	1	33	5		6
12	2	35	3		2
12	3	37	0		0
12	4	39	0		0
12	5	41	2		0
12	6	43	2		2
12	7	45	8		28
12	8	47	4		4
12	9	49	4		0
12	10	51	0		2
14	11	50	8		18
14	12	47	4		9
14	13	44	4		6
14	14	41	3		61
14	15	38	3		0
14	16	35	4		3
16	17	34	5		2
16	18	36	8		9
16	19	38	4		3
16	20	40	3		41
16	21	42	3		37
16	22	44	0		1
16	23	46	9		21
16	24	48	6		6
16	25	50	8		27
18	26	49	13		9
18	27	46	4		1
18	28	43	8		8
18	29	40	5		7
18	30	37	8		28
20	31	37	9		21
20	32	39	9		13
20	33	41	0		0
20	34	43	3		16
20	35	45	5		24
20	36	47	2		2
10	37	50	2		1
10	38	47	9		4
10	39	44	6		9
10	40	41	16		19
10	41	38	0		2
10	42	35	0		23
8	43	34	4		0
8	44	36	26		12
8	45	38	10		6
8	46	40	10		15
8	47	42	4		25
8	48	44	2		65
8	49	46	8		11
8	50	48	6		3
8	51	50	4		7
6	52	49	6		25
6	53	46	4		10
6	54	43	2		18
6	55	40	5		14
6	56	37	18		16
4	57	37	9		18
4	58	39	6		8
4	59	41	6		9
4	60	43	20		2
4	61	45	11		13
4	62	47	6		4
Total for 62 fields:			366		756

L_A for grain boundary $= \frac{\pi}{2} \cdot P_L = \frac{\pi}{2} \frac{5.9}{0.55} = 16.9$ cm/cm^2

L_A for twin boundary $= \frac{\pi}{2} \frac{12.2}{0.55} = 34.8$ cm/cm^2

$\overline{X}$ for grain boundary = 5.9
σ for grain boundary = 4.9

$\overline{X}$ for twin boundary = 12.2
σ for twin boundary = 13.4

TABLE 41 Precipitate Particle Density

SAMPLE: Semix 4-2-4 (Y)$_2$ Sample in polished condition. Magnification 400X.

Field area = 0.00149 cm^2

A denotes No. of Large precipitates observed in field of view.

B denotes No. of Small precipitates observed in field of view.

X and Y denotes location of microscope stage for the data measured.

FIELD			A	B
Y	No.	X	Large	Small
12	1	33	8	68
12	2	35	1	7
12	3	37	2	11
12	4	39	1	6
12	5	41	6	13
12	6	43	5	12
12	7	45	5	6
12	8	47	5	11
12	9	49	3	20
12	10	51	3	6
14	11	50	2	7
14	12	47	0	6
14	13	44	3	303
14	14	41	5	28
14	15	38	4	14
14	16	35	1	92
16	17	34	1	30
16	18	36	1	24
16	19	38	2	23
16	20	40	5	65
16	21	42	3	146
16	22	44	1	490
16	23	46	0	52
16	24	48	3	54
16	25	50	2	40
18	26	49	0	29
18	27	46	2	23
18	28	43	1	19
18	29	40	2	8
18	30	37	3	13
20	31	37	2	8
20	32	39	2	26
20	33	41	2	22
20	34	43	1	17
20	35	45	3	19
20	36	47	3	32
10	37	50	6	36
10	38	47	4	13
10	39	44	2	20
10	40	41	3	11
10	41	38	3	3
10	42	35	0	32
8	43	34	2	33
8	44	36	0	5
8	45	38	1	5
8	46	40	1	18
8	47	42	6	5
8	48	44	3	24
8	49	46	5	14
8	50	48	2	10
8	51	50	3	15
6	52	49	2	27
6	53	46	4	8
6	54	43	2	18
6	55	40	1	8
6	56	37	0	4
4	57	37	8	21
4	58	39	4	38
4	59	41	7	24
4	60	43	6	30
4	61	45	4	18
4	62	47	5	16
Total for 62 fields:			177	2206

Area of 62 fields = 0.09238 cm^2

No. of large ppt. = 177 / 0.09238
= 1916 / cm^2

$\bar{X}$ for large ppt. = 2.9

σ for large ppt. = 2.0

No. of small ppt. = 2206 / 0.09238
= 23879 / cm^2

$\bar{X}$ for small ppt. = 35.6

σ for small ppt. = 72

TABLE 42 DISLOCATION DENSITY

SAMPLE: Semix 4-2-4 (Y) Sample in etched condition

Magnification 1000X, Area of field = 0.000238 cm^2

X and Y denote the location of microscope stage (field of view)for the data measured.

FIELD			No. of Dislocation Pits		
Y	No.	X		↓	
12	1	34		0	
12	2	35		0	
12	3	37		0	
12	4	39		0	
12	5	41		0	
12	6	43		0	
12	7	45		0	
12	8	47		0	
12	9	49		3	
12	10	50		3	
14	11	49		199	
14	12	47		13	
14	13	44		0	
14	14	41		6	
14	15	38		0	
14	16	35		0	
16	17	35		0	
16	18	36		2	
16	19	38		4	
16	20	40		0	
16	21	42		0	
16	22	44		0	
16	23	46		4	
16	24	48		0	
16	25	49		2	
18	26	47		2	
18	27	46		0	
18	28	43		580	
18	29	40		3	
18	30	37		0	
19	31	37		2	
19	32	39		0	
19	33	41		188	
19	34	43		470	
19	35	45		175	
19	36	47		0	
10	37	50		0	
10	38	47		34	
10	39	44		0	
10	40	41		202	
10	41	38		0	
10	42	35		0	
8	43	35		790	
8	44	36		165	
8	45	38		84	
8	46	40		800	
8	47	42		27	
8	48	44		7	
8	49	46		84	
8	50	48		0	
8	51	49		0	
6	52	49		0	
6	53	46		0	
6	54	43		0	
6	55	40		0	
6	56	37		480	
5	57	38		280	
5	58	39		0	
5	59	41		0	
5	60	43		0	
5	61	45		710	
5	62	47		173	

Total for 62 fields: 5492

Dislocation density = $37.2 \times 10^4/cm^2$

$\overline{X} = 88.6$

$\sigma = 195$

TABLE 43 Grain Boundary and Twin Boundary Density

SAMPLE: Semix 4-2-8 (Z) Sample in polished condition. Magnification 100X.
Field area = 0.0241 cm^2. Circumference of test circle = $\pi \cdot D$ = 0.55 cm.
A denotes No. of grain boundary intersections with circumference of test circle.
B denotes No. of twin boundary intersections with circumference of test circle.
X and Y denotes field location of the data measured.

FIELD Y	No.	X	A GB	No. of twins	B Twin
12	1	33	8		11
12	2	35	7		29
12	3	37	0		2
12	4	39	2		3
12	5	41	5		8
12	6	43	7		16
12	7	45	3		6
12	8	47	4		2
12	9	49	4		5
12	10	51	10		32
14	11	50	5		13
14	12	47	4		17
14	13	44	3		3
14	14	41	3		3
14	15	38	2		0
14	16	35	0		1
16	17	34	0		28
16	18	36	0		0
16	19	38	3		8
16	20	40	5		50
16	21	42	7		5
16	22	44	6		7
16	23	46	12		44
16	24	48	10		12
16	25	50	3		4
18	26	49	5		5
18	27	46	5		75
18	28	43	12		12
18	29	40	7		33
18	30	37	5		19
20	31	37	6		19
20	32	39	7		24
20	33	41	0		6
20	34	43	3		4
20	35	45	5		34
20	36	47	10		20
10	37	50	4		13
10	38	47	5		12
10	39	44	7		13
10	40	41	10		19
10	41	38	2		0
10	42	35	2		10
8	43	34	9		1
8	44	36	3		1
8	45	38	4		12
8	46	40	2		6
8	47	42	12		21
8	48	44	5		27
8	49	46	5		32
8	50	48	0		28
8	51	50	6		15
6	52	49	10		0
6	53	46	2		51
6	54	43	2		45
6	55	40	5		7
6	56	37	0		2
4	57	37	6		2
4	58	39	4		68
4	59	41	2		72
4	60	43	4		54
4	61	45	8		25
4	62	47	5		16
Total for 62 fields:			302		1112

L_A for grain boundary $= \frac{\pi}{2} \cdot P_L = \frac{\pi}{2} \frac{4.87}{0.55} = 13.9$ cm/cm^2

L_A for twin boundary $= \frac{\pi}{2} \frac{17.9}{0.55} = 51.2$ cm/cm^2

$\overline{X}$ for grain boundary = 4.87
σ for grain boundary = 3.15

$\overline{X}$ for twin boundary = 17.9
σ for twin boundary = 18.3

TABLE 44 Precipitate Particle Density

SAMPLE: Semix 4-2-8 (Z) Sample in polished condition. Magnification 400X.

Field area = 0.00149 cm^2

A denotes No. of Large precipitates observed in field of view.

B denotes No. of Small precipitates observed in field of view.

X and Y denotes location of microscope stage for the data measured.

FIELD			A		B
Y	No.	X	Large		Small
12	1	33	0		6
12	2	35	0		10
12	3	37	1		5
12	4	39	1		7
12	5	41	0		16
12	6	43	0		9
12	7	45	0		1
12	8	47	2		8
12	9	49	3		31
12	10	51	0		49
14	11	50	0		6
14	12	47	0		4
14	13	44	0		3
14	14	41	0		2
14	15	38	0		10
14	16	35	1		2
16	17	34	0		22
16	18	36	0		0
16	19	38	0		23
16	20	40	0		1
16	21	42	3		27
16	22	44	0		13
16	23	46	0		35
16	24	48	0		37
16	25	50	4		13
18	26	49	0		86
18	27	46	1		12
18	28	43	0		11
18	29	40	0		26
18	30	37	0		7
20	31	37	2		57
20	32	39	1		51
20	33	41	0		46
20	34	43	0		79
20	35	45	0		33
20	36	47	1		44
10	37	50	3		30
10	38	47	0		24
10	39	44	0		17
10	40	41	1		6
10	41	38	2		4
10	42	35	2		12
8	43	34	1		3
8	44	36	4		3
8	45	38	2		11
8	46	40	0		2
8	47	42	8		17
8	48	44	4		14
8	49	46	5		9
8	50	48	2		7
8	51	50	1		7
6	52	49	5		15
6	53	46	4		15
6	54	43	0		16
6	55	40	0		2
6	56	37	0		28
4	57	37	0		1
4	58	39	0		6
4	59	41	0		3
4	60	43	0		8
4	61	45	0		3
4	62	47	0		1
Total for 62 fields:			64		1056

Area of 62 fields = 0.09238 cm^2

No. of large ppt. = 64 /0.09238 = 693 / cm^2

$\bar{X}$ for large ppt. = 1.0

σ for large ppt. = 1.67

No. of small ppt. = 1056 /0.09238 = 11430 / cm^2

$\bar{X}$ for small ppt. = 17.0

σ for small ppt. = 18.3

ORIGINAL PAGE IS OF POOR QUALITY

TABLE 45 DISLOCATION DENSITY

SAMPLE: Semix 4-2-8 (Z) Sample in etched condition

Magnification 1000X, Area of field = 0.000238 cm^2

X and Y denote the location of microscope stage (field of view)for the data measured.

FIELD			No. of Dislocation Pits		
Y	No.	X		↓	
12	1	34		8	
12	2	35		31	
12	3	37		5	
12	4	39		131	
12	5	41		0	
12	6	43		6	
12	7	45		6	
12	8	47		10	
12	9	49		2	
12	10	50		7	
14	11	49		0	
14	12	47		11	
14	13	44		1	
14	14	41		7	
14	15	38		0	
14	16	35		0	
16	17	35		0	
16	18	36		0	
16	19	38		5	
16	20	40		12	
16	21	42		33	
16	22	44		18	
16	23	46		340	
16	24	48		0	
16	25	49		41	
18	26	47		0	
18	27	46		0	
18	28	43		7	
18	29	40		159	
18	30	37		12	
19	31	37		114	
19	32	39		0	
19	33	41		57	
19	34	43		6	
19	35	45		272	
19	36	47		0	
10	37	50		73	
10	38	47		3	
10	39	44		2	

FIELD			No. of Dislocation Pits		
Y	No.	X		↓	
10	40	41		1	
10	41	38		5	
10	42	35		0	
8	43	35		3	
8	44	36		0	
8	45	38		0	
8	46	40		0	
8	47	42		18	
8	48	44		1	
8	49	46		6	
8	50	48		480	
8	51	49		195	
6	52	49		68	
6	53	46		10	
6	54	43		76	
6	55	40		0	
6	56	37		2	
5	57	38		0	
5	58	39		0	
5	59	41		0	
5	60	43		30	
5	61	45		162	
5	62	47		55	

Total for 62 fields: 2491

Dislocation density = $16.9 \times 10^4 /cm^2$

$\bar{X}$ = 40.2

σ = 86.9